THE PHYSICAL REVIEW

VOLUME 47 | *Second Series* | NUMBER 11

JUNE 1, 1935

Published for the

AMERICAN PHYSICAL SOCIETY

by the

AMERICAN INSTITUTE OF PHYSICS

Incorporated

LANCASTER, PA., AND NEW YORK, N. Y.

The American Physical Society

OFFICERS OF THE SOCIETY

R. W. Wood, *President*
The Johns Hopkins University
Baltimore, Maryland

F. K. Richtmyer, *Vice President*
Cornell University
Ithaca, New York

W. L. Severinghaus, *Secretary*
Columbia University
New York, New York

G. B. Pegram, *Treasurer*
Columbia University
New York, New York

John T. Tate, *Editor*
University of Minnesota
Minneapolis, Minnesota

L. B. Loeb, *Local Secretary for the Pacific Coast*
University of California
Berkeley, California

The Physical Review

BOARD OF EDITORS

John T. Tate, *Editor*

J. W. Buchta, *Assistant Editor*

Associate Editors

K. K. Darrow
J. C. Hubbard
A. E. Ruark

A. Ellett
L. A. Turner
G. E. Uhlenbeck

W. V. Houston
R. S. Mulliken
I. I. Rabi

The Physical Review, which was established [illegible] 1893, is a journal of experimental and [illegible]retical physics. It is published for the American Physical Society by the American Institute of Physics Incorporated. There are two volumes annually with twelve issues in each volume.

[illegible] for publication should be submitted to [illegible], University of Minnesota, Minneapolis, [illegible].

[illegible] all correspondence concerning papers in the [illegible] publication, should be addressed to the Editorial [illegible] American Institute of Physics, 11 East 38th [illegible], New York, New York.

Subscriptions [illegible] United States and Possessions and [illegible], $5.00; Foreign, $16.50. Subscriptions and orders [illegible] back numbers should be addressed to Prince and [illegible], Lancaster, Pennsylvania, or to the American Institute of Physics, 11 East 38th Street, New York, [illegible].

[illegible] is not accepted for the *Physical Review* but [illegible] is called to the *Review of Scientific Instruments with News and Views*, a companion publication of [illegible], and a medium through which the field of physics can be reached most effectively. Rates and other information will be furnished on request to the Editorial Secretary.

Changes of address and complaints of failure to receive the *Physical Review*, in the case of members of the American Physical Society, should be addressed to the Treasurer; in the case of other subscribers, to the Editorial Secretary. New copies can be sent free in response to complaints of non-delivery only if notice of non-delivery is received within three months of date of issue.

The Physical Review is published semi-monthly at Prince and Lemon Streets, Lancaster, Pennsylvania.

Entered at the Post Office at Lancaster, Pennsylvania, as second class matter.

Acceptance for mailing at special rate of postage provided for in section 1102, Act of October 3, 1917, authorized September 6, [illegible].

THE
PHYSICAL REVIEW
A Journal of Experimental and Theoretical Physics
VOL. 47, NO. 11 JUNE 1, 1935 SECOND SERIES

An Apparent Effect of Galactic Rotation on the Intensity of Cosmic Rays

ARTHUR H. COMPTON, *University of Chicago and Oxford University* AND IVAN A. GETTING, *Oxford University*

(Received April 12, 1935)

Doppler effect studies of the globular clusters and the extra galactic nebulae have shown a motion of the earth of about 300 km/sec. toward about declination 47°N and right ascension 20 hr. 40 min., which is due chiefly to the rotation of the galaxy. Calculation shows that because of this motion the intensity of cosmic rays at sea level on an unmagnetized earth should be about 1.2 percent greater on the front side than on the back. Taking into account the earth's magnetic field, it is estimated (assuming the cosmic rays reaching the earth to consist of protons and electrons) that the diurnal variation at latitude 45° due to this motion should be, within a factor of 2, equal to 0.1 percent, with its maximum at 20 hr. 40 min. sidereal time. Data published by Hess and Steinmaurer show a sidereal time variation having just this amplitude and phase. While this agreement gives a strong presumption that the cause of this sidereal time variation is the earth's motion through space, another possible explanation is also considered. Experimental methods for making a definite test are outlined. The implication of a galactic rotation effect would be that the cosmic rays originate beyond our galaxy.

DR. HOWARD LOWRY has called our attention to the possibility that the motion of the earth through space may appreciably affect the intensity of cosmic rays. If these rays approach the earth from a source external to the galaxy, the effect due to our motion with the rotation of the galaxy should be perceptible, and comparison with existing cosmic-ray data shows a sidereal diurnal variation of just the anticipated type. If further experiments show this variation to be really due to the galactic rotation we shall have direct evidence of the very remote origin of cosmic rays, and a new method of determining the state of the earth's motion relative to the rest of the universe.

According to data kindly supplied us by Professor J. H. Oort, the rotational motion of our portion of the galaxy is in the galactic plane, directed toward 20 hr. 55 min. right ascension and 47°N declination, with a probable error of a few degrees. The most precise estimate of the speed has been made from the Doppler shifts of 18 globular clusters,[1] giving 275 ± 50 km/sec. Observations of the Doppler effect of extragalactic systems give 380 ± 110 km/sec. velocity in about the same direction.[2] Other methods give nearly the same result. In addition, the sun has a small individual motion of about 20 km/sec. The resultant velocity should be toward about $\alpha=20$ hr. 40 min., $\delta=+47°$ at about 300 km/sec. It would appear from the analysis by Oort[2, 3] of the motions of the remote galaxies, that the peculiar velocities of these systems are probably smaller than 80 km/sec. This means that if the cosmic rays come uniformly from all parts of the remote cosmos, our speed relative to their source is probably about that of the galactic rotation.

This motion with a speed of about 0.1 percent that of light will affect the intensity of the in-

[1] C. Strömberg, Astrophys. J. **61**, 357 (1925).
[2] E. Hubble, Proc. Nat. Acad. Sci. **15**, 270 (1929).
[3] J. H. Oort, Bull. Ast. Inst. Netherlands **6**, 155 (1931).

coming cosmic rays by changing both the energy of the cosmic-ray particles and the number received per second. Imagine, as in Fig. 1, the earth moving along AB with a speed βc, where $\beta \ll 1$, and imagine cosmic-ray particles with a speed γc, almost equal to that of light, moving in the direction CB, at an angle θ with the direction of the earth's motion. By making use of the relativity expressions for addition of velocities and for kinetic energy, it can then be shown that the energy of each particle relative to the moving earth is, to the first order of small quantities,

$$E' = E(1+\alpha\beta(\sqrt{2}-1)\cos\theta)/(1-\beta\cos\theta), \quad (1)$$

where E is its energy relative to an observer at rest, and $\alpha = 1-\gamma$. If $\alpha \ll 1$, we may thus write without sensible error,

$$E' = E/(1-\beta\cos\theta). \quad (2)$$

If E is equated to $h\nu$, this becomes the usual expression for the Doppler effect with light.

To calculate the increase in the rate at which the cosmic-ray particles impinge on unit surface drawn normal to the direction of motion AB, let $AC = \gamma c$ be the distance traveled by a particle in unit time. Then to the first order of β the time required for a particle from C to reach B is

$$\tau = (\gamma c - \beta c\cos\theta)/\gamma c = 1-(\beta/\gamma)\cos\theta,$$

or, again by neglecting $1-\gamma$ when multiplied by β,

$$\tau = 1-\beta\cos\theta. \quad (3)$$

Assume for convenience a constant number of particles per unit path. The number striking a stationary unit surface at B within a range of directions $d\theta$ and in the time interval τ is then proportional to

$$n = (1-\beta\cos\theta)\cdot\cos\theta\cdot 2\pi\sin\theta d\theta, \quad (4)$$

while during the same interval the number striking the surface moving from A to B is

$$n' = 1\cdot\cos\theta'\cdot 2\pi\sin\theta d\theta. \quad (5)$$

From Fig. 1, however to the first order of β,

$$\sin\theta = \sin\theta'/(1-\beta\cos\theta')$$

and

$$d\theta = d\theta'/(1-\beta\cos\theta').$$

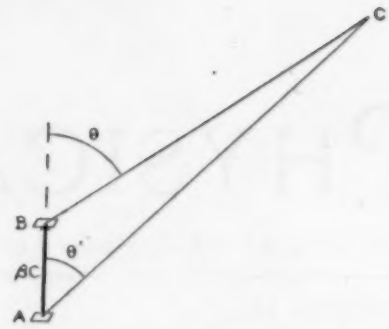

FIG. 1.

Thus by Eq. (5),

$$n' = \cos\theta'\cdot 2\pi\sin\theta' d\theta'/(1-\beta\cos\theta')^2, \quad (6)$$

where the primed angles are those observed from the moving surface. Within the same observed range of angles, therefore, the rate of receiving particles is thus increased by the motion in the ratio

$$n'/n = 1/(1-\beta\cos\theta)^2. \quad (7)$$

Since the intensity is the energy of the particles received per second per unit area, on combining Eqs. (7) and (2) we have, for the rays incident at an angle θ with the direction of motion,

$$I'/I = 1/(1-\beta\cos\theta)^4. \quad (8)$$

This is the counterpart of the fact previously shown by one of us[4] that the Doppler change in intensity of light from a moving source is equal to the 4th power of its change in frequency.

With coincidence counting tubes, arranged to record the radiation from a narrow range of directions, we should be concerned, except for the absorption by the atmosphere, with Eq. (7). With an ionization chamber it is the average effect from all angles with which we are concerned. Let us suppose that the direction of motion is toward the zenith (condition for maximum intensity). We may then weight roughly the contribution from the various directional zones by assuming to a sufficient approximation that when measured near sea level the intensity of the rays per unit solid angle falls off because of atmospheric absorption about as $\cos^2\phi$, where ϕ is the zenith angle. The number of particles received from the direction zone ϕ to $\phi+d\phi$ will

[4] A. H. Compton, Phys. Rev. **21**, 490 (1923).

thus be proportional to

$$\cos^2\phi \cdot 2\pi \sin\phi d\phi. \tag{9}$$

The mean energy of the incident particles is thus

$$\bar{E}' = \frac{\int_0^{\pi/2} E' \cos^2\phi \sin\phi d\phi}{\int_0^{\pi/2} \cos^2\phi \sin\phi d\phi}. \tag{10}$$

By writing Eq. (2) in the form

$$E' = E(1+\beta\cos\varphi), \tag{11}$$

its equivalent to the first power of β, we obtain on integration of Eq. (10)

$$\bar{E}' = E(1+\tfrac{2}{3}\beta). \tag{12}$$

At the surface of the atmosphere with an isotropic distribution of the rays, the ratio of the intensity in the moving system to that in the stationary system should similarly be, by Eq. (8):

$$\frac{I_0'}{I_0} = \frac{\int_0^{\pi/2}[2\pi \sin\theta d\theta/(1-\beta\cos\theta)4]}{\int_0^{\pi/2} 1\pi \sin\theta d\theta} = 1+2\beta, \tag{13}$$

to the first power of β.

The ionization observed in an ionization chamber depends, however, upon the fraction of the energy which penetrates the atmosphere and the fraction absorbed within the chamber. We may assume that the intensity is a function of the depth z below the surface of the atmosphere such that

$$I/I_0 = f(z); \tag{14}$$

but when the energy of the incident particles is increased by the factor $(1+\epsilon)$ the intensity follows a new function of the depth,

$$I'/I_0' = f_1(z) = f(z/(1+a\epsilon)). \tag{15}$$

This says that the "penetrating power" has been increased by a factor $(1+a\epsilon)$, a conception which may be strictly valid for exponentially absorbed particles, but expresses only roughly the effect of the increased energy on "range" particles. Since $-dI/dz$ is the energy per second spent per cm³ as the rays traverse the atmosphere, the rate of ionization per cm³ of the air is

$$i = -kdI/dz, \tag{16}$$

where k is the number of ions produced per unit energy (about 30 ions per electron volt), and i is nearly proportional to the ionization current measured in an ionization chamber. From Eqs. (15) and (14) we have thus for the ratio of the ionization observed on the moving earth to that on the earth at rest,

$$\frac{i'}{i} = \frac{dI'/dz}{dI/dz} = \frac{I_0'}{I_0}\frac{(d/dz)f[z/(1+a\epsilon)]}{(d/dz)f(z)} = \frac{I_0'}{I_0}\frac{1}{1+a\epsilon}\frac{f'[z/(1+a\epsilon)]}{f'(z)}. \tag{17}$$

We may write

$$f'[z(1+a\epsilon)] = f'(z-\delta z),$$

where $\delta z = a\epsilon z$. Also

$$f'(z-dz) = f'(z) - (d/dz)f'(z)\delta z \quad [\delta z \ll z]$$
$$= f'(z) - f''(z)\delta z.$$

Thus

$$f'[z/(1+a\epsilon)]/f'(z) = 1-[f''(z)/f'(z)]\delta z = 1+m\delta z = 1+ma\epsilon z,$$

where

$$m \equiv -f''(z)/f'(z). \tag{18}$$

Eq. (17) may thus be written

$$i'/i = (I_0'/I_0)(1+ma\epsilon z)/(1+a\epsilon) = (I_0'/I_0)[1+a\epsilon(mz-1)]. \tag{19}$$

According to Eq. (12) we may use $\frac{2}{3}\beta$ for ϵ, and Eq. (13) gives the value of I_0'/I_0 as $1+2\beta$. The effective value of a cannot differ greatly from 1. With these values, expression (19) becomes to the first power of β,

$$i'/i = 1+(5/4)\beta+(3/4)\beta mz, \tag{20}$$

or for the fractional change in intensity

$$\delta i/i = (i'-i)/i = \beta(5/4+(3/4)mz). \tag{21}$$

In this expression, as we have seen, β is presumably about 0.001, z is the depth below the surface of the atmosphere, and m, defined by Eq. (18) may be calculated from the experimental ionization *vs.* depth curve for any value of z.

Using the depth ionization data collected by

Eckart,[5] we calculate from Eqs. (18) and (21) the values of m given in Table I and of $\delta i/i$ for

TABLE I. *Predicted amplitude of variation of intensity at various depths, due to motion of $\beta=0.001$. (Eq. (21).)*

Depth (kg/cm^2=z)	I (ions)	m	$\delta i/i$
0.3	126	5.5	0.002
0.5	31	8.6	.004
0.7	9.1	9.0	.006
1.0	2.9	6.3	.006
1.5	1.54	4.4	.006
2.0	1.03	1.8	.004
3.0	.61	1.7	.005

various depths below the surface of the atmosphere. In the neighborhood of sea-level (1 kg/cm^2), this means a difference of 1.2 percent between the front and the back sides of the earth.

There are, however, two factors which must prevent observing this full effect, the deflection of the cosmic-ray particles by the earth's magnetic field, and the inclination of the earth's axis relative to the motion in question. If δ is the declination of the direction of motion, λ the latitude of the observer and θ the hour angle between the observer's meridian and the direction of motion, then the angle ϕ between the observer's zenith and the direction of motion is given by

$$\cos\phi=\sin\delta\sin\lambda+\sin\delta\cos\lambda\cos\theta. \quad (22)$$

The factor by which the predicted variation should be reduced is

$$F=\tfrac{1}{2}(\cos\phi_{\max.}-\cos\phi_{\min.}). \quad (23)$$

The best available data for testing the prediction have been collected by Hess and Steinmaurer[6] on the Hafelekar, at an altitude of 2300 meters and a latitude 47°N. At this station, by Eqs. (22) and (23), we get $F=0.496$.

The effect of the magnetic field cannot be calculated with precision. If we assume the composition of the cosmic rays suggested by one of us,[7] the rays reaching the earth consist of a penetrating component of protons, and a less penetrating component of electrons, apparently about equally divided between positrons and negatrons. The protons and electrons seem to comprise about 40 percent and 60 percent, respectively, of the rays as observed at 2300 meters. The protons constitute the rays which show a latitude effect at 47 degrees, and are thus strongly bent by the earth's magnetic field. Protons of each energy should show a maximum at a different sidereal time, and these times will be distributed throughout the entire 24 hours. It is unlikely therefore that this component can contribute appreciably to a diurnal variation. The electron component on the other hand must have such great energy to traverse the atmosphere that its curvature should be considerably less. If, as Johnson's new results seem to show,[8] there are about equal numbers of positrons and electrons, the magnetic curvatures will diffuse the rays in both directions, thus lessening the diurnal variation, but will not alter the phase of the maximum. A reasonable estimate would seem to be that the variation due to this component should be between 10 percent and 50 percent as great as if they were undeflected. Taking these various factors together, we may anticipate a total diurnal variation under the conditions of Hess and Steinmaurer's experiments, within perhaps a factor of 2, equal to 0.1 percent. Its maximum should most probably occur close to the sidereal time, 20 hr. 40 min., when the earth's motion is toward the zenith.

This calculation is directly comparable with the experiments of Hess and Steinmaurer,[6] in which the average results of a complete year of observations, after making the necessary corrections, have been plotted against the sidereal time. In Fig. 2, are shown: (1) the effect as predicted above, of 0.05 percent amplitude and with its maximum at 20 hr. 40 min. sidereal time; (2) Hess and Steinmaurer's data averaged over half-hour periods, taken from their Fig. 5; and (3) the same data averaged over 3-hour periods. It will be seen that there is a definite sidereal time variation whose phase and amplitude are very close to those predicted. A least-squares analysis of these data, kindly carried through for us by Mrs. Ardis T. Monk, gives for the first harmonic an amplitude of $0.043\pm.0045$ percent with its maximum at 21 hr. 31 min.$\pm$23 min. Thus the effect is almost 10 times the probable

[5] C. Eckart, Phys. Rev. **45**, 851 (1934).
[6] V. F. Hess and R. Steinmaurer, Sitzungsber. Preuss. Ak. Phys.-Math. Kl. **15** (1933).
[7] A. H. Compton, Proc. Phys. Soc. London, April, 1935. A. H. Compton and H. A. Bethe, Nature **134**, 734 (1934).
[8] T. H. Johnson, Phys. Rev. in press (1935).

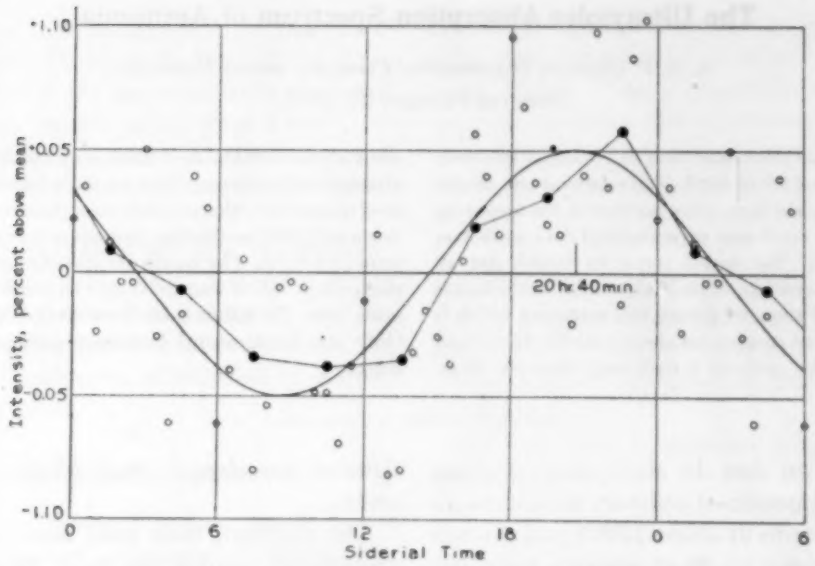

FIG. 2. Percentage variation in intensity of the cosmic rays with sidereal time. Curve, predicted effect due to galactic rotation. Data, Hess and Steinmaurer; open circles, half-hour means; solid circle, 3-hour means.

error, and cannot therefore be ascribed to chance.

No other data of such precision are available which are suitable for testing this sidereal diurnal effect. In the records of Steinke for 1929[9] little if any effect is evident, whereas his data for 1926[10] seem to show about the same magnitude of effect as those of Hess and Steinmaurer.

Messerschmidt has pointed out that if the solar diurnal variation differs at different seasons of the year, the annual mean will show an apparent sidereal time variation. It should be possible to test this suggestion in two ways. (1) Measurements of the same type as those of Hess and Steinmaurer, if made in the southern hemisphere, should show a sidereal time variation due to the earth's motion with its maximum at the same sidereal time. If, however, the effect is due to a seasonal difference in the solar time variation, the apparent sidereal maximum in the annual mean as observed in the southern hemisphere should differ in phase by 12 hours as compared with the northern hemisphere. (2) There should be a difference in the cosmic-ray intensity in the northern and southern hemispheres due to the earth's motion. Since the earth's magnetic field does not bend the approaching rays from the northern to the southern hemisphere, or *vice versa*, we may expect this difference to be almost as great as if no magnetic field were present. According to Eq. (22), the 24 hour mean of the component of motion in the direction of the zenith is proportional to sin δ sin λ. For northern and southern stations at 45° latitude, and taking δ as +47 degrees, this means that the average intensity at the northern station should be, according to Table I, about 0.6 percent greater than at the southern station. Though existing data are not of sufficient precision to show this difference, the predicted effect is of sufficient size to be measurable with some precision by using the more refined meters now in use.

While we must await some such measurements before we can consider the effect due to the rotation of the galaxy as established, the quantitative agreement with the predictions as shown in Fig. 2 gives a strong presumption in its favor. Its existence would imply that an important part of the cosmic rays originates outside of our galaxy. If its magnitude is found to be as great as we have predicted, it will imply that practically all the cosmic radiation has an extragalactic origin.

[9] E. Steinke, Zeits. f. Physik **42**, 570 (1927).
[10] E. Steinke, Zeits. f. Physik **64**, 48 (1930).

The Ultraviolet Absorption Spectrum of Ammonia

A. B. F. DUNCAN, *Department of Chemistry, Brown University*

(Received February 28, 1935)

The discrete absorption spectrum of ammonia has been photographed from 2300 to 850A. The experimental results of other workers in the long wave portion of the spectrum are confirmed, and much new experimental data at shorter wavelengths found. The bands down to 1665A are all diffuse because of predissociation. Below 1665 all the bands are very sharp and show rotational fine structure which is partly resolved. True continuous absorption (in distinction to that produced by pressure broadening) does not begin until about 1200A. At 1150A and below the continuous absorption is so strong that no more bands could be measured accurately. Sharp bands exist, however, at least as far down as 1085A, so the first ionization potential should be at least 11.3 volts. The bands are classified in four v' progressions which fall in four different electronic states, all of the same type. All bands come from $v=0$ of the normal state. Only one fundamental frequency appears in the excited states.

IT is well known that the absorption spectrum of gaseous ammonia at ordinary temperatures and pressures begins at about 2200A and extends into the ultraviolet.[1, 2] Most workers have not observed the spectrum at wavelengths shorter than 1900A, but the measurements of Leifson extend as far as 1500A. In the present work the spectrum was photographed at room temperature, with moderately high dispersion and very high resolving power from 2300 to 850A.

The vacuum grating spectrograph and light source have been described.[3, 4] The ammonia used was obtained from the very pure liquid used for conductivity work in the laboratory of Professor C. A. Kraus. It was redistilled in vacuum and evaporated into a large storage bulb attached to the spectrograph. The spectrograph was filled by means of small calibrated volumes to pressures of 0.015 to 1 mm. No absorption was apparent at lower pressures, and higher pressures served merely to bring out weaker parts of the fine structure, of which not much use was made. Since at normal incidence only about 1000A of the spectrum could be photographed at one time, it was necessary to use two settings of the grating. We were assured that all the absorption down to 1275A was really in the first order by making one exposure through fluorite. The absorption below this wavelength seems far too strong to be due to any very short wavelength bands (shorter wavelength than 650A) in the higher orders.

The standard lines used were 1215.68 (H, in absorption, narrow on most plates), 1066.662 (Si IV),[5] 1338.603 (O IV), 1371.287 (O V), 1548.195 (C IV), 1550.768 (C IV)[6] and 2066.86 (B III).[7] Measurements at the two settings of the grating gave consistently a small difference in the dispersion. With a uniform but different dispersion for each setting of the grating, bands and standard lines appearing at both settings had the same values. All bands reported were found on at least two different plates. Most of the band heads were measured in at least ten different spectra.

The first four double headed bands in the near ultraviolet were measured to within 1–5 cm^{-1}. The succeeding predissociation bands were so diffuse that the centers of gravity only could be measured. For this measurement, the two limits of the absorption band were measured on several plates at a series of regularly increasing pressures. A plot was then made of the edges against pressure, and the two curves extrapolated to crossing. This value was taken as the center of gravity and the method seemed safer than extrapolating to zero pressure. Measurements by this method were reproducible to 5–20 cm^{-1}. The accuracy here rests naturally on the assumption that the

[1] S. Leifson, Astrophys. J. **63**, 87 (1926).
[2] J. K. Dixon, Phys. Rev. **43**, 711 (1933).
[3] Noyes, Duncan and Manning, J. Chem. Phys. **2**, 717 (1934).
[4] A. B. F. Duncan and J. P. Howe, J. Chem. Phys. **2**, 851 (1934).
[5] B. Edlén and J. Söderqvist, Zeits. f. Physik **87**, 218 (1933).
[6] B. Edlén, Zeits. f. Physik **85**, 85 (1933).
[7] Corrected by Noyes, Duncan and Manning to this value by intercomparison with 1931.027 (C III), and N I 1745.26, 1742.74 (Bowen and Ingram, Phys. Rev. **28**, 444 (1926)).

same meaning is to be attached to the position of maximum absorption in all the bands. The sharp bands in the rest of the spectrum were measured with a precision usually better than 5 cm^{-1}, the precision decreasing slowly with the increasing wave number/distance ratio at shorter wavelengths.

Parts of the spectrum will first be described separately, and then a general discussion of the entire spectrum given. It is necessary for this discussion to review the known facts about the normal state of ammonia, as revealed by Raman and infrared spectra.

The Normal State of Ammonia

Studies of the infrared absorption[8, 9, 10] and Raman spectrum of ammonia[11, 12] show that this molecule is a regular pyramid, whose altitude is rather small (about 0.3A). There are four fundamental vibration frequencies all of which are permitted in both types of spectra. There are some differences in the assignment of the experimental data to these frequencies, but the following interpretation seems to be that agreed on in most recent papers. In order of increasing frequency we have first $\nu_1 = 934.2, 964.3$ a non-degenerate frequency.[13] It is associated with a parallel deformation (symmetrical bending) motion in which an equilateral triangle having an hydrogen atom at each corner, vibrates as an almost rigid unit along the symmetry axis with the nitrogen atom, which is outside the plane of the triangle. In the limiting case the H−H distance is not altered. ν_2 is the corresponding perpendicular deformation frequency and appears to be 1630 in infrared and 1580 in Raman spectra. This frequency is doubly degenerate. ν_3 represents a symmetrical stretching (parallel valency) motion, and has the value 3334 cm^{-1}. It is non-degenerate. ν_4 is the corresponding perpendicular frequency and may be considered a tipping motion of the triangle relative to the N atom. Its value must be regarded as very uncertain, but it would appear to be greater than 3000 cm^{-1}. This same designation (by subscripts) of these frequencies has not been made by all investigators, but it is the one used in all the discussion following.

The Electronic States of Ammonia

The possible types of states[14, 15] are A_1, A_2 (similar to Σ^+ and Σ^- states of diatomic molecules), and E. The selection rules are different for two cases:

(1) The electric moment is parallel to the symmetry axis

$$A_1 \rightarrow A_1, \qquad A_2 \rightarrow A_2.$$

(2) The electric moment is perpendicular to the symmetry axis

$$A_1 \rightarrow E, \qquad A_2 \rightarrow E.$$

The normal state is most probably A_1, therefore the excited states found are either A_1 or E, depending on the direction of the electric moment.

The Diffuse Bands (2200–1675A)

Most of these bands have been photographed by Dixon and Leifson and partly analyzed by Dixon, who studied the effect of temperature on the bands and was able to observe many bands arising from high levels of the normal state. The bands found in this research are given in Table I

Table I. *The diffuse bands* (cm^{-1}).

Leifson	Dixon	Duncan	Leifson	Dixon	Duncan
44247			50556	50675	50663
45246			51440	51600	51555
46157	46140	46126 *	52317	52407 (1900A)	52501
	46200	46202	53265		53444
47003	47030	47010 *	54206		54411
	47090	47069	55135		55341
47869	47925	47914 *			56278
	47975	47962			57271
48768	48890	48803			58255
		48868			59202
49686	49790	49712			

* These first three bands are accompanied by weaker branches called satellites by Dixon. They were not investigated thoroughly in this work but were about the same number and had the same values as those found by Dixon.

[8] D. M. Dennison and J. B. Hardy, Phys. Rev. **39**, 938 (1932).
[9] D. M. Dennison, Rev. Mod. Phys. **3**, 280 (1931).
[10] P. Lueg and K. Hedfeld, Zeits. f. Physik **75**, 599 (1932). References to much other work given here.
[11] E. Amaldi and G. Placzek, Zeits. f. Physik **81**, 259 (1933).
[12] C. M. Lewis and W. V. Houston, Phys. Rev. **44**, 903 (1933).
[13] The very interesting explanation of this double value of the frequency is given in the above papers of Dennison.
[14] R. S. Mulliken, Phys. Rev. **43**, 279 (1933).
[15] J. E. Leonard-Jones, Trans. Faraday Soc. **30**, 70 (1934).

TABLE II. *Band heads (complete list)* (cm^{-1}).

V''	Series I calc.	Series I obs.	Series II calc.	Series II obs.	Series III calc.	Series III obs.	Series IV calc.	Series IV obs.
0	46122	46126(4)	60130	60136(1)	69748	69765(5)	82857	82857(6)
		884		933		904		986
1	47008	47010(4)	61081	61069(3)	70669	70669(6)	83847	83843(8)
		904		957		926		1029
2	47902	47914(5)	62046	62026(5)	71607	71595(6)	84871	84872(8)
		889		998		960		1056
3	48804	48803(6)	63025	63024(6)	72564	72555(7)	85931	85928(9)
		909		998		989		
4	49714	49712(7)	64019	64017(7)	73539	73544(8)		
		951		1008		990		
5	50632	50663(7)	65028	65025(6)	74532	74534(7)		
		892		1017		1027		
6	51558	51555(8)	66051	66042(7)	75543	75561(8)		
		946		1049		1021		
7	52492	52501(10)	67088	67091(8)	76572	76583(9)		
		943		1049		1045		
8	53434	53444(9)	68140	68140(8)	77619	77628(10)		
		967		1052		1045		
9	54384	54411(8)	69206	69192(6)	78685	78673(8)		
		930		1056		1092		
10	55342	55341(6)	70287	70248(4)	79768	79767(6)		
		946		1068		1065		
11	56308	56287(6)	71382	71316(0)	80869	80832(8)		
		985				1052		
12	57282	57272(5)			81989	81884(8)		
		983						
13	58264	58255(2)						
		954						
14	59254	59209(0)						

together with the measurements of Leifson and Dixon (those which are due to absorption in the *cold* gas) for comparison. The last bands of the series were not found by Leifson probably because his absorbing column was too short.

The agreement of the present measurements with those of Dixon is good in the first three double headed bands. The fourth band is here found to be double headed (because of the long column used) while Dixon gives only the center. The agreement with Leifson is not very good but the general trend of differences is about the same.

It seemed best to accept Dixon's vibrational analysis with one modification. He used two frequencies to explain the upper state differences. His high difference, 2720, is almost exactly three times the lower one, 890, so that every third band falls in a 2700 v' progression. Only two bands (in addition to the $v''=0\ v'=0$ band) were used in this progression, and attempts to fit the higher frequency bands observed in the present work into a 2700 progression required that that difference vary in a very irregular and unconvincing manner. It seems that intensities should be quite different in combination bands and in simple overtones, and members of the 2700 progression (n 2700) should be quite different from bands of the type n 2700$+n'$ 890. This is clearly found not to be the case here, where the intensities increase in a most regular manner up to $v'=8$ and afterwards decrease regularly to $v'=14$. Furthermore, the upper state frequency 2720 must be interpreted as a modification of ν_3 and it is difficult to see physically why this type of frequency should be so greatly lowered. All bands observed here (long wave head used for the double headed bands) fit, within the limit of experimental error, a very simple formula

$$\nu(\mathrm{cm}^{-1}) = 46{,}157 + 878(v'+\tfrac{1}{2}) + 4(v'+\tfrac{1}{2})^2 - 475, \quad (1)$$

where 475 is used for $\omega_e(v''+\frac{1}{2})+x_e\omega_e(v''+\frac{1}{2})^2$, $(v''=0)$, and accordingly all bands in this region are interpreted as members of one v' progression.

Dixon's interpretation of the two heads as being two rotational branches seems essentially correct, although it is doubtful whether they are P and R branches. The difference in direction of shading in these branches found by Dixon, could not be found here. All the branches in-

TABLE III. *Sub-bands in series III and IV* (cm^{-1}).

Heads											
					Series III						
		69765(5)			*254*	70019(4)				*722*	70487(4)
		70669(6)			*322*	70991(5)					
		71595(6)	*216*	71811(3)	*312*	71907(5)	*415*	72010(2)			
		72555(7)	*219*	72774(5)	*298*	72853(6)					
		73544(8)	*207*	73751(5)	*310*	73854(5)					
		74534(7)	*208*	74742(3)	*317*	74851(7)				*673*	75207(4)
		75561(8)	*238*	75784(4)	*253*	75814(6)	*433*	75994(6)	*513* 76074(2)	*585*	76146(2)
		76583(9)	*219*	76802(6)	*278*	76861(?)**	*388*	76971(6)	*505* 77088(2)	*600*	77183(0)
		77628(10)	*138*	77766(5)	*268*	77896(8)	*440*	78069(8)	*491* 78119(0)		
		78673(8)	*89*	78762(7)	*258*	78931(0)	*409*	79082(7)			
		79767(6)	*67*	79834(8)*	*318*	80085(0)			*665* 80432(0)	*815*	80618(5)
		80832(8)			*278*	81110(6)			*645* 81477(0)	*765*	81597(3)
		81884(8)			*263*	82146(5)			*620* 82504(0)	*722*	82606(2)
					Series IV						
82704(1)	*153*	82857(6)			*387*	83244(3)			*543* 83600(4)		
83717(3)	*126*	83843(8)			*433*	84276(6)					
84749(4)	*123*	84872(8)			*402*	85274(7)					
85769(4)	*159*	85928(9)									
86839(5)											

Unassigned
78860 (3)
84960 (1)

* Doubtful on basis of intensity.
** Emission lines in source here.

cluding the satellites appear to be shaded to the red.

THE SHARP BANDS (1675–1150A)

It is possible to arrange all the remaining bands heads into three progressions which obey the following series formulas. The progressions are referred to as series II, III and IV. The arrangement was made not merely on the basis of constant differences, but also intensities, appearance of the bands by direct examination of plates and enlargements, and variation of the appearance with pressure were considered. The same bands would have been picked out as belonging to the progressions if differences had not been obtained until after the arrangement had been made. The series formulas, in the same form as Eq. (1) follow:

$$\nu = 60{,}135 + 936.28(v' + \tfrac{1}{2}) + 7.22(v' + \tfrac{1}{2})^2 - 475, \quad (2)$$

$$\nu = 69{,}769 + 902.56(v' + \tfrac{1}{2}) + 9.04(v' + \tfrac{1}{2})^2 - 475, \quad (3)$$

$$\nu = 82{,}851 + 954.2\ (v' + \tfrac{1}{2}) + 17.2(v' + \tfrac{1}{2})^2 - 475. \quad (4)$$

The bands observed are given in Table II with their intensities (on a scale of ten). Values calculated from the above formulas are included for comparison.

Series II consists of very sharp bands which have their intensity maxima at a short wavelength head. There is definite shading to the red of the most intense portions. As many as twenty or thirty "lines" (or groups of intense lines very close together) may be measured in some of the bands, but it is very doubtful that much resolution of the true rotational lines has been accomplished. The "lines" will therefore not be listed, but merely the most intense heads. The last two members of the series would fit the formula better if higher powers of $(v' + \frac{1}{2})$ were considered, and we would expect that the interaction of vibration and rotation would be considerable here. Leifson photographed five of the bands in this series, but regarded them as diffuse. The reason for this is not apparent for they are certainly very sharp here. Leifson's values[16] for the "centers" agree however fairly well with the heads reported here.

The next progression, series III, slightly overlaps series II and its bands have a somewhat different appearance. Series IV is very similar to series III and the following remarks apply to both series. Each band appears to be multiple headed, the number of heads ranging from two to six. Two heads are always much stronger than the others and of the two, the long wave one is

[16] The values are 61,957, 62,932, 63,938, 64,977, 66,006 cm^{-1} and correspond to $v' = 3, 4, 5, 6$ and 7 of this series.

somewhat the stronger, and is considered the "head" of the band and is the one listed in Table II. This head has the same significance as the heads in series II. The other absorption maxima are separated from the main head by approximately constant differences in any one series. These branches which look like separate bands are all shaded to the red. It does not appear possible to explain these branches as being due to independent vibrational transitions, for the differences involved are much too small even for difference frequencies. Electronic multiplets should be excluded because of the character of the excited states, but in any case the multiplicity cannot be as large and as variable as would be required here.

In Table III are given all the measurements of intense absorption in series III and IV (with intensities on a scale of ten in parentheses). The other absorption maxima accompanying each head and considered the other more intense rotational branches are given in the same horizontal row as the head. The differences *from the head* are indicated in italics.

Toward the end of series IV the continuous absorption begins to get rather strong. It is for this reason that series IV is so short. Additional bands can be seen on the plates and on enlargements, but could not be measured accurately and are not reported. No additional progressions could be found. Series IV really seems to extend as far as 1085A = 92,165 cm^{-1} = 11.36 e.v. It would appear that the first ionization potential should be at least as great as this, but not necessarily much greater. The value usually given by more direct measurement is 11.3 e.v.

Discussion

We may now survey the ammonia spectrum as a whole. The four progressions may all be interpreted as v' progressions all coming from $v = 0$ in the normal state. The four progressions must be in four different electronic states since the differences between the first members are far too large to be vibrational differences and are of the order of magnitude of electronic term differences. According to the electronic selection rules, and the experimental fact that only parallel vibrations are found in the excited electronic states, all these states must be of the same type as the normal state (either A_1 or A_2, but more probably A_1). The fact that the four 0,0 bands do not form a Rydberg series does not present a very serious argument against the excited states being all of the same type.[17]

These four progressions involve only the frequency ν_1. This fact introduces such a great simplification in the discussion that it seemed very important to verify it as well as possible. Accordingly the appearance and intensities were disregarded (since consideration of these requires the above progressions, with *only* the frequency ν_1), and an extensive search made for other approximately constant differences made from a complete table of differences. It was of course possible to find pairs of bands in series III and IV (if all the absorption maxima in Table III were considered as equally probable band heads) which could be attributed to modifications of ν_2 and ν_3, but only pairs could be found, and no two pairs seemed to have any connection by numbers which could be considered as even greatly modified normal frequencies. Normal state differences should have almost exactly the values of the normal Raman and infrared frequencies, or be exact multiples of these, and no differences at all fulfilled this requirement. So we must conclude that the use of frequencies[18] other than ν_1 results in progressions which are too short to be convincing, are very great in number and cannot be further classified, and that the most elementary intensity rules are violated.

The four progressions are sufficiently long and the data exact enough to obtain what should be fairly reliable values for the first anharmonic constants in the series formulas. These are analogous to the $x_e\omega_e$ constant of diatomic molecules. The most noteworthy fact about them are

[17] R. S. Mulliken, J. Chem. Phys. 1, 494 (1933).

[18] The objection may be made following Dixon's discussion that the other frequencies exist in the excited states, and are unstable, and that after light absorption of ν_1, ammonia goes over into one of the other frequencies and dissociates. It would appear that this would lead to a continuous or a least a predissociation spectrum in all the states, neither of which is observed except in part of the first state. The cause of the predissociation in this state may be found elsewhere, probably in an additional repulsive level with which the normal state does not combine optically.

that they are all negative[19] and increase with increasing electronic excitation. The constant seems to change sign after the fourteenth member of series I and after the tenth member of series II, but there are too few bands and these have too low intensities to determine a new slope of the $E(v'+1)-E(v')/n$ curves. No determination of the spectroscopic heat of dissociation is therefore possible here.

It was first thought that series II was a continuation of series I, since the last member of series I is separated from the first member of series II by 927 cm^{-1}. The predissociation would then cease abruptly at $v=14$ in the combined series. The main reason for rejecting this idea was because of the quite different slopes of the first difference/n curves for the bands in series I and II making it impossible to find a formula to fit the combined series. The problem of finding an explanation for the two intensity maxima in the combined series also could not be solved.

Another general experimental fact which seems rather important concerns the intensities in the progressions. The maximum of intensity in series I occurs at $v=7$–9, in series II at $v=7$ in series III at $v=8$ and in series IV at about the same value, although the continuous absorption is too strong here to get a reliable estimate. Application of the Franck-Condon principle here indicates that "r_e" is changed considerably in all the excited states relative to the normal state, but at least the first three electronic excited states, and probably the fourth have a similar "r_e". This quantity is to be regarded as depending on the height of the pyramid and at least one other dimension of the molecule, as the N−H or H−H distance.

With the rotational structure of the bands completely resolved in the excited states, and a satisfactory interpretation of this made, the dimensions of the molecule could be exactly calculated in these states from the changes in A and C. Differences in A and B might even be discovered. It would seem impossible to ever accomplish this in series I because of the predissociation. It would be impossible with present instruments in series III and IV because of the large wave number/distance ratio. Series II could be studied more completely from this standpoint with instruments of greater dispersion (our resolving power was most probably limited by the plates used). A discussion of rotational structure will be postponed until this is done.

The continuous absorption at the end of series IV suggests that decomposition would be produced directly by light absorption there, and we might expect from the character of the vibration that all three hydrogens would be split off simultaneously. It is to be noted that the energy becomes just large enough to do this in this part of the spectrum. Absorption to the second and higher excited states could be followed by return of the molecule to the first excited state, and it could decompose there due to the predissociation in that state. This process should be accompanied by fluorescence in the near ultraviolet and visible. This prediction will be tested experimentally.

[19] This is common in polyatomic molecules which have been studied from this standpoint. J. H. Clements, Phys. Rev. **47**, 224 (1935), H. C. Urey and H. Johnston, Phys. Rev. **38**, 2131 (1931).

The Infrared Absorption Spectrum of Silane

WENDELL B. STEWARD AND HARALD H. NIELSEN, *Mendenhall Laboratory of Physics, Ohio State University*

(Received April 15, 1935)

The spectrum of silane has been investigated to beyond 13.0μ. Bands, enumerated in the order of their intensities, were located at 11.0μ (910 cm^{-1}), 4.6μ (2183 cm^{-1}), 3.17μ (3153 cm^{-1}), 3.23μ (3095 cm^{-1}), 5.5μ (1820 cm^{-1}) and 2.3μ (4360 cm^{-1}). Four of these regions have been investigated under higher dispersion and partially resolved. The spectrum appears quite similar, except for certain details, to that of methane and by analogy the above bands have been identified as ν_4, ν_3, $\nu_1+\nu_4$, $\nu_3+\nu_4$, $2\nu_4$ and $2\nu_3$. From these values one may determine ν_1 which takes the value 2243 cm^{-1}. By the methods developed by Dennison and Johnston one may determine the moment of inertia which from the most probable value for the spacing between lines takes the value $I_0=8.9\times10^{-40}$ g cm^2.

INTRODUCTION

THE absorption by methane in the infrared has been extensively studied by a number of investigators.[1] Two very intense bands were measured by Cooley, each of which showed a very simple rotational structure. The data of Cooley have served as very convincing evidence that the methane molecule is a regular tetrahedron in shape with the hydrogens at the corners and the carbon atom at their center of gravity. As is well known such a model would have only two optically active vibration frequencies both of which are triply degenerate and both arising from what is essentially a vibration of the carbon atom in the field of the hydrogen atoms. Moreover, such a model should have an extremely simple rotational character since all of its principal moments of inertia would be alike. In fact, all the bands should be of the parallel type with a separation between lines equal to $\Delta\nu=h/4\pi^2I_0$ where h is Planck's constant and I_0 the moment of inertia. Cooley verified these general characteristics, but found that the spacing between lines in the two optically active fundamental bands was different, an effect which has been explained by Teller and Tisza[2] and more recently by Dennison and Johnston[3] as due to an interaction between rotation and vibration.

It has seemed very likely that the silane molecule would be very similar to that of methane and it was therefore thought of interest to investigate its spectrum, looking for many of the same details observed in the spectrum of methane. In an earlier communication[4] a preliminary report of this experiment was made. Four regions of absorption, enumerated in the order of their intensities were reported lying at wavelengths 10.5μ, 4.58μ, 3.187μ and 5.2μ. When compared with the spectrum of methane these were given the assignments ν_4, ν_3, $\nu_1+\nu_4$ or $\nu_3+\nu_4$ and $2\nu_4$, respectively, in the notation of Dennison. Three of these regions have since been studied under higher dispersion and have been at least partially resolved into fine structure. In addition a search for weaker bands has been carried out.

We are indebted to Professor Warren Johnson of the Chemistry Department of the University of Chicago for a quantity of silane gas free from impurities. Because of its violently explosive character, extreme caution had always to be exercised to keep the gas away from air or oxygen. Three cells of lengths 6 cm, 30 cm and 150 cm, all

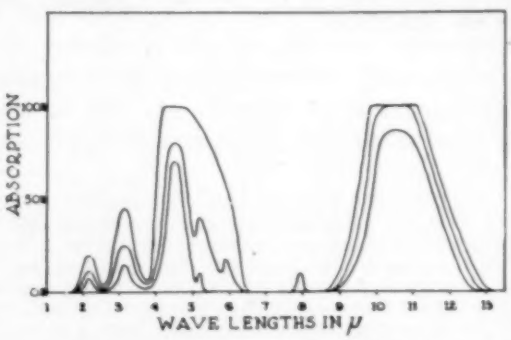

FIG. 1. Exploration curve made with a Wadsworth spectrometer and rocksalt prism.

[1] W. W. Coblentz, Publ. of Carnegie Inst., Washington, D. C. (1905); J. P. Cooley, Astrophys J. **62**, 73 (1925); J. Ellis, Proc. Nat. Acad. Sci. **13**, 202 (1927); A. Adel and V. M. Slipher, Phys. Rev. **46**, 902 (1934).

[2] Teller and Tisza, Zeits. f. Physik **73**, 791 (1932).

[3] D. M. Dennison and M. Johnston, Phys. Rev. **47**, 93 (1935).

[4] W. Steward and H. H. Nielsen, J. Chem. Phys. **2**, 712 (1934).

fitted with rocksalt windows were used in measuring various parts of the spectrum.

A prism exploration curve extending from 1.0μ to 13.0μ was first made before measurements with the diffraction gratings were begun. These were made with a Wadsworth spectrometer equipped with a rocksalt prism by using all three of the above-mentioned cells. The prism curve is reproduced in Fig. 1.

The grating spectrometer used was similar to that designed by Meyer and used by him and Barker and their collaborators at the University of Michigan. In this case a two-meter collimating mirror was used and for this experiment the spectrometer was equipped with two echellette gratings ruled by Wood at Johns Hopkins University, one with 3600 lines per inch for the 3.5μ region; the other with 800 lines per inch for the 10.0μ region. For recording purposes a vacuum thermocouple built by Dr. Norman Wright at the University of Michigan was used in conjunction with a Moll thermal relay and a Leeds and Northrup high sensitivity galvanometer.

Experimental Results

The 3.2μ region

This absorption region is made up of two badly overlapping bands. These bands, their centers lying at 3.17μ (3153 cm^{-1}) and 3.23μ (3095 cm^{-1}) appear to correspond to the absorption region in methane near 2.3μ observed by Cooley. These have been partly resolved into rotational structure, but it is difficult to observe any regularity in the line spacing because of the bad overlapping. For the band at 3153 cm^{-1} the spacing between lines is estimated to be 4.7 cm^{-1} while for that at 3095 cm^{-1} it appears to be about 9.7 cm^{-1}. The bands are both characterized by extremely broad Q branches converging toward lower frequencies. To make the absorption measurements in this region it was found most satisfactory to use the 30-cm cell. Measurements were made at intervals of 0.5 cm^{-1} along the band, the spectrometer slit here being about 0.6 cm^{-1}. The data were recorded in terms of galvanometer deflections instead of in percentage absorption for each circle setting. The procedure seemed justifiable since while the region does overlap with the 3.16μ region of atmospheric water-vapor absorption, the spectrometer box could be sufficiently well dried out to make the falsification completely negligible. In Fig. 2 is shown the absorption pattern of this region, and wavelengths and frequency positions of the principal lines, to which arbitrary numbers have been assigned, are recorded in Table I.

Table I. *Wavelengths and wave numbers of the principal lines in the 3.2μ absorption region of silane.*

No.	λ in μ	ν in cm^{-1}	No.	λ in μ	ν in cm^{-1}
1	3.4040	2937.7	18	3.2314	3094.6
2	3.3913	2948.7	19	3.2175	3108.0
	3.3901	2949.8	20	3.2123	3113.0
3	3.3802	2958.4	21	3.2050	3120.1
	3.3747	2963.2		3.2013	3123.7
4	3.3682	2968.9	22	3.1983	3126.7
5	3.3575	2978.4		3.1950	3129.9
	3.3546	2981.0	23	3.1920	3132.8
6	3.3470	2987.6		3.1886	3136.2
	3.3443	2990.2	24	3.1855	3139.2
	3.3364	2997.2		3.1823	3142.4
7	3.3344	2999.0	25	3.1796	3145.1
8	3.3250	3007.5	26	3.1716	3153.0
9	3.3150	3016.6	27	3.1637	3160.9
	3.3066	3024.3	28	3.1584	3166.2
10	3.3039	3026.7	29	3.1527	3171.9
	3.2981	3032.0		3.1496	3175.0
11	3.2946	3035.3	30	3.1444	3180.3
	3.2890	3040.4		3.1405	3184.2
12	3.2846	3044.5	31	3.1371	3187.7
13	3.2741	3054.3	32	3.1325	3192.4
	3.2707	3057.4		3.1305	3194.4
14	3.2663	3061.6	33	3.1257	3199.3
	3.2621	3065.5		3.1218	3203.3
	3.2593	3068.1	34	3.1185	3206.7
15	3.2554	3071.8		3.1157	3209.6
	3.2522	3074.8	35	3.1118	3213.6
16	3.2482	3078.6	36	3.1057	3219.9
17	3.2404	3086.0	37	3.0995	3226.3

The 4.5μ absorption region

The band at 4.5μ in silane is very intense and corresponds to the 3.3μ band in methane. This band has been resolved into a series of prominent lines on either side of a very broad Q branch which like those at 3.2μ converges toward lower frequencies. In general details this band resembles the corresponding one in the spectrum of methane, except that the lines are not single sharp lines, but groups of lines, too closely spaced for complete resolution, which appear to converge in the same direction as the Q branch. The principal peaks are separated by an average spacing of about 5.65 cm^{-1}. A cell 6 cm long filled with silane to a pressure of 6 cm of mercury was used. With the spectrometer slits set at 0.6 cm^{-1}, readings were taken at intervals along the band of 0.6 cm^{-1}

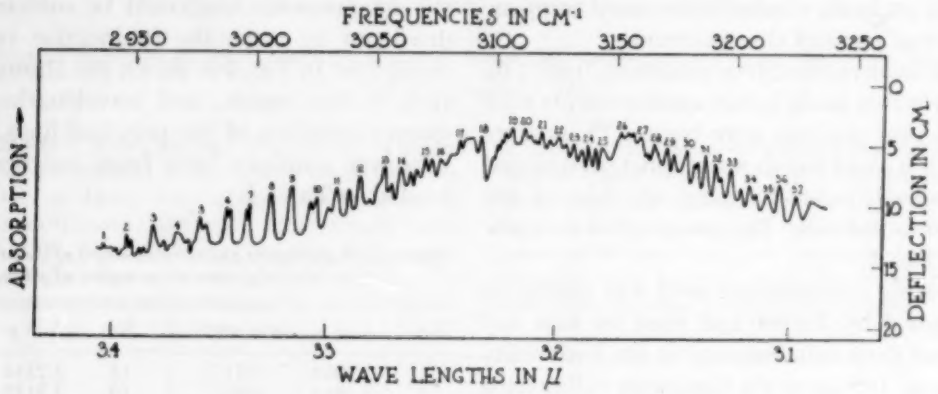

FIG. 2. Absorption pattern of silane in the 3.2μ region.

and as before galvanometer deflections only were recorded for each circle setting. The rapid falling off of deflections at the high frequency side of the band is due to the atmospheric absorption of carbon dioxide. The absorption pattern of this region is shown in Fig. 3 and wavelengths and frequency positions of the principal lines of the band, to which arbitrary numbers have been assigned, are given in Table II.

TABLE II. *Wavelengths and wave numbers of the principal lines in the 4.5μ absorption region of silane.*

No.	λ in μ	ν in cm^{-1}	No.	λ in μ	ν in cm^{-1}
−17	4.7982	2084.1	−5	4.6402	2155.1
	4.7940	2085.9		4.6342	2157.9
	4.7894	2087.9		4.6311	2159.3
−16	4.7844	2090.1	−4	4.6278	2160.8
	4.7809	2091.7		4.6227	2163.2
	3.7751	2094.2		4.6188	2165.1
−15	4.7706	2096.2	−3	4.6162	2166.3
	4.7681	2097.3		4.6097	2169.3
	4.7616	2100.1		4.6067	2170.8
−14	4.7578	2101.8	−4	4.6040	2172.0
	4.7552	2103.0		4.5950	2176.3
	4.7476	2106.3	2	4.5556	2195.1
−13	4.7436	2108.1	3	4.5440	2200.7
	4.7343	2112.2		4.5388	2203.2
−12	4.7302	2114.1	4	4.5323	2206.4
	4.7243	2116.7		4.5271	2208.9
	4.7205	2118.4	5	4.5214	2211.7
−11	4.7166	2120.2	6	4.5098	2217.4
	4.7115	2122.5	7	4.4987	2222.9
	4.7065	2124.7		4.4919	2226.2
−10	4.7038	2125.9	8	4.4877	2228.3
	4.6973	2128.9		4.4819	2231.2
	4.6929	2130.9	9	4.4767	2233.8
−9	4.6910	2131.7		4.4710	2236.6
	4.6845	2134.7	10	4.4658	2239.2
	4.6801	2136.7	11	4.4598	2242.3
−8	4.6780	2137.7	12	4.4555	2244.4
	4.6717	2140.5	13	4.4496	2247.4
	4.6677	2142.4	14	4.4451	2249.7
−7	4.6646	2143.8		4.4399	2252.3
	4.6587	2146.5	15	4.4353	2254.6
	4.6562	2147.7	16	4.4300	2257.3
−6	4.6523	2149.5			
	4.6459	2152.4			
	4.6433	2153.6			

The 10.5μ absorption region

This region also is an extremely intense one and the amount of gas used here was the same as for the 4.5μ region. With spectrometer slits of 0.7 cm^{-1} and 1.0 cm^{-1} for the high frequency and low frequency sides of the band, respectively, readings were taken along the band at intervals of 0.7 cm^{-1}. The absorption data as before were recorded in terms of galvanometer deflections and the absorption pattern of this region is shown in Fig. 4. This region corresponds to the 7.7μ region measured by Cooley in methane and in reality it resembles this region a great deal except that the rotational structure is more complex. In general the band is characterized by P and R branches and a Q branch of great intensity converging toward lower frequencies. A second absorption maximum is found near 10.2μ while yet a weaker peak (No. 1) is found near 12.0μ. These are thought to be due to centers of much weaker bands arising probably from transitions between higher vibration levels. This point should of course be further investigated and could readily be tested by remeasuring this region at much reduced temperatures. This band has only been partially resolved and the rotational structure appears to be quite irregular. This is probably due to overlapping with the other weaker bands at 10μ and 12.0μ, respectively, and perhaps also to some complex structure of each line as was observed at 4.5μ. An estimate of the

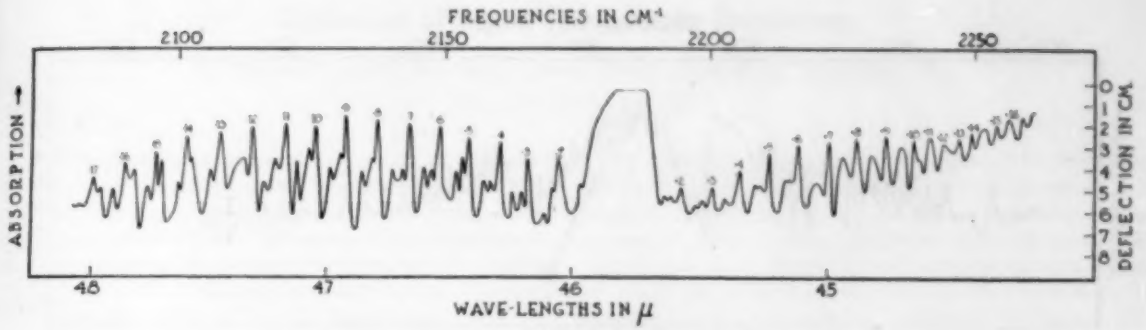

FIG. 3. Absorption pattern of silane in the 4.5μ region.

line spacing has been made from several lines near the center of the band and this leads to a value of about 3.5 cm^{-1}. Because of the irregularity of the absorption pattern, only the principal peaks, numbered quite arbitrarily, are given in Table III with their frequency and wavelength positions.

TABLE III. *The frequency and wavelength positions of the principal absorption peaks in the 10.5μ region of silane.*

No.	λ in μ	ν in cm^{-1}	No.	λ in μ	ν in cm^{-1}
	12.3721	808.3	23	10.5531	947.6
	12.3380	810.5		10.5274	949.9
	12.2246	814.7		10.5016	952.2
1	12.2189	818.4	24	10.4759	954.5
	12.1680	821.8		10.4502	956.9
	12.1339	824.1	25	10.4244	959.3
	12.1040	826.2		10.3987	961.7
2	12.0143	832.3		10.3730	964.0
3	11.9120	839.5	26	10.3562	965.6
4	11.8563	843.4	27	10.3215	968.8
	11.8270	845.5		10.2701	973.7
	11.8013	847.4		10.2449	976.1
5	11.7414	851.7	28	10.2186	978.6
6	11.6858	855.7	29	10.1761	982.7
	11.6565	857.9		10.1504	985.2
7	11.6391	859.2	30	10.1157	988.6
8	11.5793	863.6		10.0906	991.0
9	11.4979	869.7	31	10.0624	993.8
10	11.4512	873.3		10.0217	997.8
	11.4255	875.2		10.0002	1000.0
11	11.3740	879.2	32	9.9787	1002.1
	11.3399	881.8		9.9446	1005.6
12	11.3190	883.5	33	9.9099	1009.1
13	11.2801	886.2	34	9.8500	1015.2
14	11.2418	889.5	35	9.7818	1022.3
15	11.1951	893.2	36	9.7208	1028.7
16	11.0066	908.5	37	9.6568	1035.5
17	10.9384	914.2	38	9.5927	1042.5
18	10.9211	915.7		9.5664	1045.3
	10.8780	919.3	39	9.5323	1049.1
	10.8612	920.7	40	9.4725	1055.7
	10.8379	922.7	41	9.4120	1062.5
19	10.8188	924.3		9.3522	1069.3
	10.7966	926.2	42	9.3348	1071.3
	10.7673	928.7		9.3007	1075.2
20	10.7326	931.7		9.2487	1081.2
	10.6985	934.7	43	9.1882	1088.4
21	10.6596	938.1		9.1368	1094.5
	10.6129	942.2			
22	10.5872	944.5			

Discussion of experimental results

The writers desire here to make only a few general remarks concerning the interpretation of the observed bands. In general details the spectrum of silane is entirely like that of methane, a direct quantitative correspondence existing between the two. In silane, bands have been located at 2.3μ (4360 cm^{-1}), 3.17μ (3153 cm^{-1}), 3.23μ (3095 cm^{-1}), 4.6μ (2183 cm^{-1}), 5.25μ (1900 cm^{-1}) and 11.0μ (910 cm^{-1}). These correspond, respectively, to the regions at 1.80μ, 2.32μ, 2.37μ, 3.3μ, 3.9μ and 7.7μ in methane and by analogy have been designated as $2\nu_3$, $\nu_1+\nu_4$, $\nu_3+\nu_4$, ν_3, $2\nu_4$ and ν_4. This fixes the value of ν_1 as about 2243 cm^{-1}. In Table IV we summarize this assignment and give the approximate relative intensities.

It has earlier been pointed out that an essential difference exists between the 4.5μ band in silane and the corresponding 3.3μ band in methane in that each of the strong lines in silane is accom-

TABLE IV. *Summary of the assignment and relative intensities of the absorption bands of silane.*

Observed ν	Computed ν	Intensity	Identification
—	770 cm^{-1}	—	ν_2
910 cm^{-1}	—	50.0	ν_4
1260	1274	0.1	$\nu_3-\nu_4$
1680	—	—	$\nu_3+\nu_4$ (?)
1900	1820	0.1	$2\nu_4$
2183	—	20.0	ν_3
—	2243	—	ν_1
3095	—	1.0	$\nu_3+\nu_4$
3153	—	1.0	$\nu_1+\nu_4$
4360	—	.1	$2\nu_3$

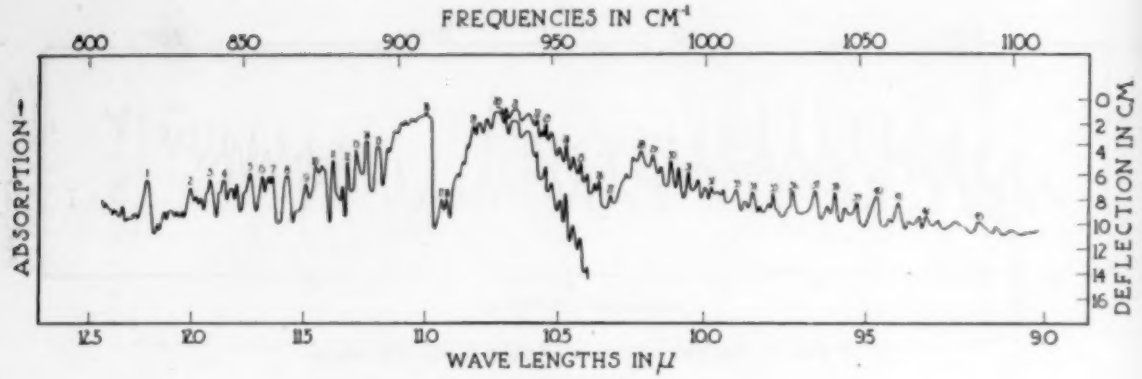

FIG. 4. Absorption pattern of silane in the 10.5μ region.

panied by satellites, while in the methane band each line is single. For this effect no adequate explanation is available. Certainly the other isotopes of silicon are too rare to account for these peaks. Each line occurs as a group of unresolved components which appear to converge in the same direction as the Q branch and it is suggested that the explanation of this satellite effect is in some way intimately associated with the convergence of the lines in the band. It is hoped to consider this point in more detail some time later when measurements on the spectrum of GeH_4 and new measurements on the bands in CH_4 under higher dispersion than previously, now under way in this laboratory, are completed.

If we interpret the two minor maxima in the long wavelength region as due to upper stage bands, then by knowing the spacings in the two bands it is possible, after the method of Dennison and Johnston, to compute the moment of inertia of the silane molecule. Taking the spacings in the 4.5μ band and the 11.0μ band to be 5.7 cm^{-1} and 3.5 cm^{-1}, respectively, we obtain, following Dennison and Johnston, the value for the moment of inertia $I_0 = 8.9 \times 10^{-40}$ g cm^2. This leads to a value of 2.31×10^{-8} for the distance between two hydrogen atoms, and a value of 1.54×10^{-8} for the distance between the silicon atom and a hydrogen atom.

In conclusion we desire to express our appreciation to Professor Warren C. Jonson of the University of Chicago for supplying us with the silane gas used in this experiment and to the National Research Council for a grant-in-aid. The donation of several pieces of optical sodium chloride by the International Salt Company of Scranton, Pennsylvania is acknowledged with gratitude.

Collisions of Alpha-Particles in Deuterium

E. POLLARD* AND H. MARGENAU, *Sloane Physics Laboratory, Yale University*

(Received April 12, 1935)

An investigation is made of the yields of deuterons emitted from deuterium under bombardment by alpha-particles from a polonium source. Three different but complementary experimental arrangements are employed: (1) The yield of deuterons projected forward is measured as a function of the alpha-particle velocity, the impinging alpha-particles being of nearly homogeneous velocity. (2) Absorption measurements are made on the deuterons projected forward by alpha-particles of all velocities up to the polonium limit. The results are found to agree with those of (1). (3) The yield of deuterons is measured as a function of the angle of projection for two different alpha-particle velocities.

To permit comparisons, similar experiments were made with ordinary hydrogen. As theoretical implications of this work may be mentioned: (1) Anomalous scattering begins at greater relative alpha-particle energies for deuterium than it does for hydrogen. Thus it is found that the radius at which the deuteron field becomes non-Coulombian is smaller than the corresponding radius for the proton. (2) An irregularity found in the deuteron yield for impinging alpha-particles of 2.6 MV. is interpreted as a resonance phenomenon. (3) The angular variation in the deuteron yield is of a nature not easily explained by Taylor's theory of scattering. This matter is discussed in some detail.

THE experimental basis of our knowledge of the field of force surrounding nuclei is largely derived from observations on the scattering of charged particles by the nuclear fields. Such observations have been made on the scattering of alpha-particles by hydrogen, helium and other light elements by various workers and in each case have given information about both the nature of the scattering process and the limits of the attractive nuclear field. Experiments on the scattering of alpha-particles by deuterium are of particular interest since any differences observed from the behavior in impacts with protons must be due to the additional neutron. At the same time there may exist nuclear resonance phenomena of the type first discussed by N. F. Mott[1] which would affect the nature of the scattering.

Experiments by Rutherford and Kempton[2] indicate a general similarity between the nuclear field of the deuteron and that of the proton. These authors point out, however, the desirability of further work on the question and suggest that more detailed investigations may bring to light differences in the scattering phenomena due to protons and deuterons. The present work exhibits such differences.

The scattering of alpha-particles in hydrogen was thoroughly investigated long ago by Chadwick and Bieler.[3] They determined the angular distribution of projected protons for alpha-particles of various velocities. In this paper we present similar data for projected deuterons, investigating their behavior in greater detail. In order to provide a certain basis of comparison we have repeated in part the work of Chadwick and Bieler on hydrogen, using an automatic method of counting instead of observing scintillations. The results are in substantial agreement with theirs.

From the yield of deuterons projected in a forward direction by alpha-particles of various energies the conclusion is drawn that the deviation of the nuclear field from the Coulomb type, which in the case of the proton occurs when the alpha-particle is about 4.6×10^{-13} cm from its center, takes place for the deuteron at the smaller distance of 3.2×10^{-13} cm.

The variation of proton yield with angle of projection provides an interesting test of present hypotheses of the nucleus. Taylor[4] has worked out a theory of this variation which assumes a proton potential of the usual crater type, and applied it to the results of Chadwick and Bieler. A similar analysis will be made in this paper for the results on deuterons, and it will be shown that, while for low velocities of the bombarding alpha-particles there is no violent disagreement between the experimental results and Taylor's

* Sterling Fellow.

[1] N. F. Mott, Proc. Roy. Soc. **A133**, 228 (1931).

[2] Lord Rutherford and A. E. Kempton, Proc. Roy. Soc. **A143**, 724 (1934).

[3] J. Chadwick and E. S. Bieler, Phil. Mag. **42**, 923 (1921).

[4] H. M. Taylor, Proc. Roy. Soc. **A136**, 605 (1932).

theory, the simple model of the nucleus breaks down when the alpha-particles have a greater speed.

It is not implausible to suppose that an alpha-particle and a deuteron can form a combination of temporary stability in the scattering process, since this would correspond to an energy state of the known nucleus ${}_3Li^6$. A similar combination of an alpha-particle and a proton, on the other hand, seems less likely because of the very high charge-to-mass ratio of the resulting structure. This implies that an alpha-particle and a deuteron can enter into what may be called a resonance interaction. Such resonance should have a definite effect upon scattering phenomena, an effect indeed for which a qualitative theory exists.[1] Its occurrence may be quite common, but is difficult to observe if the scattering nucleus is heavy, for the effect decreases with increasing mass. The deuteron presents a favorable chance of its observation since the effect itself is large and the projected nuclei have longer ranges and can therefore be counted with relative ease. A resonance interaction of this type has been found for alpha-particle energies of 2.6 MV.

Experiments on the Forward Projection of H and D Nuclei

1. Scattering of alpha-particles by a Coulomb field

The early experiments of Rutherford showed that if alpha-particles fall on scattering nuclei of medium or high atomic number they suffer deflection according to the Rutherford-Darwin relation. This formula is derived by classical dynamics on the hypothesis that the nuclei repel the alpha-particles according to the inverse square law. The formula is unaltered if derived by wave-mechanical theory providing the field is strictly Coulombian for the energies of the alpha-particles used. Later experiments on the deflection of alpha-particles by nuclei of low charge showed that the Rutherford-Darwin law does not hold for close collisions. Thus it is concluded that for these collisions the inverse square law ceases to hold. Accordingly a determination of the least energy of alpha-particles which, for direct collisions, cease to be deflected as expected by the formula, gives some measure of the distance at which the *attractive* field of the nucleus becomes effective.

In the case of collisions with hydrogen nuclei it is very much easier to observe the projected nuclei than the deflected alpha-particles since their greater range renders them easily detectable. The theory of the projection of such nuclei has been worked out by Darwin, who shows that the number of nuclei projected per second into a given solid angle at an angle θ to the direction of the incident alpha-particle is

$$n = A/V^4(1/M+1/m)^2 \sec^3\theta. \qquad (1)$$

A is a constant for a fixed arrangement of target and source.
M, V are the mass and velocity of alpha-particle.
m is the mass of the nucleus.

It follows that the total number projected within a cone of half-angle θ about the direction of the alpha-rays is

$$F = (A\pi/V^4)(1/M+1/m)^2 \tan^2\theta. \qquad (2)$$

Then providing the angle θ does not vary, a test of this relation can be made by determining either n or F for different incident particle velocities. Both n and F should diminish rapidly with increasing velocity by reason of the $1/V^4$ factor. If we consider the *range* of the impinging particle the diminution of yield with increasing range is less rapid, being approximately proportional to $R^{-4/3}$. While in experiments on variation of yield with angle of projection, to be described later, the quantity n was observed, it is more convenient for the present purpose to determine F.

Our experimental arrangement therefore was constructed to allow a determination of the number of hydrogen or deuterium nuclei projected within a constant angle for varying ranges of the incident alpha-particle. Since the nuclei are projected approximately in the direction of the impinging alpha-particles we speak of "forwards projection."

2. Arrangement of apparatus

The general arrangement of apparatus can be seen from Fig. 1. A is the alpha-particle source, of polonium deposited on a silver disk of 1 cm diameter and of strength about 20 millicuries. A test showed that the spread of alpha-particle

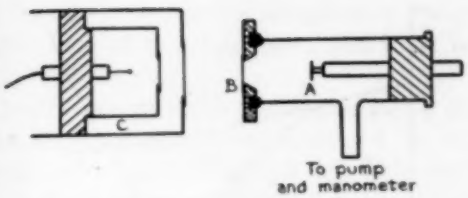

FIG. 1. Diagram of apparatus used in experiments on forward projection.

ranges did not exceed 0.3 cm. B is the target of hydrogen or deuterium. This was deposited on a foil of aluminum of air equivalent, in some cases, 0.9 cm, in others 2.2 cm, which was waxed over a number of holes situated in a circle of about 1.6 cm diameter. Both larger and smaller apertures were used, and also a small zone in which the holes were confined to the space between circles of 0.7 cm and 1.4 cm diameter. For layers of hydrogen we used either powdered $Ca(OH)_2$ deposited from an alcohol suspension or a thin film of vaseline. For deuterium we used $Ca(OD)_2$ shaken up with CCl_4 and painted over the aluminum. The $Ca(OD)_2$ proved more difficult to obtain in thin layers than the $Ca(OH)_2$—probably because of a trace of metallic calcium left in after its preparation. We found, by weighing, that the $Ca(OD)_2$ layers varied in average thickness from 0.2 cm to 0.6 cm air equivalent. The uniformity was poor but in the thinner layers the total spread in the range of the incident particles could not be very large. Since there is danger that $Ca(OD)_2$ can change into $Ca(OH)_2$ if moisture is present, we used a fresh layer every few days. That a layer is stable for a period of days was directly shown in magnetic deflection experiments. In order to prevent the $Ca(OD)_2$ powder from dropping off or being blown off while the pressure in the space AB was changed, the layer was covered with either a thin gold or aluminum leaf. Blank experiments showed that the yield of disintegration products from aluminum was negligible compared to that of the projected hydrogen nuclei.

The projected nuclei produced in the target were counted by the proportional Geiger counter C of the form described by Pollard and Eaton.[5] The aperture of C was of diameter 1 cm in some experiments and 0.6 cm in others, according to the degree of angular definition required. The distance AB was varied about 4 cm; BC about 2.5 cm. By introducing known pressures of oxygen into the space AB the range of the alpha-particles impinging on the target could be changed slowly and the corresponding yield of projected nuclei counted. The distance BC and the angle subtended by the aperture B at the counter were carefully chosen to enable the detection of the projected nuclei at as small ranges as possible. The main difficulty encountered in verifying the Rutherford-Darwin formula is in detecting the recoil nuclei at such low energies. Where the formula holds the ranges of the recoil protons or deuterons are (for forwards projection) about 6 cm and fall off rapidly in range (proportionally to $\cos^3\theta$) for angles greater than 20°. The shortest recoil range that can reach the counter is about 4 cm. If wide apertures permitting large angles between the alpha-particle and the recoil nucleus are used it is inevitable that at low alpha-particle energies a proportion of the protons or deuterons do not reach the counter. Our mean angle was in general not greater than 20°, which means that the exact shape of the curves for alpha-particle ranges less than 1.4 cm (for protons) or 1.2 cm (for deuterons) is uncertain.

In counting the particles we used mainly a method of photographic recording of an oscillograph trace. Counting by a relay and impulse counter is somewhat uncertain for low alpha-particle energies since the particles entering the counter opening are of differing ranges and so produce deflections of differing sizes.

3. Experimental results

The first experiments were made on recoil protons and were intended to enable investigation of the range of incident alpha-particles at which the falling yield of recoil protons expected from the Rutherford-Darwin formula gives way to the rising yield due to anomalous scattering. In Fig. 2 the results of one such experiment (made with a target in the form of an annulus) are given. It will be seen that the yield curve turns upward at an alpha-particle range of 1.75 cm. This is in good agreement with the values found by Chadwick and Bieler, which do not,

[5] E. Pollard and W. W. Eaton, Phys. Rev. **47**, 597 (1935).

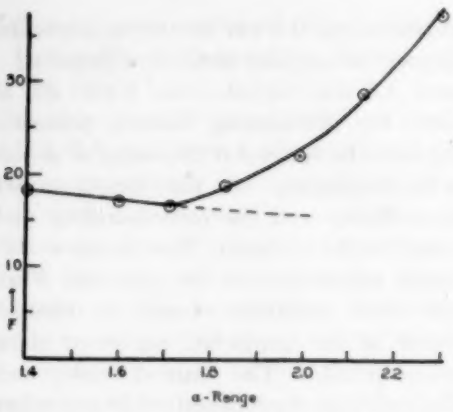

FIG. 2. Yield of protons per minute *vs.* alpha-particle range in cm air equivalent. Broken line represents classical yield (Eq. (2)).

however, fix this minimum so definitely. The yield curve for low energies follows, at least approximately, the Rutherford-Darwin formula. Taylor[4] has used the results of Chadwick and Bieler to derive the radius of the potential well used to explain the anomalous scattering. His results show that this radius is very nearly equal to the distance of closest approach for which the classical theory first ceases to hold. We can make an estimate of the radius of the potential well by calculating the distance of closest approach corresponding to an alpha-particle of range 1.75 cm. The value found is 4.6×10^{-13} *cm*. The ranges are correct to 0.05 cm.

The results of a similar experiment on a layer of $Ca(OD)_2$ are shown in Fig. 3. Here the target was contained within a circular hole. It will be seen that there is a rapid drop between 1.15 and 1.35 cm followed by a rather more rapid rise than observed for protons. In this run a special attempt was made to detect the recoil deuterons of low energy: their behavior appears to be classical in the region 1.0 to 1.15 cm though we do not wish to assert this positively. The absolute value at the minimum is so low that it seems certain that there is a drop below the expected classical value before the rising yield begins. In Fig. 4 a curve is given for rather higher ranges. It gives the yield from a small central opening, and shows that the yield rises to a maximum at 1.6 cm range, falling from there to 1.7 cm and rising smoothly afterward. This curve represents the results of a total of five runs on different

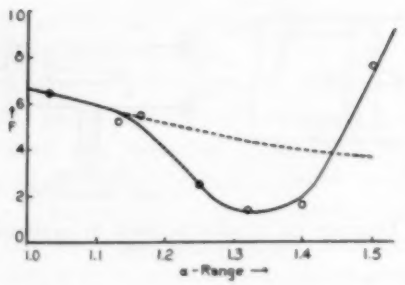

FIG. 3. Yield of deuterons per minute *vs.* alpha-particle range in cm air equivalent. Broken line represents classical yield (Eq. (2)).

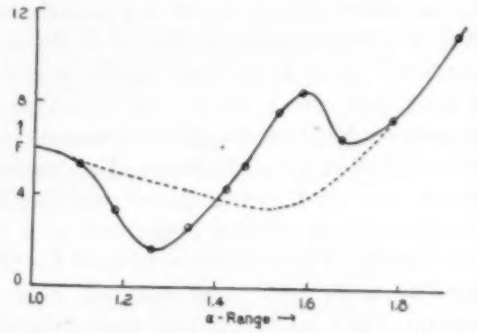

FIG. 4. Yield of deuterons per minute *vs.* alpha-particle range in cm air equivalent. Broken line represents probable trend if resonance were absent.

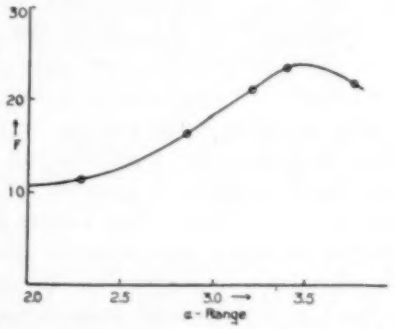

FIG. 5. Yield of deuterons per minute *vs.* alpha-particle range in cm air equivalent.

occasions with different layers of $Ca(OD)_2$. Because of the uncertainty in the thickness of the layer the alpha-particle ranges cannot be relied on to much better than 0.1 cm. A curve similar to this, but taken with a somewhat thicker layer and therefore less accurate, was published before.[6]

[6] A preliminary account of this experiment with this explanation has been given. Nature **135**, 393 (1935); Phys. Rev. **47**, 571 (1935).

In that account there is also given a comparison curve for ordinary hydrogen, which we are not here reproducing.

In Fig. 5 a curve for higher energies is plotted. This shows a steady rise up to 3.4 cm incident range, after which there is a fall. This maximum is not so definitely established as the earlier one. Experiments with higher energy alpha-particles will be needed to determine its precise nature.

4. Discussion of these results

If one supposes the mutual potential of the alpha-particle and the hydrogen nucleus to be of the crater type the expected features of scattering yields are as follows: first, a fall according to the classical theory for low energies, second, a rise as the intensity of the wavelet scattered from the inside of the crater increases. This supposes there are no critical energy levels. It is known, however, from experiments in which heavier nuclei are disintegrated that such critical energy levels for which the intensity of the wave function inside the nucleus is abnormally high do exist. Such levels should influence the scattering of alpha-particles even if there is no disintegration. Mott[1] has calculated the ratio of expected to classical scattering at energies near such a resonance level. He finds for this ratio, calculated for a scattering angle of 180°:

$$R=(1-\beta \sin 2P)^2+\beta^2(1-\cos 2P)^2. \qquad (3)$$

Here $\beta=137v/2Zc$ where v is the velocity of the incident alpha-particle and P is a phase angle which usually increases by π as v passes across the region of resonance. Z is the atomic number. An examination of formula (3) shows that for Z greater than about 4 and ordinary alpha-particle velocities R takes the form of a dip followed by a greater rise and a fall to unity. For aluminum, for instance, the greatest value of R is about 1.5.

In the case of very light elements formula (3) presents a different appearance. The dip is then absent, and the rise is considerably greater. The drop to unity, predicted by (3), is dependent upon the assumption that P increases to π, which means that there are no further deviations from classical behavior for greater velocities. If penetration occurs even within the resonance region, as it clearly does for elements of small atomic number, R will not return to unity but the yield will gradually merge into the general rise characteristic of anomalous scattering due to penetration. This obvious deviation from Mott's theory is also apparent in the experiments on disintegration of Be and B by resonance.

Formula (3) refers to resonance scattering by a state of zero angular momentum and does not purport to describe the general phenomenon of resonance scattering in a quantitative way, but it will serve us as a guide. The sharp drop at 1.15 cm range seen in Fig. 3 followed by the rise to a maximum at 1.6 cm seen in Fig. 4 has the general features associated with *resonance scattering*. We suggest that the region 1.15 – 1.7 cm corresponds to the band of energies grouped around an energy level of the composite nucleus ${}_5Li^6$. The fact that the yield does not fall to the classical value is due to the circumstance that penetration occurs independently of the resonance process as just noted.[6] The mean energy of the alpha-particles causing resonance is 2.6 MEV. In our previous publication we have stated the value 3.1 MEV. This discrepancy is due to the fact that we have there taken as the range corresponding to resonance that associated with the *maximum* of the yield curve.

The occurrence of this resonance phenomenon renders it difficult to determine the minimum at which the anomalous scattering due to the non-Coulombian field begins to be superposed on the classical scattering. If we take the minimum as experimentally found at 1.3 cm alpha-particle range, the corresponding distance of closest approach, is 3.4×10^{-13} *cm:* while if we estimate, from the trend of the rise after 1.7 cm range, that but for resonance the classical law would hold as far as 1.5 cm range we find 3.0×10^{-13} *cm.* The latter is more probably the true value. In arriving at these figures, account has been taken of the greater mass of the deuteron, in consequence of which an alpha-particle of a given energy approaches more closely to the deuteron than the proton. In either event it is seen that the radius at which normal penetration into the nucleus begins is *definitely less for deuteron-alpha-particle interaction than for proton-alpha-particle interaction.* The smaller radius for the deuteron field is more in accordance with the fields existing between heavier elements and alpha-particles. This may be linked with the fact that in heavier

nuclei, as in the deuteron, there is roughly an equal number of neutrons and protons while the proton itself is in this sense abnormal. The abnormality of proton fields has been pointed out by Cockroft at the London Conference and is discussed by Pollard.[7]

Experiment on Absorption of Projected Protons

To place the position of the minima in Figs. 2, 3 and 4 beyond doubt, another independent experiment on the absorption of the projected protons was made. For this purpose the tube was filled, first with H_2, then with D_2 at atmospheric pressure, and the source was pulled back sufficiently far so that no alpha-particles would reach C. Various absorbing foils of aluminum were placed between B and C, and the number of protons or deuterons passing through was counted by the method employed before. The deuterium used in this experiment was obtained from 98 percent heavy water by the reaction: $Ca+2D_2O \rightarrow Ca(OD)_2+D_2$.

If now one plots the yield of particles against air equivalent of the absorption in the path of the projected protons one obtains curves which will here be called integral curves and which are related to those of Figs. 2, 3, 4 as follows: Suppose that we integrate the yield curve of Fig. 2 from right to left, beginning at some extreme value of the range R_0 and stopping at some variable smaller value R. The ordinates of the integral curve are then the areas thus obtained, subtracted from the total area to the left of R_0; the abscissae of the integral curve are the corresponding values of R_0-R, but on an extended scale. Thus there should be associated with a minimum of the previous yield curves a flattening of the integral curves.

This is seen to be the case in Fig. 6 which represents the data obtained. By extra absorption is meant the air equivalent thickness of the aluminum foils, exclusive of the absorption which occurs in the gas and in the closing foil. The flattening on the deuteron curve appears to the left of the flattening on the proton curve, which shows definitely that the deuteron minimum lies at a smaller alpha-particle range. The distance

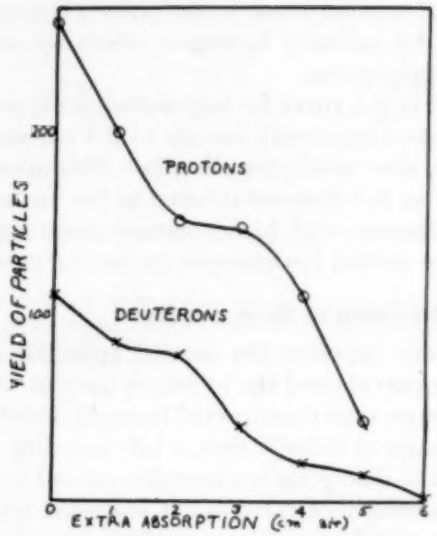

Fig. 6. Yield of particles per minute *vs.* absorption, exclusive of gas, in the path of the particles.

along the abscissae between the flatter portions of the two curves, $\Delta A'$ is about 1 cm.

It is possible even to get a numerical estimate of the distance between minima on the yield curves from the quantity $\Delta A'$ as found from Fig. 6. For it can be shown (cf. Appendix) that

$$\Delta A' = 3.2R_P' - 3.6R_D' + \Delta R_0 \qquad (4)$$

approximately, where R_P' and R_D' are, respectively, the alpha-particle ranges at which the minima on the yield curves for protons and for deuterons occur; ΔR_0 is the difference of the maximum alpha-particle range in H_2 and in D_2. But Rutherford and Kempton[8] have found these to be equal, so that $\Delta R_0 = 0$. Hence, if we assume that $R_P' = 1.8$ cm, formula (4) gives for R_D' the value 1.3 cm, which is in very good agreement with our previous results.

An experiment similar to the one described in this section, but for hydrogen only, has also been reported by Pose and Diebner.[8] Instead of hydrogen gas they use a paraffin layer, which has certain advantages over the method here required for comparison with the deuterium results. They find two flat portions on the integral curve, and correspondingly deduce two minima on the yield curve. Neither of these minima agrees well with

[7] E. Pollard, Phys. Rev. **47**, 611 (1935).

[8] H. Pose and K. Diebner, Zeits. f. Physik **90**, 773 (1934); see also E. Frank, Zeits. f. Physik **90**, 764 (1934).

the one in our curves as to position on the alpha-range scale. We consider it by no means impossible that there exist irregularities in the proton yield curves at higher energies than those here investigated and are continuing our measurements in that region; but we have found no minimum at an alpha-particle range of about 2.3 cm, where one reported by Pose and Diebner should have occurred.

Experiments on the Projection at Varying Angles

A simple test of the current theory of anomalous scattering is afforded by investigating the variation of yield with the angle between the projected nucleus and the incident alpha-particle. In order to carry this out we used apparatus as illustrated in Fig. 7. This shows the view from above. *A* is a small brass pillar supporting the source, *B* is an arm rotating about a pin at *C*. *D* is the target, supported on an aluminum foil of 2.2 cm air equivalent, and kept in place by a thin aluminum leaf. *E* is the counter. The scale of the diagram is indicated. The rotating arm was firmly fixed to a pointer on the outside of the enclosing brass box and the angular setting could be read off on a metal scale. The opening at the target was a single hole of 0.7 cm diameter and the counter was placed 3.5 cm from the opening in most of the experiments. The pin attaching the arm to the pointer was surrounded thickly with tap grease and the enclosing box evacuated. If the pump is kept running the vacuum can be held while the arm *B* is rotated. The distance *AC* was 4.5 cm. With this arrangement our maximum angular spread was 20°, our mean spread 10°.

In order to avoid uncertainties in connection with the zero-setting of the apparatus, readings were taken alternately to the left and to the right of the zero scale position. When the readings were plotted the peak of the yield curve was slightly displaced from the scale zero. The position of the peak was then chosen as the zero angle.

In Fig. 8 the yield of deuterons is plotted against θ, the angle which the projected deuterons make with the direction of the incident alpha-particles. The upper curve refers to an energy of 5.2 MEV. corresponding to a residual alpha-range of 3.7 cm. Beyond 25° the yield drops strongly. We feel that from there on the experimental points are somewhat uncertain because of the spread in θ. For the range of the deuterons decreases with increasing θ, and at a mean angle of 25° the particles projected at extreme angles begin to stop short of the counter. A reasonable correction based on the geometry of the apparatus would raise the points, but not enough to justify the supposition that the curve swings into a classical course at this angle. For the lower curve of Fig. 8 the alpha-particle energy is 3.3 MEV, the range 1.9 cm. Here, also, we have taken observations with the same apparatus on protons, but for only one energy, and the yield curve is reproduced in the figure.

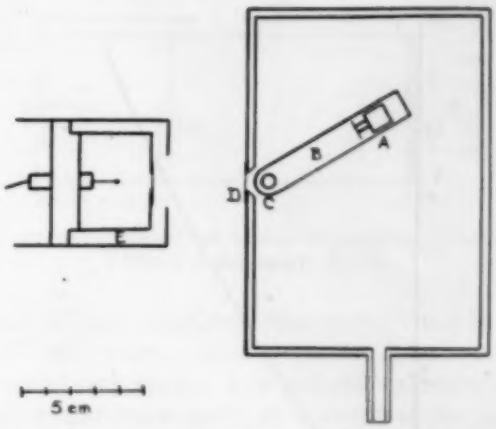

Fig. 7. Diagram of apparatus used in experiments on projection at different angles.

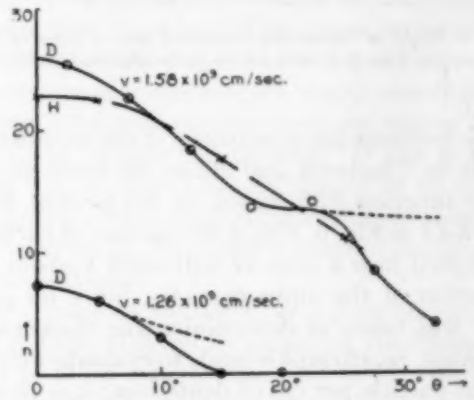

Fig. 8. Yield of deuterons (continuous), or protons (broken line), per minute *vs.* average angle of projection. *v* refers to velocity of alpha-particles. Dashed lines represent estimates of true curves, allowing for stoppage at extreme angles.

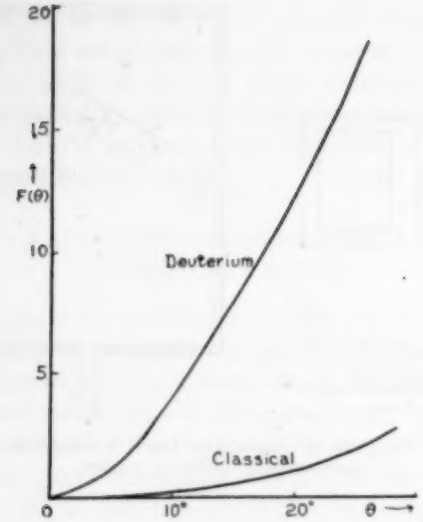

FIG. 9. Yield of deuterons projected into a cone of half-angle θ *vs.* θ. Lower curve is the classical yield.

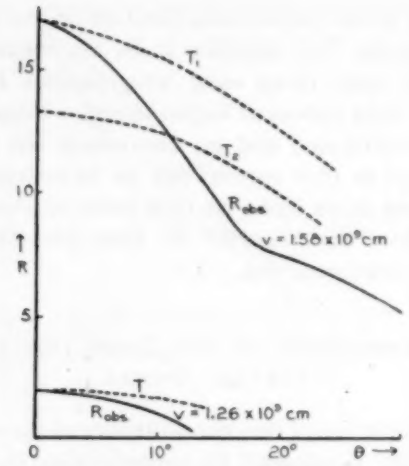

FIG. 10. Ratio of observed to classical yield *vs.* angle of projection. T_1 and T_2 are curves based on Taylor's theory.

To facilitate the comparison of our results with those of Chadwick and Bieler we have plotted their function $F(\theta)$, based on the present data, against θ in Fig. 9. $F(\theta)$ is the number of particles projected into a cone of half-angle θ about the direction of the alpha-particles. Since no great care was taken in determining the thickness of the films, no attempt is made to evaluate $F(\theta)$ per alpha-particle per cm of deuterium; it is plotted in arbitrary units. But the classical curve has been adjusted to the same scale as the deuterium curve. The hydrogen curve on this diagram is almost indistinguishable from the deuterium curve and has not been drawn.[9] It is in good agreement with Chadwick and Bieler's data, falling, as it does, somewhere between their 2.9 cm and 4.3 cm alpha-range curve.

Our results may be considered in the light of Taylor's[4] theory of scattering. He shows that if one assumes the alpha-particle wave scattered by the anomalous field of the nucleus to be spherical, the yield of protons can be expressed in terms of a quantity K_0 which, physically, refers to the phase by which the wave in a Coulomb field must be displaced toward the origin of the field in order to fit it smoothly to the wave inside the well. The assumption of a spherical wave is largely justified for the example at hand since even with the highest alpha-particle energy here used the nuclear obstacle is considerably smaller than the length of the incident alpha-waves. The former is about 3×10^{-13} cm, the latter 18.5×10^{-13} cm.

For the ratio R of observed to classical yields at various angles of projection θ Taylor finds

$$R=|e^{(-i/\gamma)\log\cos^2\theta}+i\gamma\cos^2\theta(e^{2iK_0}-1)|^2,$$

where $\gamma=hv/4\pi e^2$. (5)

Given a nuclear model, K_0 is a calculable function of the alpha-particle velocity v, but not of θ.

To find R from the experimental data the classical yield under the same conditions had to be determined. This was done by measuring the yield, at one particular angle and with the same arrangement, for alpha-particle energies low enough so that the scattering would be classical. Then, to compute the variation in angle of classical scattering Eq. (1) was used. The resulting R is plotted in Fig. 10.

If K_0 in (5) is adjusted so that R agrees with our data at $\theta=0°$, the value of K_0 is 41.5°. For greater angles, the theory then predicts the dotted curve T_1. This does not drop sharply enough to be in accord with experiment. Adjustment at $\theta=0$ can also be made by choosing K_0 to be $-26°$, but then the theoretical curve drops even less sharply. There are no other values of K_0

[9] It is evident that this way of plotting the data obscures the detailed character of the yield curves at small angles. Conversely, if yield curves are to be derived from Fig. 9, the procedure would entail very considerable uncertainties.

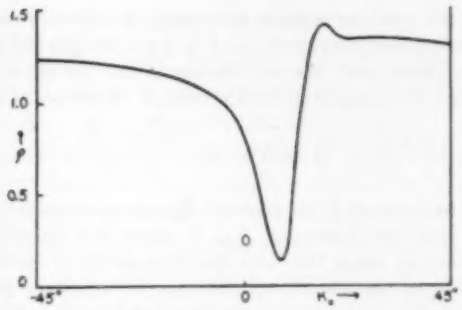

FIG. 11. $\rho = R(0°)/R(20°)$ from Taylor's theory for different values of K_0. v is taken to be 1.58×10^9 cm/sec. to agree with the experimental case.

which produce a fit at 0°. Attempts of fitting the curves at other angles (curve T_2) do not improve matters. The lower curve is explained somewhat better by Taylor's theory, but again the theoretical curve T falls less rapidly than the experimental one. In this case, $K_0 \sim 37.5°$. Agreement becomes better for smaller alpha-particle energies, as might be expected.

This test of the theory may not be entirely conclusive, since it depends quite essentially upon an accurate knowledge of the classical yield under the same circumstances, which, because of experimental difficulties, is known less well than the actual yield. To avoid this uncertainty we may proceed as follows.

The ratio R_0/R_{20}, where R_0 is observed divided by classical yield at $\theta = 0$ and R_{20} the same quantity for $\theta = 20°$, is independent of the classical yield except for a factor in θ. It is known from our experiments with considerable accuracy and has the value 2.2 for an alpha-particle velocity $v = 1.58 \times 10^9$ cm/sec. If we calculate R_0/R_{20} from Taylor's theory for this velocity but varying K_0, we obtain a function which is graphically shown in Fig. 11. Between 45° and 135° there is a monotone decrease in the ratio which causes the ends of the curve shown to join. It will be seen that R_0/R_{20} is confined to values lower than 1.5, and hence can never reach the experimental value. We feel this to be a rather definite contradiction between Taylor's theory and our data, and one which is not likely to be removed by merely including parameters K_1, K_2, etc., to take account of waves of finite angular momentum, but still maintaining a spherically symmetrical potential distribution. We regard it as more probable that the model of a fixed

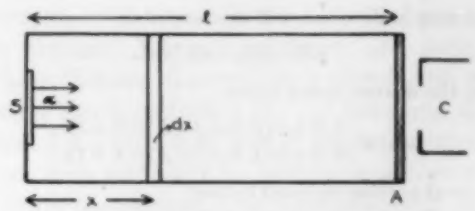

FIG. 12. Arrangement of source of particles, absorbing material and counting device.

potential hole is at fault. Margenau,[10] and Breit and Yost[11] have discussed similar instances of failure of such models. It is well also to remember in this connection that, as a result of the spin and the magnetic moment of the deuteron, its field may not be spherically symmetrical. The range of the asymmetries would undoubtedly be greater than the extent of the usual nuclear hole. In that case the neglect of scattered waves of greater angular momentum would constitute a serious error and the theory in its simple form could not be expected to hold. It can be seen from Fig. 8 that Taylor's theory is in better agreement with the results for hydrogen, although the value of R_0/R_{20} is still somewhat outside the theoretical limit.

In conclusion we desire to express our thanks to Dr. L. R. Hafstad for preparing the Po-source used in these experiments, and to Dr. Burnam and Dr. West for providing the radon tubes from which the source was made. We also benefited by the continued interest shown by Professor Kovarik in this work.

APPENDIX

Derivation of formula

Let the source of alpha-particles be at S. (cf. Fig. 12.) The particles projected forward have their origins throughout the gas between S and A, A being the absorbing foil. (We shall consider only particles which are projected forward.) The question is: How many particles will be measured by the counting device C as the absorbing thickness A is varied?

Let $f(R)$ be the number of particles shot forth from a slab of gas of thickness 1 cm air equivalent, by alpha-particles of residual range R cm. The range of the projected particles is nearly proportional to R; we shall suppose it to be KR. The number of particles dN which originate in the layer dx will be $dN' = f(R_0 - x)dx$, if R_0 is the total range of the alpha-particles. They will be measured if $K(R_0 - x) > l - x + A$, otherwise not. Hence the number of particles

[10] H. Margenau, Phys. Rev. **46**, 613 (1934).
[11] G. Breit and F. L. Yost, Phys. Rev. **47**, 608 (1935).

originating in dx which will be counted is

$$dN=f(R_0-x)\lambda(x)dx$$

where the discontinuous factor

$$\lambda(x)=\begin{cases}1 \text{ if } x<(KR_0-l-A)/(K-1)\\ 0 \text{ if } x\geqq(KR_0-l-A)/(K-1).\end{cases}$$

The total number counted is then

$$N=\int_0^l f(R_0-x)\lambda(x)dx=\int_0^{(KR_0-l-A)/(K-1)} f(R_0-x)dx.$$

From this expression it follows at once that

$$dN/dA=-f\left[\frac{(l+A-R_0)}{(K-1)}\right]\Big/(K-1).$$

This expression is a maximum when f is a minimum, let us say for the value $f(R')$. R' is the value of the range at which the yield curve has a minimum, i.e., the value which was determined previously (cf. Fig. 2 for protons and Figs. 3–5 for deuterons). We see, therefore, that the value of A for which the integral curve is flattest, A', is related to R' by

$$f\left(\frac{l+A'-R_0}{K-1}\right)=f(R'), \quad \text{or} \quad \frac{l+A'-R_0}{K-1}=R'.$$

Now the value of K for protons, K_P, is approximately 4.2, while that for deuterons, K_D, is about 4.6, as may be computed by using the facts that momentum is conserved in the alpha-particle impact and that, for equal energies, a deuteron has nearly twice the range of a proton. We are thus led to the formula

$$\Delta A'=A_p'-A_D'=(K_p-1)R_p'-(K_D-1)R_D'+\Delta R_0$$

which was used in the text of this paper.

JUNE 1, 1935 PHYSICAL REVIEW VOLUME 47

Spectral Characteristics of Electrically Exploded Mercury

H. P. KNAUSS AND A. L. BRYAN, *Mendenhall Laboratory of Physics, Ohio State University*

(Received April 1, 1935)

The spectrum obtained by sending 300 amp. from a 150-volt generator through a small stream of mercury is found to be characterized by great broadening of many of the lines, and by a strong continuous background. In the region between 2537 and 1950A, the continuous emission is strong enough, and sufficiently clear of emission lines, to be useful for absorption experiments. The continuous emission is ascribed to recombinations in which the kinetic energy plays a part, and the broadening of lines is ascribed to the strong electric fields of ions near the emitting atom.

INTRODUCTION

THE spectra obtained by allowing a condenser charged to a high potential to discharge through fine wires were studied by Anderson[1, 2] and his colleagues. They obtained spectra characteristic of metallic vapors at very high temperatures. The character of the spectrum was observed to change quickly from continuous emission, to the spark spectrum, and then the arc spectrum of the metal. By confining the explosion to a small volume, the absorption spectrum of the metal was obtained. The spectra, both emission and absorption, extended far into the ultraviolet, because of the high temperatures developed.

A modified form of this source of light was adopted by Mott-Smith and Locher[3] to illuminate a Wilson cloud chamber, taking advantage of the high intrinsic brilliancy and the short duration of the light; however, instead of employing a high voltage condenser discharge, they used a very high current obtained by connecting a 150-volt storage battery of very low internal resistance directly across a tiny stream of mercury which served instead of a fine wire. A commutator arrangement was used to permit the current to flow for a very short time at the instant when the photograph of the cloud chamber tracks was desired.[4]

The present investigation was undertaken to see whether the spectrum obtained by the "explosion" of mercury includes a region of continuous emission suitable for use in absorption experiments, with particular reference to the region between 2500 and 1850A, in which quartz prisms provide good dispersion.

[1] J. A. Anderson, Astrophys. J. **51**, 37 (1920).
[2] Anderson and Smith, Astrophys. J. **64**, 295 (1926).
[3] Mott-Smith and Locher, Phys. Rev. **38**, 1399 (1931).

[4] The authors acknowledge with thanks the information and suggestions given them by Dr. Locher personally.

Experimental Procedure

The energy for exciting the mercury was obtained from a motor-generator capable of delivering 300 amperes at 150 volts. A magnetically operated switch was used to close the circuit momentarily through a threadlike stream of mercury. A bank of "dry electrolytic" condensers was put in parallel with the line side of the switch in order to help the initial current to build up rapidly.

The mercury stream was formed by allowing the liquid to flow under a head of about 10 cm through a hole 0.9 mm in diameter in a steel electrode to the flat face of another steel electrode directly below at a distance of about 1 cm. The electrodes were supported in a housing of pipe fittings, the lower one being insulated by means of a quartz tube. The housing carried a quartz window waxed on, a tube for draining off the mercury, and a pipe leading to an expansion chamber which prevented the occurrence of excessive pressures. Provision was made to blow air through the housing between flashes in order to keep the housing cool.

It was found that but a very short duration of arc after the explosion was sufficient to burn the electrodes seriously, and to bring out iron lines in the spectrum. The control devised to prevent this consisted of a relay connected so as to open the actuating circuit of the magnetic switch at a definite interval after the circuit was closed by hand. The delay of the relay was achieved by putting a large inductance in series with it, and was controlled by varying the voltage applied to it by a potentiometer arrangement. Tests with a 60-cycle impulse counter showed that the switch actually was closed for about 0.03 sec.

Conditions were varied by inserting various amounts of resistance in the line, by changing the voltage of the generator, and by confining the explosion within a 0.5-cc hole in a porcelain block provided with an opening 3 mm in diameter through which light was allowed to issue. The effect of high voltage condenser discharges on the same mercury stream was also studied by using about 20,000 volts from condensers with a capacity of 0.26 mf, charged by means of the rectified output of a high tension transformer.

Light from the exploding mercury was focused on the slit of a Féry quartz spectrograph by spectrum, with considerable overlapping, but with greatest intensity wherever arc lines are thickest. Balasse observed such a spectrum most strongly developed when the arc lines and spark means of a quartz lens, and it was found that six flashes were sufficient to produce a well-exposed spectrum photograph. One flash produced about as much blackening as a 15-second exposure of a quartz mercury Labarc. Twice as many flashes were required when the 20,000-volt condenser discharge was used.

Results

In Fig. 1 the region 3150 to 2150A is shown as obtained with the Féry instrument. It gives a comparison of the ordinary quartz mercury arc spectrum with the explosion spectrum. In Fig. 2 the region 2150 to 1850 is shown as obtained with a Steinheil quartz instrument, with an aluminum spark for comparison.[5] The plate was sensitized for this region by using Eastman ultraviolet sensitizing solution. The continuous emission is quite suitable for showing absorption from 2537A at least as far as 1950A. The absorption shown in the photograph is largely that of NO, which is produced from the air in the housing and which could be eliminated by producing the explosions in an inert atmosphere.

It was found that with increasing generator voltages, the continuous spectrum becomes stronger, first in the ultraviolet, and then also toward the longer wavelengths. This is obviously not a black-body type of continuous emission. A clue to the probable explanation is furnished by the work of Balasse,[6] who established the occurrence of a continuous emission resulting from the recombination of an electron with a positive on to form a neutral atom in an excited state. The energy radiated thus is the ionization energy of the atom, less the energy of excitation retained, in addition to the kinetic energy of the recombining electron with respect to the ion. As usual, the effect of kinetic energy of varying amounts in transitions is to yield a region of continuous emission. These regions might be expected to extend over a large range of the

[5] This spectrum photograph was made by the senior author in collaboration with Dr. P. J. Flory in some unpublished work on the absorption of the NO molecule in this region.

[6] Balasse, J. de phys et rad. **5**, 304 (1934).

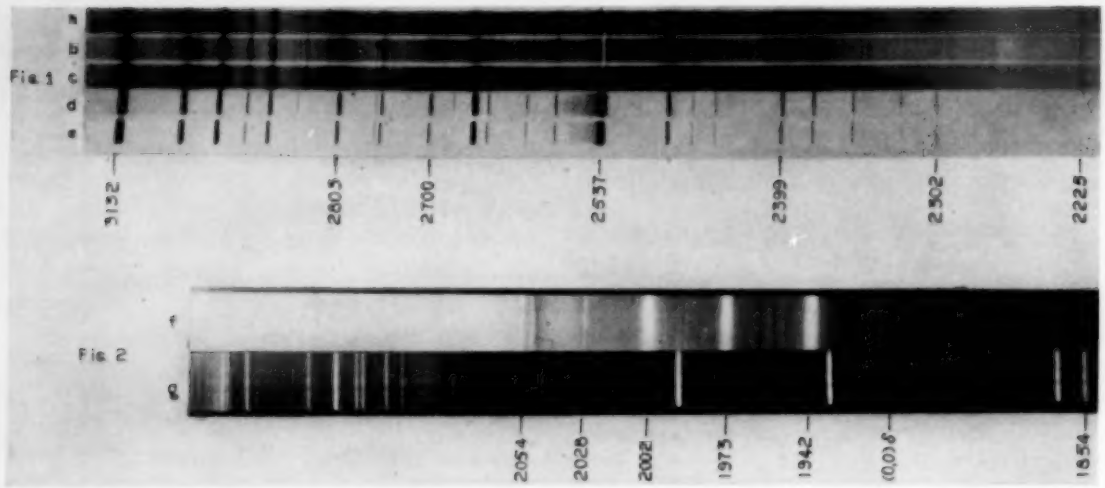

FIG. 1. Explosion spectrum of mercury compared with mercury arc. (a) 6 flashes at 150 volts; (b) and (c) each: 6 flashes at 125 volts; (d) Labarc, 160 sec.; (e) Labarc, 40 sec.

FIG. 2. Explosion spectrum of mercury with Al spark for comparison; plate sensitized with Eastman U–V solution. (f) 8 flashes; (g) condensed Al spark, 10 sec.

lines both were strong in his source. The explosion spectrum, on the contrary, shows few spark lines, but positive ions undoubtedly are present in great abundance immediately after the explosion.

As might be expected, pronounced self-reversal was observed for the resonance line, λ2537. At higher generator voltages, no additional reversals were observed. However, the confined explosion at 20,000 volts shows many absorption lines, corresponding with observations of Hori.[7] These lines have as their lower levels the three levels of the lowest ^3P state. That these levels are populated under the conditions is explained by the fact that $^3P_0$ and $^3P_2$ are metastable with respect to the ground state $^1S_0$, and that $^3P_1$ is repopulated by the absorption of λ2537 which brings the atom up from the ground state to that level.

Another characteristic of the explosion spectrum is the great broadening obtained for many of the lines, so much so that some are merged entirely with the continuous background, and others are as much as 100A wide. A summary of the ideas on the width of spectral lines was given by Weisskopf[8] in 1933. Two considerations stand out as being accountable for the extreme broadening observed here: impact damping, and Stark-effect broadening. The former merely means that if an atom in the process of emitting is struck by an ion or an electron, the quantum conditions are relaxed, and the frequency radiated differs from that of the unperturbed atom. This is substantially the same as a Stark effect produced by a rapidly changing field. Attention should be called to the fact that the earlier criteria for predicting large Stark effects, as quoted by Weisskopf, turn out to be accidental, as shown by the quantum-mechanical considerations of Condon.[9] The fields effective in shifting the energy levels of the atoms are not the relatively insignificant fields due to the voltage applied to the mercury stream, but the fields produced by positive ions formed by the explosion. Under the conditions of great density of vapor, the interatomic distances are quite small, and the corresponding fields are correspondingly enormous.

The authors acknowledge with pleasure the assistance of their colleagues, G. H. Shortley and W. H. Bennett, thanking the former for suggestions concerning the Stark effect and the latter for the loan of the source of 20,000 volts.

[7] T. Hori, Sci. Pap. Inst. Phys. and Chem. Research, Tokyo **4**, 59 (1926).

[8] V. Weisskopf, Physik. Zeits. **34**, 1 (1933).

[9] E. U. Condon, Phys. Rev. **43**, 648 (1933).

The Disintegration of the Deuteron by Impact

J. R. OPPENHEIMER, *Berkeley, California*

(Received March 29, 1935)

High energy deuterons can be disintegrated by their impact with nuclei. For deuteron energies $\sim 2\times 10^7$ e.v., the corresponding neutron yield can be of the order of 1 percent. The probability of the process can be calculated by taking advantage of the fact that the nuclear field varies little over the deuteron, and is then given quite simply in terms of the photoelectric absorption and the matrix elements of the nuclear field acting on the deuteron. For low energies the neutron yields are small, amounting to 3×10^{-9} for 3×10^6 e.v. deuterons in Al, and to 10^{-4} for 4×10^6 e.v. deuterons in carbon.

ACCORDING to the experiments of Chadwick and Goldhaber deuterons may be disintegrated by the gamma-rays of ThC″. The threshold for this photoelectric effect corresponds to the mass defect I of the deuteron with respect to the proton and neutron into which it disintegrates, and lies roughly at 2×10^6 e.v. Whenever deuterons of energy greater than this pass through matter, they may be disintegrated by their impact with atomic nuclei. It is this process which we wish to consider.

When the minimum time of impact T is very short compared to the periods of the deuteron τ, then we may determine the mean energy lost by the deuteron for its disintegration by applying the familiar method by which Bohr derived the atomic energy losses of fast particles. This gives for the energy loss per cm

$$\Delta E/\Delta x=[4\pi Z^2e^4/(2M)v^2]N\ln(\tau/T). \quad (1)^*$$

Here N is the number of nuclei/cm³, Ze their charge, v the deuteron velocity and $2M$ the deuteron mass. Further

$$T=Ze^2/Mv^3, \quad \tau=\hbar/Ik, \quad (2)$$

where k is a constant of order unity, which depends on the structure of the deuteron. The cross section for disintegration is thus in this limit

$$\sigma=(2\pi Z^2e^4/Mv^2k_1I)\lambda; \quad \lambda=\ln(Mv^3\hbar/Ze^2kI) \quad (3)$$

where k_1 is again of order unity, and k_1I is the mean energy which the deuteron absorbs on disintegration. If we write[1] for the energy loss to atomic electrons

$$\frac{\Delta' E}{\Delta x}=\frac{4\pi NZe^4}{mv^2}\Lambda; \quad \Lambda=\ln\frac{mv^3}{Ze^2\kappa R}; \quad \kappa\sim 5.3; \quad R=\frac{me^4}{4\pi\hbar^3} \quad (4)$$

then the yield of neutrons from a thick target, for an initial deuteron energy W, is

$$Z(m/2M)(W/k_1I)L \quad (L\sim 1) \quad (5)$$

where L is the average over the energy range of the deuteron of the ratio λ/Λ. For high energies ($\sim 3\times 10^7$ e.v.) and large Z this gives yields of the order of 1 percent. It therefore seems of interest to investigate this process for lower energies, where the assumption $T\ll\tau$ can no longer be made.

We can make this calculation very simply insofar as we may neglect the variation of the field of the nucleus over the deuteron. This in turn will be permissible whenever the dimensions d of the deuteron are small compared to the distance of closest approach with the nucleus. Since d cannot be smaller than $\hbar/(MI)^{\frac{1}{2}}$, we must have

$$\hbar/(MI)^{\frac{1}{2}}\ll Ze^2/Mv^2. \quad (6)$$

This condition does not contradict $T\ll\tau$ when

$$n=Ze^2/\hbar v\gg 1. \quad (7)$$

The condition (7) is well satisfied except for the lightest elements, for all deuteron energies which are likely to be available; and we shall assume the validity of (7) in the following work.

* This is the mean energy transferred, by the impact of a nucleus of velocity v on a deuteron initially at rest, to the relative motion of neutron and proton with respect to their center of mass; the mean work done on the proton is just twice this.

[1] F. Bloch, Zeits. f. Physik **81**, 363 (1933).

Under these circumstances we can compute the field acting on the deuteron as though it were a point charge moving in the field of the nucleus; let us call the matrix component of this field which corresponds to an energy loss of the deuteron $=h\nu$, $\mathcal{E}_\nu$. This field will disintegrate the deuteron; if σ_ν be the cross section for photo-effect, the cross section for impact disintegration will be

$$\sigma=(c/4\pi h)\int_{I/h}^{W/h}\sigma_\nu|\mathcal{E}_\nu|^2 d\nu/\nu. \tag{8}$$

Now Bethe and Peierls have given[2] a theoretical calculation of σ_ν, which is based on the assumption that the forces between proton and neutron act appreciably only over a region small compared to the size of the deuteron and the wavelength of the photoneutron: they find

$$\sigma_\nu=\frac{2h^2\alpha}{3\pi MI}\frac{x^{\frac{1}{2}}}{(1+x)^3};\quad x>0;\quad x=h\nu/I-1. \tag{9}$$

Since when we insert this in (8) the integrand falls off fairly rapidly with ν, we may use (9) even for frequencies higher than those for which its derivation is valid; for the true value of σ_ν will give an integrand in (8) which falls off still more rapidly.

The matrix elements $\mathcal{E}_\nu$ are just $2M/e$ times the matrix elements of the acceleration of the deuteron; these are known[3] from the theory of the continuous x-ray spectrum, and assume a relatively simple form when (7) is valid. We have to remember, however, that the deuteron and nucleus have like charges, whereas the calculations on the continuous x-spectrum are made for two charges which attract each other. For our case we find

$$|\mathcal{E}_\nu|^2=\frac{16\pi^2 z^2e^2}{3^{\frac{1}{2}}}\frac{z^2e^2}{v^2}\exp\left\{-2\pi n\right.$$
$$\left.\times\left[\left(1-\frac{(1+x)I}{W}\right)^{-\frac{1}{2}}-1\right]\right\}g'\left(\frac{nI(1+x)}{2W}\right). \tag{10}$$

The function $g'(y)$ appears in the classical theory of the x-ray spectrum:

$$g'(y)=\tfrac{1}{4}\pi(3)^{\frac{1}{2}}iyH_{iy}^{(1)}(iy)H_{iy}^{(1)\prime}(iy). \tag{11}$$

A rough plot of g' has been given[4] by Kramers: for large y, $g'=1$; and g' does not deviate sensibly from this value except for very small values of y, where it is given by

$$g'(y)\to(3^{\frac{1}{2}}/\pi)\ln 2/yC,\quad \ln C=0.577. \tag{11a}$$

From (8), (9) and (10) we have

$$\sigma=(16\pi Z^2e^4/3(3)^{\frac{1}{2}}Mv^2I)\varphi(Z,W),$$
$$\varphi(Z,W)=\int_0^{W/I-1}\frac{x^{\frac{1}{2}}}{(1+x)^4}dx$$
$$\exp 2\pi n\{1-[1-(I/W)(1+x)]^{-\frac{1}{2}}\}$$
$$\times g'(nI/2W)(1+x)). \tag{12}$$

The integral for $\varphi(Z,W)$ may be evaluated for the limiting cases $\frac{nI}{2W}\gg\ll 1$, but except in these cases can hardly be written in closed form.

For $\pi nI/W\gg 1$ we find

$$\sigma=\frac{4}{\pi(3)^{\frac{1}{2}}}\frac{Z^2e^4}{Mv^2I}\left(\frac{nI}{W}\right)^{-5/2}$$
$$\exp 2\pi n[1-(1-I/W)^{-\frac{1}{2}}]. \tag{13}$$

For $nI/2W\ll 1$, on the other hand

$$\sigma=\frac{\pi}{3}\frac{Z^2e^4}{Mv^2I}\ln\frac{W}{Ink}\qquad k=e^{-1/6}C\sim 1.51$$
$$=\frac{\pi}{3}\frac{Z^2e^4}{Mv^2I}\ln\frac{Mv^3h}{Ze^2kI}. \tag{14}$$

This is in fact of the form (3), with $k=1.51$, $k_1=6$.

If we take $Z=13$, $I=2\times10^6$, $W=3\times10^6$, we may apply (13). This gives $\sigma\sim\frac{3}{4}\times10^{-27}$ cm^2, and with (4) gives a neutron yield of about 3×10^{-9}. For $Z=6$, $W=4\times10^6$, (13) is inapplicable. Here (12) and (4) give a yield of about 10^{-6}. The increase in yield with energy is very rapid.

[2] H. Bethe and R. Peierls, Proc. Roy. Soc. **A148**, 146 (1935).

[3] H. A. Kramers, Phil. Mag. **46**, 836 (1923) and G. Wentzel, Zeits. f. Physik **27**, 257 (1924) give the classical theory. Gaunt gives the quantum theoretic treatment, for unlike charges, for $n\gg1$: J. A. Gaunt, Zeits. f. Physik **59**, 508 (1930). For $h\to0$ the exponent in (10) goes to $2\pi^2(Ze^2/Mv^2)\nu$.

[4] Kramers, reference 3, pp. 858–860.

Some Higher Terms in the Spectrum of Ag II

W. P. GILBERT, *Department of Physics, Cornell University*

(Received April 6, 1935)

The spectrum of silver has been excited in a hollow cathode discharge with a helium atmosphere. Wavelength measurements were made in the region from 500 to 2600A with a 1.5-meter grating vacuum spectrograph and in the region from 4000 to 11,000A with a Zeiss 3-prism spectrograph. Starting with terms already reported by previous workers as a basis, radiations have been classified sufficiently to establish the $4d^9 6p\ ^{3,1}(P^\circ D^\circ F^\circ)$ and the $4d^9 7s$ and $8s\ ^{3,1}D$ terms. A few terms of unknown origin have been found and in addition a few lines arising from the transition $4d^9 5d$ to $4d^9 5p$ have been identified. The application of a Ritz formula to the $4d^9(^2D_{2\frac{1}{2}})ns\ ^3D_3$ series gives 134,110 cm^{-1} for the limit of this series. The absolute value of the $4d^{10}\ ^1S_0$ term with respect to the $4d^9\ ^2D_{2\frac{1}{2}}$ level of the Ag III ion is thus found to be 173,274 cm^{-1}, which corresponds to an ionization potential of 21.4 volts.

A NUMBER of investigators[1] have contributed to the analysis of the first spark spectrum of silver. With the exception of the recent contribution of Duffendack and Thomson[2] the terms established by these workers have been listed in the tables compiled by Bacher and Goudsmit.[3] In the present paper the analysis of this spectrum has been extended to higher terms.

Experimental Details

The silver spectrum was produced in a hollow cathode discharge maintained in an atmosphere of helium. The cathode was made of chemically pure silver, in the form of a cylinder 5 cm long and 2 cm in diameter. Normally, the tube was operated at 1500 volts and 200 to 400 milliamperes. The use of a spark gap in series with the lamp[4] served to bring out strongly lines of Ag III and to enhance lines arising from the higher states of Ag II while lines of Ag I and lines arising from low levels of Ag II were little affected by its use. Best results were obtained by maintaining the helium pressure as low as possible. The spectrum of the discharge was photographed from 500 to 2600A with a vacuum spectrograph equipped with a 1.5-meter grating which gave a dispersion of about 11.2A per mm. Impurity lines were used as standards. In the region from 500 to 1930A the oxygen, nitrogen and carbon lines measured by Edlén[5] and the wavelengths computed by Paschen[6] for hydrogen and helium were used. From 1930 to 2600A no satisfactory impurity lines were found so the sharp lines of Ag II as given by Shenstone[7] were employed as standards. The measurements are believed to be accurate to 0.05A (1.4 cm^{-1} at 1900A to 5 cm^{-1} at 1000A) over this region. A Zeiss three-prism spectrograph was used to photograph the region from 4000 to 11,000A. The dispersion varied from 6A per mm at 4100A to 112A per mm at 10,000A. An iron comparison spectrum furnished standards throughout this region. The accuracy of measurement varies from about 0.01A (1 cm^{-1}) at 4100A to about 1.0A (1 cm^{-1}) near 9000A. Schumann plates were employed for all photography in the vacuum region and Eastman plates of recommended types in the visible and infrared.

Extent of Excitation

The normal operation of the discharge does not excite the silver sufficiently to produce the entire spark spectrum. It is well known[8] that excitation in the hollow cathode is primarily the result of reactions in which the energy of metastable or ionized rare gas atoms is imparted to normal, metastable or ionized metal atoms. The particular type of reaction favored depends upon the physical properties of the element excited, the rare gas employed, and upon the discharge conditions. These reactions are found to produce maxima of excitation of the terms with which they are in resonance. The energy available from the helium ion corresponds to 198,300 cm^{-1} (metastable helium 159,830 cm^{-1}). Since the value of the lowest state of Ag I is 61,104 cm^{-1}

[1] Gibbs, Rev. Mod. Phys. **4**, 401 (1932).
[2] Duffendack and Thomson, Phys. Rev. **43**, 106 (1933).
[3] Bacher and Goudsmit, *Atomic Energy States*, McGraw-Hill Book Co., 1932.
[4] Gartlein and Gibbs, Phys. Rev. **38**, 1907 (1931).
[5] Edlén, Zeits. f. Physik **85**, 85 (1933).
[6] Paschen, Ber. Preuss. Akad. d. Wiss. Phys.-Math. Klasse **30**, 662 (1929).
[7] Shenstone, Phys. Rev. **31**, 317 (1928).
[8] Sawyer, Phys. Rev. **36**, 44 (1930).

and of Ag II is 173,274 cm^{-1} (total 234,378 cm^{-1}), the highest term of Ag II which would be excited to any appreciable extent because of reactions between normal silver atoms and helium ions would be 36,078 cm^{-1} below the first double ionization limit. This excitation maximum falls just above the levels of the ($d^9 6p$) configuration and has been observed by Duffendack and Thomson[2] and by the author.

However, there are two other possible reactions, namely, those between ionized silver atoms and helium ions and those between metastable silver atoms and helium ions which, if present, should produce higher excitation than this. In the present work no resonance phenomena have been observed which would indicate the presence of either of these reactions. Silver has a relatively high boiling point and at the cathode temperatures which existed in the present work the vapor pressure is low. The presence of silver atoms in the discharge space must therefore be due primarily to sputtering. As a consequence, the concentration of silver atoms is low and those present probably react only as neutral atoms.[8] In the case of Cu II,[9] the highest term found appears to have been excited by reactions between copper atoms in the $3d^9 4s^2$ state and helium ions. Unfortunately, the $4d^9 5s^2$ state of Ag I is unknown. If it be assumed, with some reason,[10] that this state is almost coincident with the $4d^{10} 5p$ state of Ag I, then the highest term of Ag II excited by reactions of this type should lie about 6500 cm^{-1} below the first ionization limit of Ag II. The fact that no resonance phenomena have been observed which would indicate the existence of such reactions therefore supports the view suggested by Blair[10] that the $4d^9 5s^2$ state of Ag I is not metastable but lies closer to the limit than the $4d^{10} 5p$ state.

The action of the spark gap, whereby these limitations are removed, is not clearly understood. It seems reasonable to attribute the higher excitation to increased sputtering action, resulting in an increase in the concentration of metal atoms in the discharge space, and to the increased potential fall in the negative glow, resulting in an increase in the energy transferred during collisions of the first kind.

[8] Kruger, Phys. Rev. **34**, 1122 (1930).
[10] Blair, Phys. Rev. **36**, 1531 (1930).

Term Values and Classifications

The new terms of Ag II determined by the present measurements as well as those reported by previous investigators are collected in Table I. The classified lines by which the new terms are established are listed in Table II. The intensities are visual estimates and are comparable only over short regions of the spectrum.

In most cases a check upon the term assignments made on the basis of ultraviolet data was afforded by the infrared data. A particular exception exists in the case of the term $4d^9 6p\ ^3P_0^\circ$. This term is based upon the single transition $4d^9 5s\ ^3D_1 - 4d^9 6p\ ^3P_0^\circ$ and for this reason may be considered questionable. Nine terms are included

Table I. *Term values for Ag II.*

Term symbol	A[a]	Absolute[b] term values cm^{-1}	Term symbol	A[a]	Absolute[b] term values cm^{-1}	Term symbol	A[a]	Absolute[b] term values cm^{-1}	Term symbol	A[a]	Absolute[b] term values cm^{-1}
$4d^{10}\ ^1S_0$	S	173274.0	$4d^9(^2D_{3\frac{1}{2}})6s\ ^3D_2$	S	52747.4	$^3D_1$	S	41773.5	$4d^9(^2D_{1\frac{1}{2}})6p\ ^3P_0^\circ$	G	37123.3
$4d^9(^2D_{3\frac{1}{2}})5s\ ^3D_3$	S	134110.1	$^3D_3$	S	52369.9	$^1G_4$	S	41763.5	$^3F_2^\circ$	G	36758.3
$^3D_2$	S	132533.0	$4d^9(^2D_{1\frac{1}{2}})6s\ ^3D_1$	S	48154.6	$^1D_2$	S	41490.1	$^3P_1^\circ$	$D\&T$	36445.5
$4d^9(^2D_{1\frac{1}{2}})5s\ ^3D_1$	S	129535.3	$^1D_2$	S	47876.2	$4d^9(^2D_{3\frac{1}{2}})6p\ ^3F_3^\circ$	G	41260.6	$^3F_3^\circ$	G	36100.6
$^1D_2$	S	127228.3	$4d^9(^2D_{3\frac{1}{2}})5d\ ^3S_1$	S	47705.1	$4d^9(^2D_{1\frac{1}{2}})5d\ ^3F_2$	S	41125.1	$^3D_1^\circ$	$D\&T$	36051.7
$4d^9(^2D_{3\frac{1}{2}})5p\ ^3P_2^\circ$	S	93101.8	$^3G_5$	S	46613.5	$^1F_3$	S	41082.2	$^1D_2^\circ$	G	35807.7
$^3F_3^\circ$	S	91106.9	$^3G_4$	S	46600.9	$4d^9(^2D_{3\frac{1}{2}})6p\ ^3F_4^\circ$ —	G	40848.5	? 7_3 —	G	34640.7
$^3P_1^\circ$	S	89653.1	$^3P_2$	S	46513.8	? 1_4 —	G	40589.3	? 8_3 —	G	34046.7
$^3F_4^\circ$	S	89608.8	$^3P_1$	S	46510.3	$4d^9(^2D_{3\frac{1}{2}})6p\ ^3P_1^\circ$ —	$D\&T$	40435.9	? 9_3 —	G	32311.7
$^3D_3^\circ$	S	88077.7	$^3D_3$	S	46069.0	$^3D_2^\circ$ —	G	40357.8	$4d^9(^2D_{1\frac{1}{2}})7s\ ^3D_2$	G	28800.1
$4d^9(^2D_{1\frac{1}{2}})5p\ ^3P_0^\circ$	S	87136.0	$^3F_3$	S	45789.5	$^3D_3^\circ$ —	G	40255.9	$^3D_3$	G	28655.0
$4d^9(^2D_{3\frac{1}{2}})5p\ ^3D_3^\circ$	S	86817.7	$^3D_2$	S	45757.0	? 2_1 or $_2$ —	G	40135.8	$4d^9(^2D_{1\frac{1}{2}})7s\ ^3D_1$	G	24195.6
$4d^9(^2D_{1\frac{1}{2}})5p\ ^3F_3^\circ$	S	86390.3	$^3F_4$	S	45672.2	? 3_2 —	G	39684.6	$^1D_2$	G	24094.9
$^3F_2^\circ$	S	84143.7	$^3P_0$	B	44745.2	? 4_3 —	G	38933.4	$4d^9(^2D_{3\frac{1}{2}})8s\ ^3D_3$	G	18188.7
$^1P_1^\circ$	S	83383.0	$4d^9(^2D_{3\frac{1}{2}})6p\ ^3P_2^\circ$ —	G	42550.9	$4d^9(^2D_{1\frac{1}{2}})5d\ ^1S_0$	B	38824.6	$^3D_2$	G	18117.2
$^3D_1^\circ$	S	82943.5	$4d^9(^2D_{1\frac{1}{2}})5d\ ^1P_1$	S	42518.0	? 5_3 or 2 —	G	38479.3	$4d^9(^2D_{1\frac{1}{2}})8s\ ^3D_1$	G	13583.2
$^1D_2^\circ$	S	82390.6	$^3G_4$	S	42027.7	? 6_2 —	G	37861.5	$^1D_2$	G	13535.2

[a] This column refers to worker by which the term has been established. S = Shenstone; B = Blair; $D\&T$ = Duffendack and Thomson; G = Gilbert.
[b] Term values referred to $4d^9\ ^2D_{3\frac{1}{2}}$ level of Ag III as zero. The proper limit is indicated in column one. The double ionization limit has a separation of 4607 cm^{-1}.

TABLE II. *New classifications in Ag II.*

Int.	λ(air)	ν(vac.)	Classification
15	9000.9	11106.9	$4d^9 6s\ ^3D_1 - 4d^9 6p\ ^3F_2^\circ$
1*ur*	8998.7	11113.3	$6s\ ^1D_2 - 6p\ ^3F_3^\circ$
2	8772.2	11396.5	$6s\ ^3D_1 - 6p\ ^3F_2^\circ$
12	8747.6	11428.6	$6s\ ^1D_2 - 6p\ ^1P_1^\circ$
0	8725.5	11457.5	$6p\ ^3D_2^\circ - 7s\ ^3D_2$
8	8704.7	11484.9	$6s\ ^3D_2 - 6p\ ^3F_2^\circ$
0	8540.6	11705.6	$6p\ ^1D_2^\circ - 7s\ ^1D_2$?
15	8492.5	11771.9	$6s\ ^1D_2 - 6p\ ^1F_3^\circ$
0	8457.7	11820.3	$6s\ ^1D_2 - 6p\ ^3D_1^\circ$
0	8431.1	11857.6	$6p\ ^3D_1^\circ - 7s\ ^3D_1$
25	8403.8	11896.1	$6s\ ^3D_1 - 6p\ ^3F_2^\circ$
15	8379.5	11930.6	$6s\ ^3D_2 - 6p\ ^3P_1^\circ$
0	8362.6	11954.7	$6p\ ^3D_1^\circ - 7s\ ^1D_2$
20	8324.4	12009.6	$6p\ ^1F_3^\circ - 7s\ ^1D_2$ $6s\ ^3D_2 - 6p\ ^3D_2^\circ$
6	8297.7	12048.2	$6p\ ^3F_4^\circ - 7s\ ^3D_3$
8	8287.3	12063.3	$6s\ ^1D_2 - 6p\ ^1D_2^\circ$
8	8263.2	12098.5	$6s\ ^3D_1 - 6p\ ^3D_1^\circ$
15	8254.7	12110.9	$6s\ ^3D_2 - 6p\ ^3D_3^\circ$
2	8224.5	12155.4	$6s\ ^3D_3 - 1_4$
8	8100.1	12342.2	$6s\ ^3D_1 - 4d^9 6p\ ^1D_2^\circ$
0*ur*	8096.4	12347.8	$6p\ ^1P_1^\circ - 7s\ ^1D_2$
1	8023.0	12460.7	$6p\ ^3F_2^\circ - 7s\ ^3D_2$
25	8005.4	12488.1	$6s\ ^3D_3 - 6p\ ^3D_2^\circ$
1	7957.3	12563.6	$6p\ ^3F_3^\circ - 7s\ ^3D_1$
6	7930.2	12606.5	$6p\ ^3F_3^\circ - 7s\ ^3D_2$
0	7439.4	13438.3	$6s\ ^3D_2 - 4_3$
5	7239.2	13809.9	$6s\ ^3D_3 - 4_3$
1*d*	7198.3	13888.3	$6s\ ^3D_3 - 5_1 \text{ or } 3$
1	6998.6	14284.7	$5_1 \text{ or } 3 - 4d^9 7s\ ^3D_1$
1*ur*	6893.5	14502.4	$4d^9 6s\ ^3D_3 - 6_2$
2	6716.9	14883.8	$6s\ ^3D_3 - 6_2$
1	6402.7	15614.0	$6s\ ^3D_2 - 4d^9 6p\ ^3F_2^\circ$
1	6278.7	15922.6	$6s\ ^3D_3 - 6p\ ^1P_1^\circ$
1	4650.93	21499.7	$3_2 - 8s\ ^3D_2$
2	4530.31	22067.4	$6p\ ^3D_2^\circ - 8s\ ^3D_2$
1	4515.46	22140.0	$6p\ ^3D_3^\circ - 8s\ ^3D_2$
2	4494.89	22241.3	$6p\ ^3D_3^\circ - 8s\ ^3D_3$
1*d*	4488.54	22272.8	$6p\ ^1D_2^\circ - 8s\ ^1D_2$
1	4479.07	22319.8	$6p\ ^3P_1^\circ - 8s\ ^3D_2$
1	4449.18	22469.8	$6p\ ^3D_1^\circ - 8s\ ^3D_1$
2	4430.56	22564.2	$6p\ ^1F_3^\circ - 8s\ ^1D_2$
4	4412.01	22659.1	$6p\ ^3F_4^\circ - 8s\ ^3D_3$
1	4364.21	22907.3	$6p\ ^1P_1^\circ - 8s\ ^1D_2$
1	4333.19	23071.2	$6p\ ^3F_3^\circ - 8s\ ^3D_3$
3	4319.65	23143.5	$6p\ ^3F_2^\circ - 8s\ ^3D_2$
1	4313.57	23176.1	$6p\ ^3F_2^\circ - 8s\ ^3D_1$
	λ(vac.)		
4	2186.40	45737.3	$4d^9 5p\ ^3D_3^\circ - 4d^9 5d\ ^1F_3$
0	2101.40	47587.3	$5p\ ^3F_4^\circ - 5d\ ^3G_3$
3	2089.97	47847.6	$5p\ ^3F_4^\circ - 5d\ ^1G_4$
7	2088.50	47881.2	$5p\ ^3P_1^\circ - 5d\ ^3D_1$
3	2060.59	48529.8	$5p\ ^3F_4^\circ - 5d\ ^1F_3$
5	2026.54	49345.8	$5p\ ^3F_3^\circ - 5d\ ^1G_4$
4	1998.98	50025.5	$5p\ ^3F_3^\circ - 5d\ ^1F_3$
10	1967.38	50829.0	$5p\ ^3P_1^\circ - 5d\ ^1S_0$
4	1937.53	51612.1	$5p\ ^3P_1^\circ - 5d\ ^1D_2$
1	1866.06	53588.8	$5p\ ^1D_2^\circ - 7s\ ^3D_2$
0	1860.38	53736.0	$5p\ ^1D_2^\circ - 7s\ ^3D_2$
1	1842.06	54287.0	$5p\ ^3D_1^\circ - 7s\ ^3D_2$
5	1827.24	54727.3	$5p\ ^1P_1^\circ - 7s\ ^3D_2$
3	1806.92	55342.8	$5p\ ^3F_3^\circ - 7s\ ^3D_2$
5	1802.28	55486.5	$5p\ ^3F_3^\circ - 7s\ ^1D_2$
6	1732.04	57735.7	$5p\ ^3F_2^\circ - 7s\ ^3D_2$
8	1723.63	58017.1	$5p\ ^3D_3^\circ - 7s\ ^3D_2$
5	1719.30	58163.2	$5p\ ^3D_2^\circ - 7s\ ^3D_2$
1	1718.38	58194.3	$5p\ ^1D_2^\circ - 7s\ ^3D_1$
2	1715.45	58293.7	$5p\ ^1D_2^\circ - 7s\ ^1D_2$
4	1702.20	58747.5	$5p\ ^3D_1^\circ - 7s\ ^3D_1$
2	1686.73	59286.3	$5p\ ^1P_1^\circ - 7s\ ^1D_2$
12	1682.82	59424.1	$5p\ ^3D_2^\circ - 7s\ ^3D_2$
5	1665.34	60047.8	$5p\ ^3F_3^\circ - 7s\ ^1D_2$
10	1644.50	60808.8	$5p\ ^3F_4^\circ - 7s\ ^3D_3$
1	1639.38	60998.7	$5p\ ^3P_1^\circ - 7s\ ^3D_2$
3	1607.86	62194.5	$5p\ ^3F_2^\circ - 7s\ ^3D_1$
4	1605.22	62296.8	$5p\ ^3F_2^\circ - 7s\ ^1D_2$
4	1604.94	62307.6	$5p\ ^3F_3^\circ - 7s\ ^3D_3$
8	1601.22	62452.4	$5p\ ^3F_3^\circ - 7s\ ^3D_2$
5	1594.25	62725.4	$5p\ ^3D_3^\circ - 7s\ ^1D_2$
3	1587.75	62942.6	$5p\ ^3P_2^\circ - 7s\ ^3D_1$
1	1565.35	63883.5	$5p\ ^3D_2^\circ - 7s\ ^3D_1$
10	1555.16	64302.1	$5p\ ^3P_2^\circ - 7s\ ^3D_2$
0	1551.65	64447.5	$5p\ ^3P_2^\circ - 7s\ ^3D_2$

Int.	λ(vac.)	ν(vac.)	Classification
0	1532.19	65266.1	$5p\ ^1P_1^\circ - 8s\ ^3D_2$
0	1527.72	65457.0	$5p\ ^3P_1^\circ - 7s\ ^3D_1$
1	1525.40	65556.6	$5p\ ^3P_1^\circ - 7s\ ^1D_2$
0	1514.52	66027.5	$5p\ ^1F_3^\circ - 8s\ ^3D_2$
6	1492.23	67013.8	$5p\ ^3F_3^\circ - 7s\ ^1D_2$
1	1457.08	68630.4	$5p\ ^3D_3^\circ - 8s\ ^3D_2$
0	1455.62	68699.2	$5p\ ^3D_2^\circ - 8s\ ^3D_2$
0	1453.19	68814.1	$5p\ ^1D_2^\circ - 8s\ ^3D_1$?
0	1451.28	68904.7	$5p\ ^3P_2^\circ - 7s\ ^3D_1$
0	1449.12	69007.4	$5p\ ^3P_2^\circ - 7s\ ^1D_2$
0	1441.74	69360.6	$5p\ ^3D_1^\circ - 8s\ ^3D_1$
0	1431.68	69848.0	$5p\ ^1P_1^\circ - 8s\ ^1D_2$
0	1429.40	69959.4	$5p\ ^3D_2^\circ - 8s\ ^3D_2$
1	1416.26	70608.5	$5p\ ^3F_4^\circ - 8s\ ^1D_2$
2	1400.15	71420.9	$5p\ ^3F_4^\circ - 8s\ ^3D_3$
0	1399.51	71534.9	$5p\ ^3P_1^\circ - 8s\ ^3D_2$
0	1373.50	72806.7	$5p\ ^3F_3^\circ - 8s\ ^3D_1$
0	1372.57	72856.0	$5p\ ^3F_3^\circ - 8s\ ^1D_2$
0	1371.44	72916.1	$5p\ ^3F_2^\circ - 8s\ ^3D_2$
2	1370.02	72991.8	$5p\ ^3F_2^\circ - 8s\ ^3D_2$
0	1364.60	73281.5	$5p\ ^3P_2^\circ - 8s\ ^1D_2$
0	1334.97	74913.1	$5p\ ^3P_2^\circ - 8s\ ^3D_2$
1	1180.96	84676.9	$5s\ ^1D_2 - 6p\ ^3P_2^\circ$
8	1163.21	85969.0	$5s\ ^1D_2 - 6p\ ^3F_3^\circ$
4	1152.15*	86794.3	$5s\ ^1D_2 - 6p\ ^1P_1^\circ$
6	1151.11	86872.7	$5s\ ^1D_2 - 6p\ ^3D_2^\circ$
5	1149.77	86973.9	$5s\ ^1D_2 - 6p\ ^3D_3^\circ$
3	1148.20	87092.8	$5s\ ^1D_2 - 2_1 \text{ or } 1$
1	1132.55	88296.3	$5s\ ^1D_2 - 4_3$
0	1126.74	88751.6	$5s\ ^1D_2 - 5_1 \text{ or } 3$
1	1122.32	89101.1	$5s\ ^3D_1 - 4d^9 6p\ ^1P_1^\circ$
2	1118.99	89366.3	$5s\ ^1D_2 - 6_2$
5	1118.56	89400.7	$5s\ ^3D_1 - 2_1 \text{ or } 1$
0	1113.00	89847.3	$5s\ ^3D_1 - 3_2$
1	1111.32	89983.1	$5s\ ^3D_2 - 4d^9 6p\ ^3P_2^\circ$
5	1105.34	90469.9	$5s\ ^1D_2 - 6p\ ^3F_2^\circ$
5	1101.50*	90783.3	$5s\ ^1D_2 - 6p\ ^1P_1^\circ$
5	1098.22	91056.4	$5s\ ^3D_1 - 5_1 \text{ or } 3$
4	1097.35	91128.6	$5s\ ^1D_2 - 4d^9 6p\ ^1F_3^\circ$
1	1096.74	91179.3	$5s\ ^1D_2 - 6p\ ^3D_1^\circ$
8	1095.60	91274.2	$5s\ ^3D_2 - 6p\ ^3F_2^\circ$
2	1093.85	91420.2	$5s\ ^1D_2 - 6p\ ^1D_2^\circ$
7	1092.19	91559.2	$5s\ ^3D_3 - 6p\ ^3P_2^\circ$
2	1090.82	91674.2	$5s\ ^3D_1 - 6_2$
4	1085.79*	92098.8	$5s\ ^3D_3 - 4d^9 6p\ ^3P_1^\circ$
8	1084.87	92176.9	$5s\ ^3D_3 - 6p\ ^3D_2^\circ$
4	1083.67	92279.0	$5s\ ^3D_3 - 6p\ ^3D_3^\circ$
4	1082.25	92400.1	$5s\ ^3D_3 - 2_1 \text{ or } 1$
8	1082.11	92412.0	$5s\ ^3D_1 - 4d^9 6p\ ^3P_0^\circ$
0	1080.07	92586.6	$5s\ ^1D_2 - 7_2$
6	1077.83	92779.0	$5s\ ^3D_1 - 4d^9 6p\ ^3F_2^\circ$ $5s\ ^3D_2 - 6p\ ^3F_3^\circ$
6	1076.99	92851.4	$5s\ ^3D_2 - 3_2$
12	1072.23	93263.6	$5s\ ^3D_2 - 4d^9 6p\ ^3F_3^\circ$
5	1069.69*	93485.0	$5s\ ^3D_1 - 6p\ ^3D_1^\circ$
5	1069.25	93523.5	$5s\ ^3D_2 - 1_4$
6	1068.37	93600.5	$5s\ ^3D_2 - 4_3$
1	1066.91	93728.6	$5s\ ^3D_1 - 4d^9 6p\ ^1D_2^\circ$
1	1066.61	93755.0	$5s\ ^3D_2 - 6p\ ^3D_2^\circ$
10	1065.49	93853.5	$5s\ ^3D_2 - 6p\ ^3D_3^\circ$
4	1063.20	94055.7	$5s\ ^3D_2 - 5_1 \text{ or } 3$
3	1058.99	94429.6	$5s\ ^3D_3 - 3_2$
7	1056.28	94671.9	$5s\ ^3D_2 - 6_2$
6	1050.67	95177.4	$5s\ ^3D_3 - 4_3$
4	1047.23	95490.0	$5s\ ^3D_1 - 8_2$
0	1044.14	95772.6	$5s\ ^3D_2 - 4d^9 6p\ ^3F_2^\circ$
4	1040.69*	96090.1	$5s\ ^3D_2 - 6p\ ^1P_1^\circ$
1	1038.95	96251.0	$5s\ ^3D_2 - 6_2$
5	1036.99	96432.9	$5s\ ^3D_2 - 4d^9 6p\ ^1F_3^\circ$
2	1036.41	96486.9	$5s\ ^3D_3 - 6p\ ^3D_1^\circ$
3	1033.84	96726.8	$5s\ ^3D_3 - 6p\ ^1D_2^\circ$
1	1028.55	97224.2	$5s\ ^3D_1 - 9_2$
6	1021.53	97892.4	$5s\ ^3D_2 - 7_2$
2	1020.29	98011.3	$5s\ ^1D_2 - 4d^9 6p\ ^1F_3^\circ$
1	1017.26	98303.3	$5s\ ^3D_3 - 6p\ ^1D_2^\circ$
5	1015.37	98486.3	$5s\ ^3D_2 - 8_2$
15	1005.32	99470.8	$5s\ ^3D_3 - 7_2$
5	999.38	100062.	$5s\ ^1D_2 - 8_2$
5	997.80	100220.	$5s\ ^3D_2 - 9_2$
1	982.33	101799.	$5s\ ^3D_2 - 9_2$
30	752.80*	132837.	$4d^{10}\ ^1S_0 - 4d^9 6p\ ^3P_1^\circ$
25	730.83*	136831.	$4d^{10}\ ^1S_0 - 6p\ ^1P_1^\circ$
3	728.73*	137225.	$4d^{10}\ ^1S_0 - 6p\ ^3D_1^\circ$

* Classification by Duffendack and Thomson.[3] *ur* unresolved line; *d* diffuse line.

whose origin is unknown but which possibly arise from the configuration $4d^8 5s5p$. These terms are designated by numbers with the assigned j value as subscript. A few additional lines arising from the transition $4d^9 5p - 4d^9 5d$ have been identified. Among these, the line $4d^9 5p\ ^3P_1^\circ - 4d^9 5d\ ^1S_0$ is of interest in that it confirms Blair's $4d^9 5d\ ^1S_0$ term.

The extension of the $4d^9 ns\ ^{3,1}D$ series permits the calculation of the series limit by means of a Ritz formula. The application of this formula to the $4d^9 6s$, $7s$ and $8s\ ^3D_3$ terms yields 134,110 cm^{-1} as the limit of this series with respect to the $4d^9\ ^2D_{2\frac{1}{2}}$ term of Ag III. The $4d^{10}\ ^1S_0$ term of Ag II is 39,164 cm^{-1} below $4d^9 5s\ ^3D_3$. Thus the absolute value of the $4d^{10}\ ^1S_0$ term of Ag II is 173,274 cm^{-1} with respect to the $4d^9\ ^2D_{2\frac{1}{2}}$ level of the Ag III ion. This corresponds to an ionization potential of 21.4 volts. By the application of a Rydberg formula to the $4d^9 5s$ and $6s\ ^3D_3$ terms, Shenstone[7] obtained a value of 21.9 volts for this quantity. The Ritz formula for the $4d^9 ns\ ^3D_3$ series is:

$$T_m = 134{,}110 - \nu = RZ^2/[m - 3.07285 - 8.047\times 10^{-7}(T_m)]^2.$$

Of the $4d^9 ns\ ^{3,1}D$ series, the $^3D_3$ and $^3D_2$ series converge to the $4d^9\ ^2D_{2\frac{1}{2}}$ state of Ag III and the $^3D_1$ and $^1D_2$ series converge to $4d^9\ ^2D_{1\frac{1}{2}}$. The calculation of the limits for these four series by means of a Ritz formula should yield the separation of the $4d^9\ ^2D$ terms of Ag III with considerable accuracy. The results are as follows:

Series	*Term value of $4d^9 5s\ ^3D_3$	Limit in Ag III
$ns\ ^3D_3$	134,110 cm^{-1}	$4d^9\ ^2D_{2\frac{1}{2}}$
$^3D_2$	134,111	$^2D_{2\frac{1}{2}}$
$^3D_1$	138,716	$^2D_{1\frac{1}{2}}$
$^1D_2$	138,718	$^2D_{1\frac{1}{2}}$

* As obtained from the series indicated in column one and referred to the limit indicated in column three.

From the average of these results, the separation of, the $4d^9\ ^2D$ terms of Ag III should be 4607 cm^{-1}. This is in agreement with the separation reported by Gibbs and White[11] and with that recently found by the author in his analysis of the Ag III spectrum the results of which will soon be published. Thus the correctness of the classifications here reported is further confirmed.

The author acknowledges with pleasure the advice and criticism of Professor R. C. Gibbs during the course of this investigation. He is also indebted to Dr. C. W. Gartlein for the design of the Schüler tube and for assistance in some of the experimental work.

[11] Gibbs and White, Phys. Rev. **32**, 318 (1928).

JUNE 1, 1935 PHYSICAL REVIEW VOLUME 47

Neutron-Proton Interaction

Part I. The Binding Energies of the Hydrogen and Helium Isotopes

EUGENE FEENBERG, *Research Laboratory of Physics, Harvard University*

(Received April 1, 1935)

In the present state of nuclear theory it is reasonable to assume, for particles bound in the same nucleus, that the neutron-proton interaction operator can be represented fairly well by a potential function $J(r)$. By taking $J(r)$ to have the form $Ae^{-\alpha r^2}$, which is well adapted to the discussion of the three- and four-body problems, A and α have been determined to fit the binding energies of the deuteron and the alpha-particle. The results are roughly $A = 170$ mc^2, $1/\alpha^{1/2} = 1.3 \times 10^{-13}$ mc, with both the Wigner and Majorana theories. The computed binding energy of H^3 has the value 12.7 mc^2 (Wigner) or 11.2 mc^2 (Majorana), not very far below the experimental value of 16 mc^2. The two theories appear to be about equally good.

Section I. Introduction

THE proton-neutron nuclear model[1, 2, 3] in which the important internuclear interactions are those between neutrons and protons provides a satisfactory explanation of the most striking features of nuclear structure. These are:

(a) The large ratio of binding energies of the alpha-particle and deuteron and the general linear increase of binding energy with mass

[1] Heisenberg, Zeits. f. Physik **77**, 1 (1932); **78**, 156 (1932); **80**, 587 (1933).
[2] E. Majorana, Zeits. f. Physik **82**, 137 (1933).
[3] Wigner, Phys. Rev. **43**, 252 (1933).

number for the light and intermediate nuclei.

(b) The existence of a long series of light nuclei for which the mass number is exactly double the charge number.

(c) The general tendency, for intermediate and heavy nuclei, of the mass charge ratio to increase with increasing charge.

The first part of (a) can be understood in terms of a very large neutron-proton interaction with a range of about 10^{-13} cm. The small binding energy of the deuteron results then from the almost complete cancelation of a large kinetic energy against an only slightly larger potential energy.[4] The second part of (a) can be understood in terms of the Majorana form of exchange interaction. Item (b) implies that the neutron-neutron interaction is relatively small so that in a hypothetical series of light nuclei of given mass the most stable arrangement is the one with the largest possible number of proton-neutron interaction terms.[1] The long range Coulomb repulsive force between the protons decreases the binding energy by a term proportional to the five-thirds power of the charge number[5] and hence with increasing charge number tends to shift the most stable arrangement toward a neutron-proton ratio greater than unity. This is the explanation of (c).

For particles bound in the same nucleus, it is a plausible assumption that the neutron-proton interaction operator can be represented fairly well by a potential operator $J(r)P_{np}$ with $J(r)$ a function of the separation r and P_{np} an "exchange" operator which works on the coordinates of the two particles. This assumption is basic to the nuclear theories of Heisenberg, of Majorana and of Wigner. In the Heisenberg theory P_{np} interchanges both the space and spin coordinates of the particles, in Majorana's theory only the space coordinates are interchanged. In Wigner's theory P_{np} drops out (in other words the Wigner theory is a direct application of the Schrödinger wave equation). Only the latter two theories yield a stable alpha-particle. Because it is unsatisfactory in this respect the Heisenberg form of the exchange operator will not be considered further.

The Majorana theory provides that two particles with non-overlapping wave functions do not interact thus making long range interaction forces compatible with the observed roughly linear increase of binding energy with charge number. Under the same conditions the Wigner theory yields a dependence roughly quadratic in the charge number. With the short range forces required by the physical facts both theories, in conjunction with the Pauli principle applied separately to neutrons and to protons, make the alpha-particle a particularly stable system capable of playing the part of a secondary unit in the structure of complex nuclei. It was thought best to carry through calculations for both theories even though the Wigner theory is not acceptable for heavy nuclei.

The immediate problem is the determination of $J(r)$, a problem which Wigner[3] has already attacked with considerable success. In this paper the variation method of calculation is simplified and extended to the Majorana theory. A non-rigorous method of reducing the three- and four-body systems to "equivalent" two-body systems is also developed. It is believed that the results obtained are more accurate than those of Wigner.

The Hamiltonian operator in the Wigner theory is

$$H=-\tfrac{1}{2}\sum\Delta_i-\sum J(r_{pipj}), \qquad (1a)$$

and in the Majorana theory

$$H=-\tfrac{1}{2}\sum\Delta_i-\sum J(r_{pipj})P_{pipj}. \qquad (1b)$$

The units are $m_e c^2=510{,}000$ e.v. for energy and $(h^2/4\pi^2c^2m_em_p)^{\frac{1}{2}}=8.97\times10^{-13}$ cm for length. The operator P_{pipj} changes a function $\psi(\cdots x_{pi}\cdots x_{nj}\cdots)$ into $\psi(\cdots x_{nj}\cdots x_{pi}\cdots)$ and thus merely multiplies by ±1 any function which is symmetric or anti-symmetric with respect to interchange of the space coordinates of the particles pi and nj. The energy is given by the equation[6]

$$E^0=\int\cdots\int\psi H\psi d\tau \qquad (2)$$

in terms of the Hamiltonian, H, and the normalized wave function ψ.

The experimental facts to be correlated and explained are summarized in Table I. In computing the energies, the mass of the neutron is

[4] Wigner, Zeits. f. Physik **83**, 253 (1933).
[5] Gamow, *Atomic Nuclei and Radioactivity*, p. 19.
[6] The superscript 0 will be used to designate energies computed by the variation method.

TABLE I. *Masses and binding energies of hydrogen and helium isotopes.*

Atom	Mass	Binding energy*
H^2	2.0136 ±0.0001[7]	4.0±1.1
H^3	3.0151 ±(?)[8]	16.0±1.7 (?)
He^3	3.0163 ±0.0004[8]	13.4±1.7
He^4	4.00216±0.0002	54.0±2.2

* With respect to free neutron and hydrogen atoms.

taken as 1.0080±0.0005[9] and of the hydrogen atom as 1.0078.

SECTION II. THE TWO-BODY EQUATION

We write $J(r)$ in the form $Af(\alpha^{\frac{1}{2}}r)$. It will be necessary to make a definite assumption about the form of f, but, for the moment, all that need be stated is that f is a positive valued function which vanishes rapidly for large values of the argument. The positive valued parameters A and α are to be determined to fit the binding energies of the deuteron and the alpha-particle. Evidently A and $1/\alpha^{\frac{1}{2}}$ are directly proportional to the depth and breadth, respectively, of the potential well. We are looking for a solution of the equation

$$\{d^2/dr^2+E+Af(\alpha^{\frac{1}{2}}r)\}\varphi=0 \qquad (3)$$

which vanishes at both $r=0$ and $r=\infty$ and does not vanish anywhere else. In our problem we know the value of $E(E=-4.0)$ and will use the differential equation to obtain a relation between A and α; thus $A=A(\alpha)$ or, more conveniently $A/\alpha=g(\alpha)$. Anywhere on this line in A, α space the normal state solution of (3) has the eigenvalue $E=-4$. This procedure reduces the two-parameter potential to a one-parameter function.

It is convenient to insert here the proof of a theorem which will be needed later. Suppose that the relation $A/\alpha=g(\alpha)$ is known. Then it can be used to compute the normal state eigenvalue for arbitrary values of A and α which do not satisfy the relation: say $A=B$, $\alpha=\beta$. For let $r=m^{1/2}s$ with m a positive constant. The differential equation becomes

$$\{d^2/ds^2+mE+mBf((m\beta)^{1/2}s)\}\varphi=0. \qquad (4)$$

Now if $mE=-4$, the quantities mB and $m\beta$ are related by the equation $mB=A(m\beta)$, or $mB/m\beta=B/\beta=g(m\beta)$. Hence $m\beta$ is known and from it the required value of m. The desired eigenvalue is just $-4/m$.

Considerations of simplicity and elegance lead to the assumption that $J(r)$ belongs to the two parameter family of functions $Ae^{-\alpha r^2}$. With $J=Ae^{-\alpha r^2}$ the relation $A=A(\alpha)$ was determined by a number of numerical integrations. Table II

TABLE II. $A(\alpha)$ *for* $-E(H^2)=4.0$.

A/α	3.45	3.66	3.88	4.11	4.35	4.60	4.85	5.10	5.36
$1/\alpha^{1/2}$	0.12	0.15	0.18	0.21	0.24	0.27	0.30	0.33	0.36

gives A/α as a function of $1/\alpha^{\frac{1}{2}}$. The relation is almost linear.

With the approximate wave function

$$\varphi=(\nu/\pi)^{3/4}re^{-\nu r^2/2}$$

the variation Eq. (2) has the explicit form

$$E^0=(3/2)\alpha\sigma-A(\sigma/(\sigma+1))^{\frac{1}{2}}, \quad \sigma=\nu\alpha. \qquad (5)$$

Eq. (5) is needed for comparison with later results.

SECTION III. THE THREE- AND FOUR-BODY PROBLEMS

A suitable and fairly flexible wave function for use in (2) is obtained if we approximate to ψ by a product of functions each depending only on the distance between one pair of particles: thus

$$\psi(1, 2, 3)=u(12)u(13)v(23) \qquad (6)$$

for H^3 and He^3 and

$$\psi(1, 2, 3, 4)=u(13)u(14)u(23)u(24)v(12)v(34) \qquad (7)$$

for the alpha-particle. The u's tie together unlike particles while the v's serve to increase the average potential field in which the particles move by holding like particles together. It turns out that the v's are important in both theories and absolutely essential in the Majorana theory. With these wave functions (2) can be put in the form

$$E^0(H^3)=X(H^3)+Y(H^3)-Z(H^3), \qquad (8)$$

$$E^0(He^4)=-Q(H^3)+X(He^4)+Y(He^4)-Z(He^4), \qquad (9)$$

[7] Bainbridge, Phys. Rev. **44**, 56 (1933).
[8] Oliphant, Harteck and Rutherford, Nature **133**, 413 (1934); Proc. Roy. Soc. **A144**, 692 (1934); and Dee, Proc. Roy. Soc. **A148**, 623 (1935).
[9] Chadwick and Goldhaber, Nature **134**, 237 (1934).

in which

$$X(\mathrm{H}^3)=\tfrac{1}{2}\int\int\int\{3\,|\nabla_1 u(13)\,|^2-u(13)\Delta_1 u(13)\}\int\int\int u^2(12)v^2(23)d\tau_2 d\tau_{13},$$

$$Y(\mathrm{H}^3)=-\int\int\int v(23)\Delta_2 v(23)\int\int\int u^2(12)u^2(13)d\tau_1 d\tau_{23},$$

$$Z(\mathrm{H}^3)=2\int\int\int u^2(13)J(13)\int\int\int[u^2(12)v^2(23)]d\tau_2 d\tau_{13},$$

$$Q(\mathrm{He}^4)=\int\cdots\int u^2(23)\nabla_1 u^2(13)\cdot\nabla_1 v^2(12)\int\cdots\int u^2(24)u^2(14)v^2(34)d\tau_3 d\tau_4 d\tau_{12}, \tag{10}$$

$$X(\mathrm{He}^4)=2\int\int\int\{\,|\nabla_1 u(13)\,|^2-u(13)\Delta_1 u(13)\}\int\cdots\int u^2(14)u^2(23)u^2(24)v^2(12)v^2(34)d\tau_2 d\tau_4 d\tau_{13},$$

$$Y(\mathrm{He}^4)=-2\int\int\int v(12)\Delta_1 v(12)\int\cdots\int u^2(13)u^2(14)u^2(23)u^2(24)v^2(34)d\tau_3 d\tau_4 d\tau_{12},$$

$$Z(\mathrm{He}^4)=4\int\int\int u^2(13)J(13)\int\cdots\int u^2(24)[u^2(23)u^2(14)v^2(12)v^2(34)]d\tau_2 d\tau_4 d\tau_{13}.$$

Eq. (10) is correct for the Wigner operator and with the exception of $Z(\mathrm{H}^3)$ and $Z(\mathrm{He}^4)$ also for that of Majorana; the correct Z's in the latter theory are obtained if in the square brackets the functions $u^2(a1)$, $u^2(b3)$ are replaced by $u(a1)\cdot u(a3)$ and $u(b3)\,u(b1)$, respectively, and the same substitution applied to $v^2(a1)$, $v^2(b3)$. The symbols (W) and (M) will be used to refer to the two theories.

One result we get immediately from (10) without further calculation. In the $\mathrm{H}^3(W)$ problem, if v is replaced by a constant, Y vanishes and X and Z each reduce to twice the corresponding terms in the two-body variation problem. Hence for a constant v, the u which minimizes the three-body energy integral is the solution of the two-body equation.[3] Consequently

$$-E(\mathrm{H}^3)>-2E(\mathrm{H}^2)=8.0,\quad (W). \tag{11}$$

There is another more general argument which gives (11) again and a corresponding lower bound for the alpha-particle. The ratio of the numbers of potential and kinetic energy terms in the energy operator increases in passing from H^2 to H^3 and again in passing from H^3 to He^4. Moreover, the wave functions overlap, causing the potentials to overlap also, so that the magnitude of the effective potential in which each particle moves increases along the series H^2, H^3, He^4. Also the wave functions in all three problems have no nodes. For these reasons, and most important of all, because both the depth and breadth of the potential hole are changed together in such a manner that the binding energy of the two-body problem remains fixed at the experimental value, the exact binding energies of the three- and four-body problems must *increase* with *decreasing* effective width of the potential hole and more rapidly for the alpha-particle than for the three-body nucleus. With a hole of infinite width the kinetic energy vanishes and the potential energy is just the number of particles times the limiting value of A which is 4. This gives (11) again and the following lower bound for the binding energy of the alpha-particle:

$$-E(\mathrm{He}^4)>-4E(\mathrm{H}^2)=16.0,\quad (W). \tag{12}$$

To make clear the difficulties which must be overcome in applying the variation method to the three- and four-body problems a brief discussion of the two-body variation problem is inserted here. As the breadth of the potential well is narrowed the average correct kinetic and potential energies grow rapidly larger. This is associated with a constant value of the difference which, except for very broad holes, is a small fraction of either energy term alone. It is evident that an approximate wave function must meet more and more rigorous conditions as the hole is narrowed if the variation method is to give uniformly good results. If the wave function is not continually improved the computed binding energy will fall more and more below the correct value and for a sufficiently narrow hole will become negative. This conclusion is brought out clearly in Table III which is based on Eq. (5). At $\alpha=20$ the com-

TABLE III. *The variation method applied to* H^3.

α	K.E.*	−P.E.*	$-E$
20	18.4	19.8	1.4
30	22.6	22.7	0.1
50	27.2	24.7	−2.5

* K.E.—kinetic energy.
P.E.—potential energy.

puted energy is only thirty-five percent of the correct value. However, a comparison of the correct and approximate wave functions reveals that they agree quite well up to a distance of separation which includes eighty percent of the probability density. If $-E^0(H^2)$ is plotted against α the resulting curve is a straight line with an intercept at $\alpha=0$ having exactly the correct value, $-E(H^2)=4$. *Evidently for a sufficiently broad potential hole the variation method gives excellent results.* From Table III we draw the conclusion that if the binding energy of the three-body problem increases quite slowly with increasing α, a simple variation method is likely to yield values for $-E^0(H^3)$ which decrease with increasing α.

Returning to the many-body problem it is evident that in general the inside integrations in (10) present formidable difficulties. Fortunately there does exist a functional form for which the integration is elementary and the result simple. This form is the Gaussian error function which has already been taken for the potential. Setting

$$u=Ne^{-\nu r^2/2}, \quad v=Ne^{-\mu r^2/2} \tag{13}$$

we find after an elementary calculation the following explicit expressions for the energies with the Wigner Hamiltonian:

$$E^0(H^3)=3/2\{(2+3n+n^2)/(1+2n)\}\alpha\sigma-2A(\sigma/\sigma+1)^{\frac{1}{2}}, \qquad n=\mu/\nu, \qquad \alpha\sigma=\nu(1+2n)/(1+n), \tag{14}$$

$$E^0(He^4)=3/4\{(6+5n+n^2)/(1+n)\}\alpha\sigma-4A(\sigma/(\sigma+1))^{\frac{1}{2}}, \qquad n=\mu/\nu, \qquad \alpha\sigma=4\nu(1+n)/(3+n). \tag{15}$$

The substitution into (14) and (15) of the value of n for which the energies are as small as possible leaves expressions for the energies containing only one variable parameter:

$$E^0(H^3)=2.7991\alpha\sigma-2A(\sigma/(\sigma+1))^{\frac{1}{2}}, \qquad 2n=\sqrt{3}-1, \qquad \nu=0.7887\alpha\sigma, \tag{16}$$

$$E^0(He^4)=4.3713\alpha\sigma-4A(\sigma/(\sigma+1))^{\frac{1}{2}}, \qquad n=\sqrt{2}-1, \qquad \nu=0.6036\alpha\sigma. \tag{17}$$

The corresponding results for the Majorana Hamiltonian are

$$E^0(H^3)=6\{(2+n)/(5+n)\}\alpha\sigma-16A\{(1+2n)/(5+6n+n^2)\}^{\frac{1}{2}}(\sigma/(\sigma+1))^{\frac{1}{2}}, \qquad n=\mu/\nu, \qquad 4\alpha\sigma=\nu(5+n), \tag{18}$$

$$E^0(He^4)=6\{(2+n)/(3+n)\}\alpha\sigma-64\times 2^{\frac{1}{2}}A\{(n+1)^{\frac{1}{2}}/(n+3)^3\}(\sigma/(\sigma+1))^{\frac{1}{2}}, \qquad n=\mu/\nu, \qquad 2\alpha\sigma=\nu(3+n). \tag{19}$$

In this case the best choice of n depends on the value given to σ, but the dependence is so slight that it may be ignored. It was found by trial that $n=0.5$ and $n=0.7$ give about the best results in (18) and (19), respectively. With these values of n the expressions for the energies are

$$E^0(H^3)=2.7273\alpha\sigma-1.9098A(\sigma/(\sigma+1))^{\frac{1}{2}}, \qquad n=0.5, \qquad \nu=0.7273\alpha\sigma, \tag{20}$$

$$E^0(He^4)=4.3784\alpha\sigma-3.9606A(\sigma/(\sigma+1))^{\frac{1}{2}}, \qquad n=0.7, \qquad \nu=0.5405\alpha\sigma. \tag{21}$$

The coulomb energy corrections ΔE for He^3 and He^4 due to repulsion between the protons are computed by a first order perturbation calculation and prove to be

$$\Delta E(He^3)=(\nu+2\mu)^{\frac{1}{2}}/4, \qquad \Delta E(He^4)=(2\nu+2\mu)^{\frac{1}{2}}/4. \tag{22}$$

Numerical results obtained from (16), (17), (20), (21), (22) in conjunction with Table II are collected in the Tables IV and V.

TABLE IV. *The variation method applied to He⁴.*

α	Effective radius $\bar{\alpha}^{1/2}\times10^{13}$ cm		A	Eq. (17) (W) K.E.	$-$P.E.	$-E^0$	Eq. (21) (M) $-E^0$	C.E.*
20	0.224	2.00	84.4	90.2	122.1	31.9	30.6	1.5
30	0.183	1.64	117.1	121.7	156.4	34.7		1.7
40	0.158	1.42	148.8	151.2	187.9	36.7		1.9
50	0.141	1.27	180.0	179.6	218.1	38.5	36.1	2.1
75	0.116	1.04	256.4	247.2	289.0	41.8	38.6	2.5

* C.E.—Coulomb energy.

TABLE V. *The variation method applied to H³, He³.*

α	Eq. (16) (W) K.E.	$-$P.E.	$-E_0$	Eq. (20) (M) $-E_0$	He³ only C.E.*
20	39.5	44.9	5.4	4.5	1.1
50	67.9	67.2	-0.7	-2.0	1.4
75	83.7	78.0	-5.7	-7.0	1.6

* C.E.—Coulomb energy.

The rapid increase of $-E^0(\mathrm{He}^4)$ with α indicates that the variation method works quite well when applied to the four-body problem. It yields values for $E^0(\mathrm{He}^4)$ lying between 3/5 and 4/5 of the experimental binding energy, the largest value occurring for the smallest effective radius in the range 10^{-13} cm to 2×10^{-13} cm. However the method is unsatisfactory in the three-body problem as Table V shows. The striking feature of Table V is that $-E^0(\mathrm{H}^3)$ decreases with decreasing effective radius and actually becomes negative for sufficiently small values of $1/\alpha^{\frac{1}{2}}$. But this result we had reason to anticipate. It is proper to compare $2E^0(\mathrm{H}^2)$ with $E^0(\mathrm{H}^3)$ (because there are two potential terms in the three-body Hamiltonian and only one in the equation for the deuteron. The tables show that the kinetic energy of H^2 is less than half that of H^3). From the tables it is seen that $2E^0(\mathrm{H}^2)-E^0(\mathrm{H}^3)$ increases as the effective radius is made smaller showing that the variation method is less unsatisfactory for H^3 than for H^2.

The energy intercept at $\alpha=0$ is equal to the limiting value of the coefficient of $(\sigma/(\sigma+1))^{\frac{1}{2}}$ in the energy formula. The minimum property of the variation method and the fact that the actual binding energy $-E(\mathrm{H}^3)$ must increase with α yields (11) again and a new result

$$-E(\mathrm{H}^3)>7.64, \quad (M). \tag{23}$$

The energies given by the Majorana theory lie above those of the Wigner theory as required by a general theorem due to Eckart[10] on the relation between the two forms of the interaction operator.

SECTION IV. THE METHOD OF THE "EQUIVALENT" TWO-BODY EQUATION

The results of the preceding section indicate that the effective radius of interaction falls somewhere in the range 10^{-13} to 2×10^{-13} cm. To get a more definite result we might attempt to improve the variation method by using better wave functions. But any simple change in the wave function immediately complicates the calculation many-fold and is not likely, in the case of H^3, to yield better results than we already have in (11) and (23). We must help ourselves in some other way. The method adopted by the writer is based on analogy and considerations of plausibility although it appears that a rigorous justification may be possible.

We observe that the variation Eqs. (5), (16), (17), (20) and (21) all have the form

$$E^0=3\beta'\sigma/4m-B(\sigma/(\sigma+1))^{\frac{1}{2}} \tag{24}$$

with suitable choice of m, β' and B. But in the case of the general two-body problem with reduced mass m (24), is obtained from the equation

$$\{d^2/ds^2+E'+Be^{-\beta s^2}\}\varphi=0 \tag{25}$$

in which $\beta=\beta'/2m$ and $s=(2m)^{\frac{1}{2}}r$ (cf. fine print in Section II). We therefore associate with each many-body problem an equation of the form (25) in which B and β have the following values fixed by direct comparison of (24) with (16), (17), (20) and (21):

$$\left.\begin{aligned} B&=4A\\ \beta&=2.9142\alpha\end{aligned}\right\}\mathrm{He}^4(W),$$

$$\left.\begin{aligned} B&=2A\\ \beta&=1.8660\alpha\end{aligned}\right\}\mathrm{H}^3,\ \mathrm{He}^3,\ (W),$$

$$\left.\begin{aligned} B&=3.9606A\\ \beta&=2.9189\alpha\end{aligned}\right\}\mathrm{He}^4,\ (M), \tag{26}$$

$$\left.\begin{aligned} B&=1.9098A\\ \beta&=1.8182\alpha\end{aligned}\right\}\mathrm{H}^3,\ \mathrm{He}^3,\ (M).$$

[10] Eckart, Phys. Rev. **44**, 109 (1933).

Note that in each case B and β are uniquely determined without regard to the value assumed for m. Now by the minimum property of the variation method, the lowest eigenvalue of (25), say E', lies below the corresponding E^0.

For the deuteron E' is the correct eigenvalue. In the case of the alpha-particle the depth and breadth of the "equivalent" potential are so large that (24) is able to yield fairly good results and hence is closely correlated with the differential Eq. (25). Since (25) is the correct deuteron equation and is closely related to the He^4 problem, the correlation between (24) and (25) should also be reasonably close for H^3 which falls between the deuteron and the alpha-particle and possesses the same type of nodeless wave function. We are led to suppose that E' should lie fairly close to the eigenvalue of the associated many-body problem. It is then obviously possible, although not necessary, to interpret (25) in terms of a physical model: for H^3, a neutron interacting with a deuteron, the neutron spins being parallel; in the case of the alpha-particle, the interaction of two deuterons with antiparallel spins or a neutron interacting with He^3 (neutron spins antiparallel). Values of E' computed in part directly by numerical integration and partly by the method described in Section II are presented in Table VI which should be compared with Tables IV and V based on the cruder method of Section III. It is seen that $-E'(He^4)$ crosses the experimental binding energy in the neighborhood of $\alpha = 50$. Here the computed coulomb energy for He^3 has the value 1.4. If this coulomb correction is subtracted from the *experimental* difference $E(He^3) - E(H^3) = 2.6$ there is left a remainder of 1.2 mc^2 which must be ascribed primarily to small *attractive* forces acting between the neutrons in H^3. But the approximate wave functions are too large for small separations and too small for large separations. Also the second order coulomb correction is negative. Hence this coulomb correction is probably excessive. Furthermore it is likely that for small separations the actual proton-proton potential lies far below the coulomb value and even changes sign.[11] All these considerations indicate that the proton-proton interaction in He^3 may be somewhat smaller than 1.4 mc^2 with the consequence that the neutron-neutron interaction energy in H^3 may be larger than 1.2 mc^2. In any event the sum of the two corrections should be small enough to permit a direct comparison of $-E(He^4)$ with the experimental value of 54 mc^2.

TABLE VI. *The "equivalent" two-body method.*

	β	α	$-E'$		β	α	$-E'$
$He^4(W)$	80.0	27.5	43.7	$He^4(M)$	105.1	36.0	47.2
	104.9	36.0	49.1		157.6	54.0	57.1
	120.0	41.2	51.9		200.3	68.6	64.0
	157.4	54.0	59.3				
	200.0	68.6	66.8	$H^3(M)$	36.4	20.0	9.0
					90.9	50.0	10.1
$He^3(W)$	37.3	20.0	10.2		136.4	75.0	10.7
	93.3	50.0	11.7				
	140.0	75.0	12.8				

We then find with the Wigner theory that $-E(He^4) = 54$ at the point $\alpha = 45 (1/\alpha^1 = 0.149$ or 1.34×10^{-13} cm), $A = 165$. The corresponding point for the Majorana theory is $\alpha = 48 (1/\alpha^1 = 0.144$ or 1.29×10^{-13} cm), $A = 174$. At these points the computed binding energy of H^3 is greater than $-E'(H^3) + 1.2 = 12.7$ (W) or $-E'(H^3) + 1.2 = 11.2$ (M). The agreement with the experimental value of 16.0 ± 1.7 is good enough to serve as a justification for the original assumption that the neutron-proton interaction operator can be represented fairly well by a potential function in the case of binding. The uncertainty in the method of calculation is too great to permit any conclusion about the relative merits of the two theories for the light nuclei. Incidently in all cases the normal state eigenvalue of the "equivalent" equation is the only energy level in the discrete spectrum.

It is a pleasure to acknowledge the help derived from discussions with Professor Van Vleck. The writer is very much obliged to Professor Hans Bethe for pointing out an error in the first draft of the paper.

[11] White, Phys. Rev. **47**, 573 (1935).

Neutron-Proton Interaction

Part II. The Scattering of Neutrons by Protons

EUGENE FEENBERG, *Research Laboratory of Physics, Harvard University*

(Received April 11, 1935)

It may be that also for free particles, as well as in the case of binding, the neutron-proton interaction operator can be represented by a potential $J_1(r)$. Because the conditions of binding and of scattering are so different there is no reason to expect J_1 to be identical with J, the potential for binding. The inequalities $J_1<J$ and $\partial J_1/\partial W<0$ (W denotes the kinetic energy) should hold if some part of the potential results from a polarization of each particle in the field of the other or from a high frequency exchange process. For slow neutrons a thirty percent *decrease* in the magnitude of the interaction in going from binding to free particles yields an *increase* in the cross section for scattering by protons of several hundred percent over the value given by J. This larger value is required by recent measurements. The rapid fall of the experimental cross section with increasing W requires that J_1 decrease steadily as W is made larger in accordance with the relation $J_1(r, v) = e^{-g(\beta_0 v+v^2/c)}J(r)$. Here g is a positive constant, v is the relative velocity of the colliding particles and $\beta_0 c$ is identified with the average relative velocity of the particles in the deuteron.

IN Part I of this paper[1] it was shown that the binding energies of the hydrogen and helium isotopes can be understood in terms of a neutron-proton interaction potential, $J(r)=Ae^{-\alpha^2 r^2}$, with $A=170\ m_e c^2$, $1/\alpha^1=1.3\times10^{-13}$ cm. These values are averages of those obtained from the theories of Wigner and of Majorana. The differences between the theories are not relevant to the present discussion.

There appears to be no good reason for believing that the representation of the interaction operator as a potential function is in any sense exact or fundamental. In fact, any potential function which is small except for distances of separation less than 10^{-12} cm and gives the correct value for the binding energy of the deuteron will yield for the scattering cross section of neutrons by protons values in striking disagreement with the experimental facts.[2] It seems necessary to suppose that the interaction operator involves both the separation of the particles and their momenta and also (in scattering problems) in some way the collision time. In the absence of a fundamental theory the only means of bringing to light the properties of the interaction operator is to make simple rather naive assumptions and compare the consequences with experiment. We need not expect any one simple assumption to be adequate for all problems. By comparing the different assumptions required to explain different phenomena, for example, binding and scattering, something may be learned about the fundamental interaction operator. From this point of view the potential $J(r)$ is an approximate representation of the unknown fundamental operator, suitable for the description of binding.

It may be that for the scattering of neutrons by protons as well as in the case of binding, the interaction operator can be represented approximately by a potential $J_1(r)$ (Wigner theory) or $J_1(r)P_{np}$ (Majorana theory). Now since the conditions of scattering and of binding are so very different, we need not be surprised if J_1 differs from J. A value for J_1 greater than J or a J_1 increasing with increasing relative velocity of the colliding particles would be difficult to understand. But the inequalities

$$J_1(r)<J(r), \quad \partial J_1/\partial W<0, \tag{1}$$

relating J_1 to J and expressing the trend of the dependence of J_1 on the relative kinetic energy, W, of the colliding particles, are acceptable. Indeed, (1) must hold if a mutual polarization of each particle in the field of the other contributes to the interaction potential or if some part of the interaction arises from a high frequency exchange process such as that suggested by Heisenberg.[3] To insure that (1) is satisfied we write

$$J_1(r)=e^{-f(W)}J(r), \tag{2}$$

[1] See preceding paper.

[2] Massey and Mohr, Proc. Roy. Soc. **A148**, 206 (1935).

[3] Heisenberg, Zeits. f. Physik **77**, 1 (1932).

in which $f(W)$ is a positive valued monotonic increasing function of W. This involves the assumption that the effective radius of interaction changes little in passing from conditions of binding to those of free particles. The simple qualitative picture of the relation between the binding and the scattering interactions expressed by (1) and (2) is consistent with the facts.

The essential experimental facts are these:[4] For very slow neutrons the cross section for scattering by protons has the large value 13.3×10^{-24} cm^2. The cross section falls rapidly with increasing velocity coming down to 2.53×10^{-24} cm^2 ($v=1.3\times10^9$ cm/sec.), 1.41×10^{-24} cm^2 ($v=2\times10^9$ cm/sec.), and 0.73×10^{-24} cm^2 ($v=3\times10^9$ cm/sec.).

We proceed to the determination of $f(W)$ by a comparison of computed cross sections with the experimental values using first the simple model defined by the equations[5]

$$\begin{aligned} &J(r)=D, \quad 0\leqq r\leqq a=0.15,\\ &J_1(r)=D_1(W)\equiv De^{-f(W)},\\ &J_1(r)=J(r)=0, \quad r>a. \end{aligned} \tag{3}$$

Here D has the value 139 computed from the relation[6]

$$D=(\pi/2a)^2+2|E|^{\frac{1}{2}}/a+|E|(1-4/\pi^2)-(4/\pi-\pi/3)|E|^{\frac{1}{2}}(8/\pi^3)a+\cdots \tag{4}$$

connecting the depth and breadth of the hole with the energy eigenvalue of H^2.

The cross section for scattering by the potential J is[6]

$$\sigma=10.1\{1+a|E|^{\frac{1}{2}}\}/(W+|E|), \tag{5}$$

in units of 10^{-24} cm^2, subject to the condition $a|E|^{\frac{1}{2}}\ll\pi^2/8$. In our case $a|E|^{\frac{1}{2}}=0.15\times2.0=0.30$ which is small enough. This yields about one-fourth of the experimental cross section for slow neutrons and double the experimental value for fast neutrons. It is not possible to obtain agreement for *either* high or low velocities by changing a within reasonable limits.

The cross section given by J_1 is most simply expressed in terms of the quantities $p=(W)^{\frac{1}{2}}$ and $x=\pi/2-a(D_1+W)^{\frac{1}{2}}$. The scattering cross section is easily shown to be

$$\sigma=10.1a^2\frac{\{\cos pa-(\pi/2-x)\tan x\cdot\sin pa/pa\}^2}{(\pi/2-x)^2\tan^2x+(pa)^2} \tag{6}$$

in units of 10^{-24} cm^2. Only the partial wave with zero angular momentum is here considered.[7] With the aid of (6) and the experimental cross sections $f(W)$ was first determined at $p=0.0$ and $p=2.0$. The assumption that $f(W)$ is a linear function of p then yields perfect agreement with the experimental cross sections for other values of p. In this way it was found that

$$\begin{aligned} J_1(r)&=e^{-0.09(3.74+p)}J(r),\\ &=e^{-1.93(0.15+v/c)}J(r), \end{aligned} \tag{7}$$

in the case of the simple model defined by (3).

We have used (3) because of its mathematical simplicity and because the cross section depends only slightly on the precise form of the potential. The analysis of the data, by means of numerical integrations, in terms of the Gaussian error potential leads to essentially the same functional dependence on W with slightly different numerical coefficients:

$$\begin{aligned} J_1(r)&=e^{-0.105(4.26+p)}Ae^{-ar^2}\\ &=e^{-2.26(0.20+v/c)}Ae^{-ar^2}. \end{aligned} \tag{8}$$

Eqs. (7) and (8) show that the transition from binding to free particles is marked by a thirty to thirty-five percent decrease in the depth of the potential hole. It should be noted that for low velocities a relatively small *reduction* (thirty percent) in the magnitude of the interaction is accompanied by an *increase* of several hundred percent in the collision cross section. The reason for this is plain from (5). As the bottom of the potential well is raised the eigenvalue is squeezed out and vanishes at a definite depth. At this point $\sigma(0)$ is infinite. Immediately beyond this

[4] Dunning, Pegram, Fink and Mitchell, Phys. Rev. **47**, 416 (1935); Bonner, Phys. Rev. **45**, 601 (1934). See also, Dunning, Phys. Rev. **45**, 586 (1934); Chadwick, Proc. Roy. Soc. **A142**, 1 (1933); Meiter and Philipp, Naturwiss. **20**, 929 (1932).

[5] The units are $m_e c^2=510{,}000$ e.v. for energy and $(\hbar^2/4\pi^2 m_e m_p c^2)^{1/2}=8.97\times10^{-13}$ cm for length.

[6] Wigner, Zeits. f. Physik **83**, 253 (1933).

[7] For the justification of this assumption see Bethe and Peierls, Proc. Roy. Soc. **A149**, 176 (1935).

depth there exists no discrete energy level, but σ is still very large.

Table I exhibits the results of the analysis.

TABLE I. *Cross sections computed from (7) and (8).*

	Rectangular potential well (7)		Gaussian error potential (8)
p^*	x	$\sigma\times10^{24}$ cm^2	$\sigma\times10^{24}$ cm^2
0.0	0.077	13.6	13.6
0.5	0.109	5.2	
1.0	0.134	2.4	2.4
1.5	0.156	1.3	
2.0	0.173	0.78	0.78

* v (in units of 10^9 cm/sec.) $=1.40\ p$.

These results demonstrate that the inequalities (1) are consistent with the experimental cross sections. But they do more than that. The function $f(W)$ has the form $g(\beta_0+v/c)$; clearly $c\beta_0$ must be interpreted as a velocity. The only velocity other than v which can possibly be associated with the neutron-proton scattering process is the average relative velocity of the particles in the deuteron. A numerical integration yields the value $23m_e c^2$ for the internal kinetic energy of the deuteron (compare Part I. Table III); hence the average relative velocity is 0.22 c, only ten or twenty percent larger than $\beta_0 c$. Since J_1 is less than J the acceleration experienced by the particles during a collision must be somewhat less than the acceleration to which particles in the deuteron are subjected. This enables us to understand why $\beta_0 c$ is smaller than the average relative velocity of the particles in the deuteron and yet of the same order of magnitude.

Heisenberg[3] has suggested that the interaction of neutrons with protons is associated with or caused by a high frequency exchange process. The frequency is determined by the relation

$$h\nu\sim J(r)m_e c^2\sim(hc/2\pi e^2)m_e c^2. \qquad (9)$$

It is not necessary, and perhaps undesirable, to say much about the physical nature of the exchange process. The idea of exchange forces transcends in its generality the simple nuclear theories (those of Heisenberg and of Majorana) in which it has consciously been used as a guide and hence may be applied without presupposing a definite physical model. What is essential is that the frequency given by (9) is associated with the interaction. The crudest sort of classical reasoning based on the interpretation of $\beta_0 c+v$ as the average velocity of the particles during the collision suggests that the collision time has the order of magnitude $(e^2/m_e c^2)/(\beta_0 c+v)$. The number of exchanges which occur during a collision is then

$$n\sim2\nu(e^2/m_e c^2)/(\beta_0 c+v)\sim c/\pi(\beta_0 c+v). \qquad (10)$$

There is time for only two or three exchanges even with the very slowest neutrons. It is not surprising then that J_1 should decrease rapidly with increasing W. The relation

$$J_1(r)\sim e^{-\theta/\pi n}J(r) \qquad (11)$$

obtained by combining (10) with (7) and (8) brings out the point that J_1 is equal to J when n is infinite (the case of binding). It may be concluded that the experimental results on scattering are consistent with and, perhaps, even lend support to the general qualitative picture of exchange forces.

Quantum Theory of Metallic Reflection

L. I. SCHIFF AND L. H. THOMAS, *Mendenhall Laboratory of Physics, Ohio State University*

(Received April 6, 1935)

In the classical (Drude) theory of the reflection and transmission of light at a metal surface, the component of electric intensity perpendicular to the surface is discontinuous there, the remaining components of the field vectors being continuous. In a more detailed description the interaction of the light with the metal is expressed as scattering by the conduction electrons according to quantum theory. Those components of the field vectors which were continuous in the classical theory retain very approximately their values in that theory. The electric intensity perpendicular to the surface, though given approximately elsewhere by the classical theory, fluctuates widely within a few electron wavelengths of the surface. If this fluctuating field is used to calculate the surface photoelectric effect by Mitchell's method, the agreement of his result for a clean potassium surface with observation is improved. To a first approximation, the new theory predicts that the frequency at the peak of the spectral distribution curve for a clean surface of a metal depends only on the number N of free electrons per unit volume, and for different metals varies approximately as $N^{1/2}$; although the experimental results are uncertain, this is roughly the case. No calculations have been made for sensitized surfaces, but arguments based on the use of the Drude form seem to be precarious.

1. INTRODUCTION

THE classical phenomenological theory of the optical properties of metals assumes a discontinuous change in the optical constants at the surface of the metal. This implies a discontinuity in the normal component of the electric vector of the light at the surface, and hence a periodically varying surface charge density there. On the other hand, we should expect a quantum-mechanical treatment to give us a continuous electric field at the surface, and a transition layer near the surface in which the optical constants may be regarded as varying continuously from the values outside the metal to the values some distance within the metal, the latter being given by either the Drude or the Kronig theory.

In order to be able to write down the wave functions of the electrons within the metal, we must first make some simplifying assumptions about its internal structure. Kronig's[1] theory assumes that each electron moves effectively in a triply periodic potential field due to the positive ions of the lattice and the remaining electrons. It follows as a consequence of this theory that if the frequency is sufficiently greater than the reciprocal of the "relaxation time"[2] of a current set up in the lattice, the effects of the lattice are negligible, and the electrons may be treated as effectively free; for the alkali metals this seems to hold in the visible and ultraviolet regions. Zener[3] has shown indeed that the limits of transparency to ultraviolet light of the alkali metals as calculated from a free electron theory are in fair agreement with experiment. Under these circumstances, then, the electrons inside the metal may be treated as a Fermi gas. In such a treatment, we assume that apart from external disturbances, a particular electron moves in a field free space, the field of the rest of the electrons and that of the positive ions just cancelling each other. Darwin[4] has shown that in this case, the force acting on each electron is the "tube-force" or molar electric field, and not the Lorentz force.

2. THEORY FOR A GENERAL SURFACE BARRIER

We take for the wave equation representing an electron moving in a vector potential $\mathbf{A}$ and a scalar potential V (when the charge on an electron is $-e$):

$$-\frac{h^2}{8\pi^2 m}\nabla^2 u+\frac{eh}{2\pi imc}(\mathbf{A}\cdot\nabla)u-eVu-\frac{ih}{2\pi}\frac{\partial u}{\partial t}=0 \tag{1}$$

[1] R. de L. Kronig, Proc. Roy. Soc. **A124**, 409 (1929); **A133**, 255 (1931).
[2] Reference 1, p. 415 of the 1929 paper.
[3] C. Zener, Nature **132**, 968 (1933).
[4] C. G. Darwin, Proc. Roy. Soc. **A146**, 17 (1934).

for the light wave:

$$\mathbf{A}=\mathbf{B}(x)e^{-2\pi i\nu(t-(z\sin\theta)/c)}+\mathbf{B}^*(x)e^{2\pi i\nu(t-(z\sin\theta)/c)}, \qquad V=0 \tag{2}$$

($V=0$ being provided by a change of gauge[5]), and for the surface barrier:

$$V=V(x), \qquad V(-\infty)=V_1, \qquad V(+\infty)=V_0. \tag{3}$$

The metal is taken to fill the half-space on the negative side of the yz plane. $V(x)$ is an arbitrary known function representing the effect of the surface, that has the limiting values at $\pm\infty$, and $\mathbf{B}(x)$ is an unknown, but definite vector function. We first find the solutions w of the unperturbed equation ($\mathbf{A}=0$):

$$-(h^2/8\pi^2m)\nabla^2w-eVw-(ih/2\pi)(\partial w/\partial t)=0, \tag{4}$$

which, for energy $E<-eV_0$ and coefficients k_y and k_z of y and z in the exponent take the form:

$$w=\{A_1\psi_1(x)+A_2\psi_2(x)\}e^{i(k_yy+k_zz)}e^{-2\pi iEt/h}, \tag{5}$$

where[6]

$$\psi_1(-\infty)\approx e^{-ik_xx}, \qquad \psi_2(-\infty)\approx e^{ik_xx}, \qquad A_1\psi_1(+\infty)+A_2\psi_2(+\infty)\approx A_3e^{-px},$$
$$k_x^2=(8\pi^2m/h^2)(E+eV_1)-k_y^2-k_z^2, \qquad p^2=-(8\pi^2m/h^2)(E+eV_0)+k_y^2+k_z^2$$

(k_x and p are positive). Then putting $u=v+w$, v is given to a first approximation as a solution of:

$$-(h^2/8\pi^2m)\nabla^2v-eVv-(ih/2\pi)(\partial v/\partial t)=-(eh/2\pi imc)(\mathbf{A}\cdot\nabla)w. \tag{6}$$

After putting in the values of $\mathbf{A}$ and w, this may be solved by writing v in the form:

$$v=\phi_1(x)e^{i(k_yy+k_zz)}e^{-(2\pi i/h)(E+h\nu)t}e^{2\pi i\nu(z\sin\theta)/c}+\phi_2(x)e^{i(k_yy+k_zz)}e^{-(2\pi i/h)(E-h\nu)t}e^{-2\pi i\nu(z\sin\theta)/c}, \tag{7}$$

where $\phi_1(x)=a_1(x)\psi_1^{(1)}(x)+a_2(x)\psi_2^{(1)}(x), \qquad \phi_2(x)=b_1(x)\psi_1^{(2)}(x)+b_2(x)\psi_2^{(2)}(x).$ (8)

Neglecting v/c in comparison with k_x (for the greater part of the electrons, the latter is about a thousand times the former) we obtain:

$$\begin{aligned}a_1(x)&=c_1+(2\pi e/chq)\textstyle\int_0^x\psi_2^{(1)}\{i\mathbf{B}_x(s)(A_1\psi_1'+A_2\psi_2')-(k_y\mathbf{B}_y(s)+k_z\mathbf{B}_z(s))(A_1\psi_1+A_2\psi_2)\}ds,\\ a_2(x)&=c_2-(2\pi e/chq)\textstyle\int_0^x\psi_1^{(1)}\{i\mathbf{B}_x(s)(A_1\psi_1'+A_2\psi_2')-(k_y\mathbf{B}_y(s)+k_z\mathbf{B}_z(s))(A_1\psi_1+A_2\psi_2)\}ds.\end{aligned} \tag{9.1}$$

Here, $\psi_1^{(1)}$ and $\psi_2^{(1)}$ are the unperturbed solutions for $E^{(1)}=E+h\nu$, k_y, k_z; $\psi_1^{(2)}$ and $\psi_2^{(2)}$ are the unperturbed solutions for $E^{(2)}=E-h\nu$, k_y, k_z; also:

$$q^2=(8\pi^2m/h^2)(E^{(1)}+eV_1)-k_y^2-k_z^2=\mu\nu+k_x^2, \qquad \mu=8\pi^2m/h \tag{10.1}$$

(q is positive). Since $E^{(2)}$ is generally negative (for potassium this is so for $\lambda<6000$A), we have for $b_1(x)$ and $b_2(x)$:

$$\begin{aligned}b_1(x)&=d_1-(2\pi ie/ch\rho)\textstyle\int_0^x\psi_2^{(2)}\{i\mathbf{B}_x(s)(A_1\psi_1'+A_2\psi_2')-(k_y\mathbf{B}_y(s)+k_z\mathbf{B}_z(s))(A_1\psi_1+A_2\psi_2)\}ds,\\ b_2(x)&=d_2+(2\pi ie/ch\rho)\textstyle\int_0^x\dot\psi_1^{(2)}\{i\mathbf{B}_x(s)(A_1\psi_1'+A_2\psi_2')-(k_y\mathbf{B}_y(s)+k_z\mathbf{B}_z(s))(A_1\psi_1+A_2\psi_2)\}ds,\end{aligned} \tag{9.2}$$

where $\rho^2=-(8\pi^2m/h^2)(E^{(2)}+eV_1)+k_y^2+k_z^2=\mu\nu-k_x^2$ (10.2)

(ρ is positive). The primes (not to be confused with the superscripts) as in (9.1) and (9.2) will always denote differentiation with respect to x. The constants of integration in the above expressions must be adjusted so that outside the metal, v falls off exponentially, and inside, v represents (at large distances in) either waves moving away from the surface or an exponentially decreasing solution. In calculating

[5] J. Frenkel, *Wave Mechanics—Advanced General Theory*, 1934, p. 368.

[6] If $E<-eV_1$, we get exponential forms for the unperturbed solutions:

$$\psi_1(-\infty)\approx e^{\rho x}, \qquad \psi_2(-\infty)\approx e^{-\rho x}, \qquad p^2=-(8\pi^2m/h^2)(E+eV_1)+k_y^2+k_z^2; \qquad (\rho \text{ is positive.}).$$

photoelectric emission, we are concerned only with the ϕ_1 term, as that involving $E-h\nu$ corresponds to stimulated emission; for the coherent scattering, however, both terms must be considered.

The current coherent with the incident light is given in terms of the vector potential by means of the well-known formula:

$$\mathbf{j}=-e\{(h/4\pi im)(u^*\nabla u-u\nabla u^*)+(e/mc)\mathbf{A}uu^*\}. \tag{11}$$

To obtain the total current $\mathbf{J}$, we must integrate $\mathbf{j}$ over all the states of the conduction electrons according to Fermi statistics. This $\mathbf{J}$, which combines the polarization and conduction currents, is then the same as that which appears in Maxwell's equations:

$$[\nabla\times\mathbf{H}]-(1/c)\dot{\mathbf{E}}=(4\pi/c)\mathbf{J}, \qquad \mathbf{H}=[\nabla\times\mathbf{A}], \qquad \mathbf{E}=-(1/c)\dot{\mathbf{A}}, \tag{12}$$

from which we obtain the relation:

$$[\nabla\times[\nabla\times\mathbf{A}]]+(1/c^2)\ddot{\mathbf{A}}=(4\pi/c)\mathbf{J} \tag{13}$$

between $\mathbf{A}$ and $\mathbf{J}$. Eliminating $\mathbf{J}$ between (13) and the integrated form of (11), we obtain an integral equation in the vector potential $\mathbf{A}$. In the above theory, we have neglected effects due to photoelectric emission and incoherent scattering. These two are of the same order of magnitude, and the former is known experimentally to be negligibly small for calculations of this type (there is generally about one photoelectron produced per 200 incident quanta).

We simplify the integral equation in the vector potential as much as possible before approximating to its solution. Outside the metal, $\mathbf{J}=0$, and well inside the metal (where the electrons are not under the influence of the surface barrier), we have from classical theory that $\mathbf{J}=f_0\mathbf{A}$, where:

$$f_0=-e^2N/mc,\ N=\text{number of electrons per cc} \tag{14.1}$$

$$\epsilon=1+cf_0/\pi\nu^2, \tag{14.2}$$

the latter relating f_0 with the dielectric constant ϵ of the phenomenological theory; thus at large distances within the metal, $\mathbf{A}$ has the form:

$$\mathbf{A}=\mathbf{C}e^{\gamma z}e^{-2\pi i\nu(t-(z\sin\theta)/c)}+\mathbf{C}^*e^{\gamma z}e^{2\pi i\nu(t-(z\sin\theta)/c)}, \tag{15}$$

where $\mathbf{C}$ is a constant vector. Since we have assumed that the electrons are effectively free (except for the surface barrier), we expect the Drude results to apply everywhere except near the surface. The same argument that shows in the Drude theory that $\mathbf{B}_y(x)$, $\mathbf{B}_z(x)$, and $((4\pi/c)\mathbf{J}_x+(4\pi^2\nu^2/c^2)\mathbf{A}_x)$, (the tangential components of $\mathbf{A}$ and the normal component of $[\nabla\times\mathbf{H}]$) are continuous at the surface, now shows that these expressions vary only slowly, and to a first approximation may be taken to have everywhere the values given by the Drude theory. Thus we may put:

$$\begin{gathered}\mathbf{B}_y(x)=\mathbf{C}_ye^{\gamma z}, \qquad \mathbf{B}_z(x)=\mathbf{C}_ze^{\gamma z},\\ ((4\pi/c)\mathbf{J}_z+(4\pi^2\nu^2/c^2)\mathbf{A}_z)=\{\chi e^{-2\pi i\nu(t-(z\sin\theta)/c)}+\chi^*e^{2\pi i\nu(t-(z\sin\theta)/c)}\}e^{\gamma z}.\end{gathered} \tag{16}$$

We must now find $\mathbf{C}_y$, $\mathbf{C}_z$, χ, and γ from the Drude[7] theory in terms of the amplitude of the vector potential of the incident light wave. Using (15) for the light wave within the metal, we put:

$$\mathbf{A}=\{\mathbf{A}^{(0)}e^{-2\pi i\nu(t+(z\cos\theta/c)-(x\sin\theta)/c)}+\mathbf{A}^{(1)}e^{-2\pi i\nu(t-(z\cos\theta)/c-(x\sin\theta)/c)}\}+\text{conjugate},$$

for the wave outside, where $\mathbf{A}^{(0)}=(I_p\sin\theta,\ I_s,\ I_p\cos\theta)$ is the amplitude of the incident wave, and $\mathbf{A}^{(1)}=(R_p\sin\theta,\ R_s,\ -R_p\cos\theta)$ is the amplitude of the reflected wave. I_p and I_s are the components of the incident light vector parallel and perpendicular to the plane of incidence (xz-plane) respectively, θ being the angle of incidence, and R_p and R_s are similar quantities for the reflected beam. We find $\mathbf{E}$ and $\mathbf{H}$ from Maxwell's Eq. (12), and apply the boundary conditions (continuity of the tangential components of $\mathbf{E}$ and $\mathbf{H}$) at $x=0$. We also require the relation:

[7] P. Drude, *Theory of Optics* (English translation, 1907), part 2, section 2, chapter 4.

$$f_0\mathbf{A}=\mathbf{J}=(c/4\pi)[\nabla\times\mathbf{H}]-(1/4\pi)\dot{\mathbf{E}}. \tag{12.1}$$

The y-component of this vector equation gives us the value of γ:

$$\gamma^2=-(4\pi/c)(f_0+(\pi\nu^2\cos^2\theta)/c) \tag{17.1}$$

(γ is real and positive). The x- and z-components of (12.1) are equivalent, and with the boundary conditions may be made to give:

$$\mathbf{C}_x=\frac{2I_p}{\sin\theta-(1/\cos\theta-c\gamma/2\pi i\nu)(c\gamma/2\pi i\nu\sin\theta)}, \tag{17.2}$$

$$\mathbf{C}_y=\frac{2I_s}{1-c\gamma/2\pi i\nu\cos\theta}, \tag{17.3}$$

$$\mathbf{C}_z=\frac{2I_p}{1/\cos\theta-c\gamma/2\pi i\nu-(2\pi i\nu\sin^2\theta)/c\gamma}, \tag{17.4}$$

$$\chi=(4\pi f_0/c+4\pi^2\nu^2/c^2)\mathbf{C}_z, \tag{17.5}$$

in terms of the amplitude of the incident light.

3. Theory for an Infinite Barrier

The form of the potential function $V(x)$ that is easiest to treat from a mathematical standpoint is that which gives a square barrier:

$$V(x)=0,\quad x<0;\qquad V(x)=V_0,\quad x>0. \tag{3.1}$$

We shall consider in detail here the case of an infinite barrier ($V_0=\infty$). The changes in the results necessary when a finite barrier is used will be discussed later. We retain the form of $\mathbf{A}$ given by (2) for $x<0$ (the form outside the metal is unimportant). Then (5) becomes:

$$w=A_0(e^{-ik_0x}-e^{ik_0x})e^{i(k_0y+k_0z)}e^{-2\pi i\mathcal{E}t/h}, \tag{5.1}$$

which satisfies the boundary condition at $x=0$ for an infinite barrier (w vanishes); A_0 is a normalizing constant [which equals $(1/4\pi^3)^{\frac{1}{2}}$, for two electrons per h^3 of phase space]. Replacing $\mathbf{B}_y(x)$ and $\mathbf{B}_z(x)$ by their Drude values as in (16), and neglecting the slowly decreasing exponential term $e^{\gamma x}$ (which is important only for producing convergence at $-\infty$, and is practically unity near the surface), we find that the terms involving $\mathbf{B}_y$ and $\mathbf{B}_z$ cancel out of the current expression (11), and can therefore be left out of the coefficients (9.1) and (9.2) of the perturbed wave function (7). After evaluating the constants of integration in $a_1(x)$, $a_2(x)$, $b_1(x)$ and $b_2(x)$, we obtain:

$$\begin{aligned}a_1(x)&=-a_2(0)+(2\pi eA_0/chq)\textstyle\int_0^x e^{iqs}k_x\mathbf{B}_x(s)(e^{-ik_xs}+e^{ik_xs})ds,\\ a_2(x)&=-(2\pi eA_0/chq)\textstyle\int_{-\infty}^x e^{-iqs}k_x\mathbf{B}_x(s)(e^{-ik_xs}+e^{ik_xs})ds,\end{aligned} \tag{9.3}$$

$$\begin{aligned}b_1(x)&=-b_2(0)-(2\pi ieA_0/ch\rho)\textstyle\int_0^x e^{-\rho s}k_x\mathbf{B}_x(s)(e^{-ik_xs}+e^{ik_xs})ds,\\ b_2(x)&=(2\pi ieA_0/ch\rho)\textstyle\int_{-\infty}^x e^{\rho s}k_x\mathbf{B}_x(s)(e^{-ik_xs}+e^{ik_xs})ds.\end{aligned} \tag{9.4}$$

The part of the current given by (11) depending linearly on $\mathbf{A}$ is:

$$\mathbf{j}=-e\{(h/4\pi im)(w^*\nabla v-v\nabla w^*+v^*\nabla w-w\nabla v^*)+(e/mc)\mathbf{A}ww^*\}. \tag{11.1}$$

The current $\mathbf{J}$ is obtained from this by the integration:

$$\mathbf{J}=\textstyle\int_0^k\pi(k^2-k_x^2)\,\mathbf{j}dk_x \tag{18}$$

over the sphere of radius k in $k_xk_yk_z$-space; here $k=(3\pi^2N)^{\frac{1}{3}}$, for N electrons per cc of metal, and two electrons per h^3 of phase space.

To obtain the integral equation in $\mathbf{B}_z(x)$, we first find the current $\mathbf{j}$, by substituting (5.1) for w, and (7) for v, with coefficients given by (9.3) and (9.4), into the current expression (11.1). Since the exponentials cancel out, except for $e^{\pm 2\pi i\nu[t-(x\sin\theta)/c]}$, and $\mathbf{B}_z$ comes out as a factor, it is convenient to express ϕ_1 and ϕ_2 as integrals of the form:

$$\phi_1 = \int^0_{-\infty} g_1(x, s)\mathbf{B}_z(s)ds\,; \qquad \phi_2 = \int^0_{-\infty} g_2(x, s)\mathbf{B}_z(s)ds. \tag{19}$$

Doing this, we find directly that $g_1(x, s)$ and $g_2(x, s)$ are given by:

$$g_1(x, s) = -(2\pi eA_0/chq)4ik_x \sin qxe^{-iqs}\cos k_x s\,; \qquad -\infty < s < x. \tag{20.1}$$

$$g_1(x, s) = -(2\pi eA_0/chq)4ik_x \sin qse^{-iqx}\cos k_x s\,; \qquad x < s < 0. \tag{20.2}$$

$$g_2(x, s) = -(2\pi eA_0/ch\rho)4ik_x \sinh \rho xe^{\rho s}\cos k_x s\,; \qquad -\infty < s < x. \tag{20.3}$$

$$g_2(x, s) = -(2\pi eA_0/ch\rho)4ik_x \sinh \rho se^{\rho x}\cos k_x s\,; \qquad x < s < 0. \tag{20.4}$$

Then, with (11.1), these give for $\mathbf{j}_x$:

$$\mathbf{j}_x = [\int^0_{-\infty}(eh/4\pi im)\{(e^{-ik_x x}-e^{ik_x x})(A_0 g_2^{*\prime}+A_0 g_1')+ik_x(e^{-ik_x x}+e^{ik_x x})(A_0 g_2^{*}+A_0 g_1)\}\mathbf{B}_z(s)ds$$
$$-(e^2/mc)A_0{}^2 4\sin^2 k_x x\mathbf{B}_z(x)]e^{-2\pi i\nu(t-(x\sin\theta)/c)}+\text{conjugate}. \tag{21}$$

(The primes denote differentiation with respect to x, as before.) Substituting the value of $\mathbf{J}_x$ obtained from (18) and (21) into the last of (16), and equating coefficients of $e^{-2\pi i\nu[t-(x\sin\theta)/c]}$, we obtain finally the integral equation in $\mathbf{B}_z(x)$:

$$\chi = h(x)\mathbf{B}_z(x)+\int^0_{-\infty} K(x, s)\mathbf{B}_z(s)ds \tag{22}$$

(neglecting the factor $e^{\gamma x}$ in χ), where

$$h(x) = \frac{4\pi^2\nu^2}{c^2}-\frac{4\pi e^2A_0{}^2}{mc^2}\int_0^k 4\sin^2 k_x x(k^2-k_x{}^2)\pi dk_x$$
$$= \frac{4\pi^2\nu^2}{c^2}-\frac{4e^2}{\pi mc^2}\left\{\frac{k^3}{3}+\frac{k}{4}\frac{\cos 2kx}{x^2}-\frac{\sin 2kx}{8x^3}\right\}, \tag{23.1}$$

$$K(x, s) = \frac{2\pi ehA_0}{mc}\int_0^k\{-\sin k_x x[g_1'(x, s)+g_2^{*\prime}(x, s)]$$
$$+k_x\cos k_x x[g_1(x, s)+g_2^{*}(x, s)]\}(k^2-k_x{}^2)dk_x. \tag{23.2}$$

This equation cannot be solved by the usual method for treating integral equations, because the (real) function $h(x)$ has a zero on the negative real axis. However, we may rewrite (22) in the form:

$$\mathbf{B}_z(x) = \chi/[h(x)+\int^0_{-\infty}\{K(x, s)\mathbf{B}_z(s)/\mathbf{B}_z(x)\}ds] \tag{24}$$

and obtain a first approximation to the solution by taking $\mathbf{B}_z$ constant (the Drude value, except for the exponential term) under the integral sign. This gives us:

$$\mathbf{B}_z(x) = \chi/[h(x)+\int^0_{-\infty}K(x, s)ds]. \tag{25}$$

4. Application to the Theory of the Surface Photoelectric Effect

We have obtained explicitly in (16) and (25) approximate expressions for the vector potential existing inside a metal when we assume an infinite potential barrier at the surface. Before examining these in more detail, we shall consider what changes are necessary in the existing theory of the photoelectric effect to accommodate our new expressions for the vector potential, as the photoelectric

effect gives us a good opportunity to apply the present theory. A very complete treatment of the surface photoelectric effect has been given by Mitchell.[8] He assumes a finite square barrier at the surface (representing a clean surface), the vector potential inside the metal given by classical theory, and has calculated the perturbed wave functions by both the stationary and nonstationary methods. We wish to recalculate his Eq. (26), which gives the whole wave function of electrons outside the metal, by the stationary method, but using our value for the vector potential instead of that given by classical theory, and then to obtain the photoelectric current from this.

The calculation of the unperturbed function will be the same (except that we have used throughout the opposite sign for i). It should be noted that Mitchell calls the potential energy of the electron (not the scalar potential) V, and assigns to it the value $-h\nu_a$ inside the metal, and zero outside; this change of notation does not, of course, affect the final results. We shall use Mitchell's Eq. (13) for the light wave outside the metal, but our form (2) for the potential inside.[9] Since we have assumed that the amplitudes of the y and z components of the vector potential are essentially constant within the metal, we are led (as he was) to the conclusion that his functions ϕ_y and ϕ_z do not contribute appreciably to the current, as they are continuous across the boundary to a first approximation. The calculation of ϕ_x, however, will now be different, since we must replace his $\mathbf{a}_x$, which was constant, by our function $\mathbf{B}_x(x)$ inside the metal. It is necessary then to solve the differential equation in the perturbed function [Mitchell's Eq. (15)] by the method of the variation of parameters, and then to put in the condition that at large positive and large negative distances, ϕ_x is to represent a wave moving away from the surface. Doing this, we obtain instead of Mitchell's Eqs. (22) and (23):

$$\phi_x=(k_x/2q\mathbf{a}_x)\{c_xe^{-iqx}+\int^x_{-\infty}e^{-iq(x-s)}(e^{-ik_xs}-a_ke^{ik_xs})\mathbf{B}_x(s)ds$$
$$-\int^x_{-\infty}e^{iq(x-s)}(e^{-ik_xs}-a_ke^{ik_xs})\mathbf{B}_x(s)ds\}e^{i(k_yy+k_zz)}; \qquad x<0. \quad (26.1)$$

$$\phi_z=\{b_xe^{irx}-(pb_k/\mu\nu)e^{-px}\}e^{i(k_yy+k_zz)}; \qquad x>0. \quad (26.2)$$

(It will be noted that the sign of i is changed here.) We evaluate the constants b_x and c_x by means of the continuity conditions on ϕ_x and $\partial\phi_x/\partial x$ at $x=0$, and obtain for b_x:

$$b_x=-\frac{k_x}{\mathbf{a}_x(q+r)}\int^0_{-\infty}e^{-iqx}(e^{-ik_xx}-a_ke^{ik_xx})\mathbf{B}_x(x)dx+\frac{pb_k(q+ip)}{\mu\nu(q+r)} \quad (27)$$

instead of his expression (25). It is easy to show that these two expressions are equivalent when $\mathbf{B}_x(x)$ is taken constant (except for an exponential term that produces convergence at $-\infty$) and equal to $\mathbf{a}_x$. Then, finally, we obtain, corresponding to Mitchell's (26), the complete wave function outside the metal:

$$u=\{\alpha_kb_ke^{-px}e^{-(2\pi i/h)E_kt}+\lambda_x[b_xe^{irx}-(pb_k/\mu\nu)e^{-px}]e^{-(2\pi i/h)(E_k+h\nu)t}\}e^{i(k_yy+k_zz)}, \quad (28)$$

which is formally the same (except for the change in sign of i), but which has the value of b_x from our Eq. (27) instead of from his Eq. (25). The quantities α_k, b_k, a_k, p, q, r, k_x, λ_x, and μ have the same significance as in Mitchell's paper, and are tabulated here for convenience:

$$|\alpha_k|^2=\tfrac{1}{2}\ \text{(mean electron density inside metal)};$$
$$b_k=2ik_x/(ik_x+p); \qquad a_k=(ik_x-p)/(ik_x+p);$$
$$p=(\mu\nu_a-k_x^2)^{\frac{1}{2}}; \qquad q=(k_x^2+\mu\nu)^{\frac{1}{2}}; \qquad r=[k_x^2+\mu(\nu-\nu_a)]^{\frac{1}{2}}; \quad (29)$$
$$k_x^2=(8\pi^2m/h^2)(E_k+h\nu_a)-k_y^2-k_z^2;$$
$$\lambda_x=-(4\pi ie/ch)a_k\alpha_k; \qquad \mu=8\pi^2m/h.$$

[8] K. Mitchell, Proc. Roy. Soc. **A146**, 442 (1934).

[9] We shall use only the first term of (2) since the stimulated emission does not contribute to the photoelectric current, as Mitchell points out (reference 8, p. 448).

(k_x, k_y, k_z, q and μ have the same meaning as we assigned to them earlier in this paper.) That part of the normal component of the current density outside the metal which contains neither exponentially decreasing terms nor oscillating time factors (the photoelectric current) may then be obtained from our Eq. (11), or from Mitchell's (27) (which gives the correct result even though he omits the term involving $\mathbf{A}uu^*$). This gives us:

$$\begin{aligned} &\mathrm{j}_x = -(ehr/2\pi m)\,|\lambda_x b_x|^2; && k_x^2+\mu\nu > \mu\nu_a \\ &\mathrm{j}_x = 0; && k_x^2+\mu\nu \leqq \mu\nu_a. \end{aligned} \tag{30}$$

This current must, of course, be integrated over the conduction electrons before it gives the whole photoelectric current. However, because of the difficulties involved in effecting this integration even with the simpler value of the vector potential that Mitchell considers, we shall not attempt to do this here. But we can obtain a rough comparison with Mitchell's photoelectric yield curve by considering the ratio between our value and his value for b_x, and the manner in which it varies with the frequency of the incident light. In doing this, we use his Eqs. (73) and (74) for b_x and λ_x, where he has taken account of reflection and refraction at the surface of the metal according to classical theory (and change the sign of i). If we put:

$$I_0 = \int_{-\infty}^{0} e^{-iqx}(e^{-ik_x x} - a_k e^{ik_x x})\mathbf{B}_x(x)\,dx \tag{31}$$

we have for the ratio R of our value of b_x to Mitchell's value of b_x:

$$R = \frac{-k_x\mu\nu I_0 + pb_k(q+ip)\mathbf{a}_{0x}}{(ik_x^2 - pq)b_k\mathbf{a}_{tx} + pb_k(q+ip)\mathbf{a}_{0x}}, \tag{32}$$

where $\mathbf{a}_{0x} = I_p \sin\theta + R_p \sin\theta$ is the total (incident and reflected) x component of the amplitude of the vector potential outside the metal, and $\mathbf{a}_{tx} = \mathbf{C}_x$ is the x component of the classically calculated transmitted amplitude. We wish, then, to find roughly the value of R and its dependence on the frequency ν. First, however, we must evaluate I_0, using the value of $\mathbf{B}_x$ from (25).

Consider the relative magnitudes of the terms in the denominator of (25). The first term $h(x)$ is real. Put for the second term:

$$\Lambda = \int_{-\infty}^{0} K(x, s)\,ds. \tag{33}$$

The s-integration of Λ may be carried out simply and exactly and gives:

$$\begin{aligned} \Lambda = \frac{4ie^2}{\pi mc^2}\int_0^k \Bigg\{ & e^{-iqx}\Bigg[\frac{1}{\mu\nu}\left(\sin k_x x\cos qx - \frac{k_x}{q}\cos k_x x\sin qx\right)\cdot(iq\cos k_x x - k_x\sin k_x x) \\ & + \left(i\sin k_x x + \frac{k_x}{q}\cos k_x x\right)\left(\frac{q}{\mu\nu} - \frac{\cos(q+k_x)x}{2(q+k_x)} - \frac{\cos(q-k_x)x}{2(q-k_x)}\right)\Bigg] \\ & - \frac{e^{\rho x}}{\mu\nu}\Bigg[\left(\sin k_x x\cosh\rho x - \frac{k_x}{\rho}\cos k_x x\sinh\rho x\right)(\rho\cos k_x x + k_x\sin k_x x) \\ & + (\rho - \rho\cosh\rho x\cos k_x x - k_x\sinh\rho x\sin k_x x)\left(\sin k_x x - \frac{k_x}{\rho}\cos k_x x\right)\Bigg]\Bigg\}(k^2 - k_x^2)k_x\,dk_x. \end{aligned} \tag{34}$$

The k_x integration, on the other hand, is exceedingly complicated, as both q and ρ contain k_x under a radical. However, we can get an idea of the order of magnitude by assuming for purposes of integration that $k \ll (\mu\nu)^{\frac{1}{2}}$, when we can put approximately:

$$\sin k_x x \approx k_x x; \qquad \cos k_x x \approx 1; \qquad q \approx (\mu\nu)^{\frac{1}{2}}; \qquad \rho \approx (\mu\nu)^{\frac{1}{2}}.$$

We then obtain for the real and imaginary parts of Λ:

$$\Re[\Lambda]=\frac{4e^2}{\pi mc^2}\frac{2k^5}{15}\frac{1}{\mu\nu}\{\sin\xi-\xi\cos\xi\}, \tag{35.1}$$

$$\Im[\Lambda]=\frac{4e^2}{\pi mc^2}\frac{2k^5}{15}\frac{1}{\mu\nu}\{\cos\xi+\xi\sin\xi+e^{\xi}(1-\xi)-2\}, \tag{35.2}$$

where
$$\xi=(\mu\nu)^{\frac{1}{2}}x. \tag{35.3}$$

Several points now present themselves. First, $h(x)$ is an even oscillating function that has one zero on the negative real axis, and an infinite number of complex zeros a considerable distance from the real axis. Second, $h(x)$ approaches a definite limit ($\chi/\mathbf{C}_x$) as x becomes negatively infinite. Third, $\Re[\Lambda]$ is small compared to $h(x)$, except of course where the latter is zero. Fourth, $\Im[\Lambda]$ is also small compared to $h(x)$, and is positive for $0>\xi>-1.78$, after which it is negative for some distance.

The zero point[10] of $h(x)$ may be calculated approximately from the equation:

$$\frac{\pi\nu^2 m}{3e^2N}=\frac{1}{3}+\frac{\cos\eta}{\eta^2}-\frac{\sin\eta}{\eta^3}\approx\frac{\eta^2}{30}-\frac{\eta^4}{840}+\cdots, \tag{36}$$

where $\eta=2kx$. We take the value $5\cdot10^{14}$ for ν, and $1.35\cdot10^{22}$ for N (for potassium). These give:

$$\eta_0=-1.90\,; \qquad x_0=-1.29\cdot10^{-8}\text{ cm}\,; \qquad \xi_0=-0.95\,; \qquad (\partial h/\partial x)_0=(4e^2k^3/\pi mc^2)(0.094)>0.$$

Thus $\mathbf{B}_z(x)$, which is of the form:

$$\chi/\{(\partial h/\partial x)_0(x-x_0)+\Re[\Lambda]+i\Im[\Lambda]\}$$

near x_0, has a pole approximately at:

$$x=x_0-\{[\Re\Lambda]+i\Im[\Lambda]\}/(\partial h/\partial x)_0.$$

If $\Im[\Lambda]$ is positive (ν is such that $0>\xi>-1.78$), this is just below the negative real axis, and I_0 consists of its principal value (neglecting Λ) minus πi times the residue of the integrand at the pole. Again, if $\Im[\Lambda]$ is negative (ν such that $\xi<-1.78$), the pole lies just above the negative real axis, and I_0 consists of its principal value plus πi times the residue at the pole. Thus I_0 changes its value abruptly near that frequency for which $\xi=-1.78$. We can find this critical frequency approximately by putting:

$$\eta\approx-\nu(30\pi m/3e^2N)^{\frac{1}{2}}$$

from (36), and substituting for x in ξ in terms of η. We then have (in the case of potassium):[11]

$$\nu_c^{\frac{1}{2}}\approx2k\cdot1.78/(\mu\cdot10\pi m/e^2N)^{\frac{1}{2}}\,; \qquad \nu_c\approx8.45\cdot10^{14}.$$

We break up the integral I_0 into two parts of the same form:

$$I_1=\int^0_{-\infty}\mathbf{B}_z(x)e^{-iq_1z}dx\,; \qquad \delta_1=q+k_z>0$$

$$I_2=\int^0_{-\infty}\mathbf{B}_z(x)e^{-iq_2z}dx\,; \qquad \delta_2=q-k_z>0$$

such that: $I_0=I_1-a_kI_2$. We must remember that χ in reality has a small exponential term $e^{\gamma x}$ multiplying it, which is negligible except for producing convergence at $-\infty$. We thus have to evaluate an integral of the form:

$$I=\int^0_{-\infty}(e^{-iqz}/h(x))dx\,; \qquad \delta>0. \tag{37}$$

[10] This is approximately the point where the dielectric constant ϵ vanishes.
[11] For different metals, $\nu_c\propto N^{5/9}$, since $k\propto N^{1/3}$.

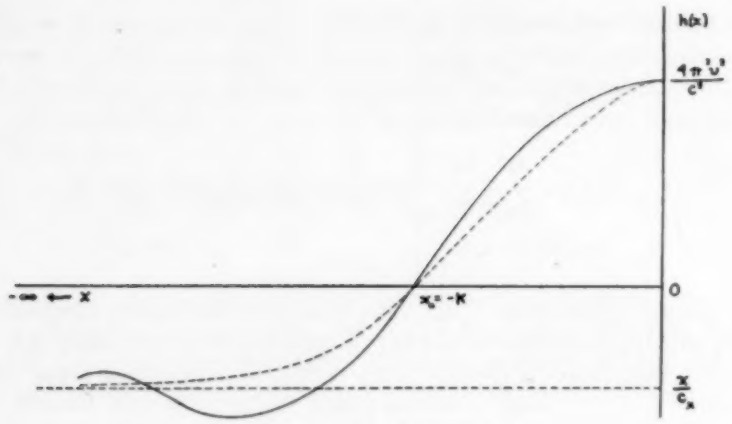

FIG. 1. The function $h(x)$.

After inserting the form (23.1) for $h(x)$ into (37), this is quite a formidable integral to evaluate, especially with the pole at x_0. However, the important features of $h(x)$ as seen in Fig. 1 (solid line) are its values at zero and $-\infty$, and the point at which it vanishes. Therefore we should expect to get a good approximation to the integral by putting instead:

$$h(x)=1/(\tau+\sigma x^2)-1/\zeta, \tag{38}$$

where $h(0)=\dfrac{1}{\tau}-\dfrac{1}{\zeta}=\dfrac{4\pi^2\nu^2}{c^2}$; $\quad h(-\infty)=-\dfrac{1}{\zeta}=\dfrac{4\pi^2\nu^2}{c^2}+\dfrac{4\pi f_0}{c}$; $\quad h(x_0)=0$; $\quad x_0=-((\zeta-\tau)/\sigma)^{\frac{1}{2}}=-K$

represented by the dotted line in the figure.

The integral (37) can then be expressed in terms of sine and cosine integrals:[12]

$$I=-(i\zeta/\delta)+(i\zeta^2/\sigma K)\{Ci(\delta K)\sin\delta K-si(\delta K)\cos\delta K-\theta\pi e^{i\delta K}\}, \tag{39}$$

where $\theta=1$, if the pole is below the negative real axis ($\nu<\nu_c$);
$\theta=0$, if the pole is above the negative real axis ($\nu>\nu_c$).

Putting (39) into the expression for I_0, we obtain:

$$I_0=\chi\{-i\zeta/\delta_1+(i\zeta^2/\sigma K)[Ci(\delta_1K)\sin\delta_1K-si(\delta_1K)\cos\delta_1K-\theta\pi e^{i\delta_1K}]$$
$$+a_k i\zeta/\delta_2-a_k(i\zeta^2/\sigma K)[Ci(\delta_2K)\sin\delta_2K-si(\delta_2K)\cos\delta_2K-\theta\pi e^{i\delta_2K}]\}. \tag{40}$$

Then, by inserting (40) into the ratio R given by (32), the latter reduces to

$$R=1+\frac{-k_x\mu\nu\chi\zeta^2 i}{\{(ik_x^2-pq)\mathbf{a}_{1z}+(q+ip)p\mathbf{a}_{0z}\}\sigma K b_k}\cdot\{[Ci(\delta_1K)\sin\delta_1K-si(\delta_1K)\cos\delta_1K-\theta\pi e^{i\delta_1K}]$$
$$-a_k[Ci(\delta_2K)\sin\delta_2K-si(\delta_2K)\cos\delta_2K-\theta\pi e^{i\delta_2K}]\}. \tag{41}$$

From (41) it is impossible to obtain a simple form for the variation with ν of $|R|^2$, this being the ratio of the new photoelectric current to that of Mitchell (for a given k_x). However, we can roughly estimate R by assigning numerical values to the quantities involved. The function $Ci(z)\sin z-si(z)\cos z$ falls off monotonically from $\pi/2$ at 0 (0.62 at 1, 0.40 at 2) approaching zero like $1/z$ as $z\to\infty$, and is therefore never large. Using a value of the frequency near ν_c, we find that $|R|\approx 6$, when $\theta=1$, and $|R|\approx 1$, when $\theta=0$. Although these results will be smoothed out somewhat when the k_x integration is

[12] See Jahnke-Emde, *Tables of Functions* (2nd ed.), p. 79, for the notation used here.

performed, it will still be true that the resulting photoelectric current will decrease rather suddenly as ν passes through the critical value, and θ changes from one to zero.

This last point is quite important, as it brings Mitchell's theoretical curve (his Fig. 2) into better agreement with experiment. On the abscissa of this curve, $(\nu-\nu_0)/\nu_0$, our critical frequency $(8.45\cdot 10^{14})$ lies at about 0.7. This means that our correction will raise his curve to the left of this point, and lower it towards the right. This will make a rather sharp peak on the low frequency side of ν_c, the position of which will nearly coincide with that of the experimental curve.[13] Detailed calculations of $|R|^2$ would be necessary before the exact forms of the experimental curve and this new theoretical curve could be compared.

This seems to indicate that the peak of the spectral selectivity curve is due principally to the effect of the pole of the vector potential function. This conclusion is confirmed by a comparison of the values of ν_c obtained by this rather rough theoretical approximation ($\nu_c \propto N^{5/9}$) with the rather uncertain experimental values for the peak of the spectral distribution curve, which in fact varies approximately as $N^{\frac{1}{2}}$ for the metals in the first three columns of the periodic table.[14]

5. Changes for a Finite Barrier

The vector potential used in the above calculations was that obtained by assuming an infinite barrier at the surface. The principal effect of making the barrier of finite height is that then the wave functions do not vanish identically at the surface, but have a small value there. This extends the transition layer slightly beyond the surface, and moves the singularity closer to the surface. Such changes would be unimportant in the theory as developed here, and the additional complications involved hardly warrant more detailed investigation at this time.

For the more complex forms of surface barriers, the theory becomes exceedingly complicated; for example, we need no longer have only one point at which the dielectric constant becomes zero. In particular, Zener's[15] argument in favor of Suhrmann's[16] theory of the selective photoelectric effect for sensitized surfaces as against that of Fowler[17] may now require reconsideration.

6. General Conclusions

We thus arrive at the conclusion that the Drude theory of the reflection of light at a metal surface, modified where necessary by Kronig's results, gives the electromagnetic field correctly except within a transition layer extending a few electron wavelengths from the surface. In this transition layer, the continuously varying electric intensity perpendicular to the surface, discontinuous in the Drude theory, does not have values near those given by that theory, but fluctuates considerably.[18] These fluctuations depend on the nature of the surface potential barrier in a complicated way, but their calculation seems to be required in the theory of the surface photoelectric effect.[19]

---

[13] This curve in Mitchell's paper was taken from a paper of R. Suhrmann and H. Theissing, Zeits. f. Physik **52**, 453 (1928).

[14] Hughes and DuBridge, *Photoelectric Phenomena*, 1932, table on p. 162; the values given there may not be, and certainly are not in the case of potassium, for really clean surfaces.

[15] C. Zener, Phys. Rev. **47**, 15 (1935).

[16] R. Suhrmann, Ergebnisse der Exakten Naturwissenschaften **13**, 148 (1934).

[17] R. H. Fowler, Proc. Roy. Soc. **A128**, 123 (1930).

[18] *cp.* the Gibbs phenomenon in Fourier series.

[19] Even in the simple case of a square barrier, it would hardly improve the results of that theory merely to average over the position of the surface, as suggested by Mitchell (reference 8, p. 461).

A Class of Perturbations of Molecular Levels

G. H. DIEKE, *The Johns Hopkins University*

(Received April 15, 1935)

By following Van Vleck and Kronig, the conditions for the occurrence of perturbations are investigated in detail for a simple case. Class A perturbations which are produced by the rotation of the molecule must have $\Lambda' = \Lambda \pm 1$. The vibrational levels cannot be perturbed in this case. There will be a constant shift between the rotational levels before and after the perturbations. When the electronic motion can be described approximately by the precession of a constant angular momentum about the figure axis, the components of the perturbation matrix can be completely calculated. For class B perturbations $\Lambda = \Lambda'$. The vibrational levels may be perturbed and there is no constant shift between the levels for high and low values of J.

IF, in the regular sequence of rotational levels of a molecule, one or several of these levels are displaced from their expected positions, such a phenomenon is called a perturbation. Very often the lines originating from these perturbed rotational levels show also abnormal intensities. Since Kronig[1] showed first the general rules for the occurrence of such perturbations, several cases have been investigated and were shown in accordance with Kronig's theory to result from the interaction of two rotational levels with the same J of two electronic states which accidentally come very close together. However, except demonstrating that the occurrence of the perturbations found was in agreement with Kronig's general rules, not much has been done in a further theoretical analysis of such perturbations. Therefore it may be useful to investigate in detail a particularly simple case, and show that the magnitude of the perturbations and all its other characteristics can be correlated with other properties of the levels. This case has been chosen because it is the simplest representative of one of the two classes of perturbations, and because it gives a key to the understanding of some pecularities of the molecular spectrum of hydrogen. It is, however, of sufficient importance to merit a special treatment. The general treatment follows closely that of Van Vleck and Kronig. The chief aim of this paper is to bring out clearly the conditions under which the different types of perturbations can occur so that a clear theoretical background is available for the discussion of some empirical perturbations which will be given in a subsequent paper.

[1] R. de L. Kronig, Zeits. f. Physik **50**, 347 (1928).

§1. GENERAL ASSUMPTIONS

An electronic state of a diatomic molecule can be specified by a number of quantum numbers. If we were dealing with electrons in a central symmetric field of force, the total orbital angular momentum would be constant and to it would correspond a quantum number L. In a real molecule, the orbital momentum is not constant, and therefore L not a true quantum number, but for higher levels of light molecules the deviations from a central symmetric field of force are not large enough to cause any trouble. The projection Λ of L on the internuclear axis is constant, no matter whether L is a good quantum number or not, if we can disregard the influence of the spin which we shall do throughout this paper.[2] Besides L and Λ, there may be several other quantum numbers, but they are not important for the following and we represent them collectively by n. It is well known that the term symbols S, P, D $\cdots$ and Σ, Π, Δ mean that L and Λ, respectively, have the values 0, 1, 2, $\cdots$.[3] Of course we have always $\Lambda \leq L$. All the $L+1$ states (L of them double) belonging to a given n and L but different Λ are called a *complex*. On the electron motion of the molecule is superimposed the vibration characterized by the quantum

[2] We restrict ourselves therefore to singlet states. The results, however, will be also applicable to many cases where the multiplicity is different from one, but the spin so loosely coupled to the rest of the molecule that its influence can be neglected. It would not be difficult to take into account the spin also in the general case, but the example would lose then much of its simplicity.

[3] In order to avoid difficulties about the internal coupling of the electrons, we may assume that L and Λ come from a single electron only, that therefore the rest of the molecule is in an $s\Sigma$ state. Some of the results apply also in more general cases, but the one stated is by far the simplest and most important one.

number V and the rotation characterized by the total angular momentum J and its projection m on an axis fixed in space. As we are not dealing with external forces, m is of no importance to us. Any given energy level is now specified completely by n, L, Λ, V and J.

In order that we may have a perturbation two energy levels must come very close together. They will have to be rotational levels belonging to two different electronic states. But the close proximity of two levels is not sufficient for a perturbation. It is necessary that the matrix component $S_{rr'}$ of a perturbing potential S must be different from zero, and we shall say that two states can perturb each other when that is the case. Kronig gave some general rules which restrict the number of perturbing pairs considerably, the chief one of these restriction rules is that J must be the same for both levels, the others we shall have to deal with later.

We can distinguish two distinct classes of perturbations. For *class A* perturbations, the perturbing force is caused by the rotation of the molecule, whereas for *class B* the perturbing forces have a different origin. Class B might again be subdivided into several subclasses, but that is unnecessary here as this paper will deal almost exclusively with class A perturbations. An investigation of the exact nature of this type of perturbations will be the subject of the rest of the paper. At the same time it will become apparent that the same cause is responsible for irregularities in the Λ-doubling observed in several molecules. These irregularities usually are not called perturbations because they are of a more systematic character. The regular Λ-doubling is also closely connected with this kind of interaction.

§2. The Hamiltonian of a Diatomic Molecule

The necessary foundation for a detailed treatment of the perturbations have been given in a very thorough paper by Van Vleck[4] and therefore it is best to start with a brief résumé of Van Vleck's results with the necessary modifications and simplifications. The principle is that first the complete wave equation of the rotating and oscillating diatomic molecule is set up. This equation can only be solved if certain small terms in the Hamiltonian are omitted. After an approximate solution of the simplified wave equation has been obtained, the result can be corrected by introducing the neglected terms as perturbing potentials and calculating their influence by the method of perturbations. The influence of these small terms will be in general small except possibly when two unperturbed levels fall close together. In that case perturbations in the special sense defined at the beginning of this paper may result.

If the nuclei of the molecule are kept fixed, i.e., if the molecule is not vibrating nor rotating, the motion of the electrons is determined by a Hamiltonian $H^{(0)}$ and the wave equation

$$(\mathbf{H}^{(0)} - W^{(0)})\Phi = 0. \tag{1}$$

Φ is a function of the coordinates of the electrons, and $\mathbf{H}^{(0)}$, $W^{(0)}$ and Φ contain the internuclear distance r as a parameter. Φ is represented by as many quantum numbers as there are degrees of freedom. It depends in a very simple way on χ, the azimuth about the internuclear axis. We have

$$\begin{aligned} \Phi^{+}{}_{n,\,L,\,\Lambda} &= \varphi_{n,\,L,\,\Lambda} \cos \Lambda\chi, \\ \Phi^{-}{}_{n,\,L,\,\Lambda} &= \varphi_{n,\,L,\,\Lambda} \sin \Lambda\chi, \end{aligned} \tag{2}$$

in which φ is independent of χ. The energy belonging to Φ^+ and Φ^- is the same. For $\Lambda = 0$ there is only one term Σ^+ with $\Phi^{+}{}_{n,\,L,\,\Lambda}$.[5]

If the molecule is left to rotate and vibrate freely, three degrees of freedom are added which are represented by the internuclear distance r, the angle θ which the internuclear axis makes with a fixed direction in space, and φ, the azimuth about this axis. If the very small motion which the center of gravity of the nuclei makes with respect to the center of gravity of the total mole-

[4] J. H. Van Vleck, Phys. Rev. **33**, 467 (1929).

[5] Because of the degeneracy for the molecule with fixed nuclei, which is due to the fact that the energy is not changed if the sense of rotation of all the electrons is reversed any linear combination of Φ^+ and Φ^- would serve just as well. The particular form (2) is most useful because it must be taken if the degeneracy is removed by the interaction of electron motion and rotation. Φ^+ remains unchanged and Φ^- changes its sign when the sense of the electron motion is reversed. If there is more than one electron we may also have Σ^- terms. We prefer to write here Π^+ and Π^-, etc., rather than the more customary Π_ϵ and Π_δ because the latter, more empirical, designation does not always make it quite clear which of the two doublet components belongs to the cos $\Lambda\chi$ and which to the sin $\Lambda\chi$.

cule (electrons included) is neglected, the wave equation becomes

$$\left\{\mathbf{H}^0-\frac{h^2}{8\pi^2\mu r^2}\left[\frac{\partial}{\partial r}\left(r^2\frac{\partial}{\partial r}\right)+\operatorname{ctg}\theta\left(\frac{\partial}{\partial\theta}-i\mathbf{M}_\xi\right)+\left(\frac{\partial}{\partial\theta}-i\mathbf{M}_\xi\right)^2+\operatorname{cosec}^2\theta\left(\frac{\partial}{\partial\varphi}-i\sin\theta\mathbf{M}_\eta-i\cos\theta\mathbf{M}_\zeta\right)^2\right]-W\right\}\psi=0. \quad (3)$$

$\mathbf{M}_\xi$, $\mathbf{M}_\eta$ and $\mathbf{M}_\zeta$ are operators corresponding to the ξ, η and ζ components of the angular momentum with respect to a coordinate system moving with the molecule. This equation is valid also if the spin is included, but in our case $\mathbf{M}$ represents the *orbital* angular momentum only.

A direct solution of (3) is obviously impossible. An approximate solution can be obtained by neglecting certain terms so that a separation of the variables is possible. We can write then

$$\psi=\Phi u(\varphi,\theta)R(r). \quad (4)$$

(4) is the solution of the approximate equation

$$(\mathbf{H}^{(0)}+\mathbf{H}^{(1)}+\mathbf{H}^{(2)}-W)\psi=0, \quad (5)$$

whereas (3) is equivalent to

$$(\mathbf{H}^{(0)}+\mathbf{H}^{(1)}+\mathbf{H}^{(2)}+\mathbf{H}^{(3)}+\mathbf{H}^{(4)}-W)\psi=0, \quad (6)$$

which contains the two extra terms $\mathbf{H}^{(3)}$ and $\mathbf{H}^{(4)}$.

$$\mathbf{H}^{(1)}=-B[\operatorname{ctg}\theta\partial/\partial\theta+\partial^2/\partial\theta^2+\operatorname{cosec}^2\theta(\partial/\partial\varphi-i\Lambda\cos\theta)^2], \quad (7a)$$

$$\mathbf{H}^{(2)}\psi=-B\Phi u(\partial/\partial r)(r^2\partial R/\partial r), \quad (7b)$$

$$\mathbf{H}^{(3)}=Bi[\operatorname{ctg}\theta(\mathbf{M}_\xi-i\mathbf{M}_\eta\mathbf{M}_\zeta-i\mathbf{M}_\zeta\mathbf{M}_\eta)+2\operatorname{cosec}\theta\mathbf{M}_\eta\partial/\partial\varphi+2\mathbf{M}_\xi\partial/\partial\theta], \quad (7c)$$

$$\mathbf{H}^{(4)}\psi=B\left[(\mathbf{M}_\xi^2+\mathbf{M}_\eta^2)\Phi-2r\frac{\partial\Phi}{\partial r}-r^2\frac{\partial^2\Phi}{\partial r^2}-\frac{2r^2}{R}\frac{\partial R}{\partial r}\frac{\partial\Phi}{\partial r}\right]Ru, \quad (7d)$$

$B=h^2/8\pi^2\mu r^2$ is also a function of r.

The procedure in solving (5) is as follows: First solve (1)

$$(\mathbf{H}^{(0)}-W^{(0)})\Phi=0,$$

which gives the electronic energy W^0 and wave function Φ both containing the parameter r. Then solve

$$(\mathbf{H}^{(1)}-W^{(1)})u=0, \quad (8)$$

from which we obtain the rotational energy

$$W^{(1)}=B[J(J+1)-\Lambda^2], \quad (9)$$

which also contains r as parameter and the rotational wave function[6] $u(\varphi,\theta)$ which is independent of r. The next step is the solution of

$$[\mathbf{H}^{(2)}+W^{(1)}(r)+W^{(0)}(r)-W]R=0. \quad (10)$$

This gives the vibrational eigenfunction R and the total energy W of the approximated molecule. We have reached now the same stage of approximation which is employed in the elementary theory of band spectra in which $W(r)$ is assumed to be given as a power series in $r-r_0$ (r_0 is the equilibrium distance). We have then the energy as function of the total angular momentum J and the vibrational quantum number V.

$$W=W_0+\sum_{l,k}Y_{lk}(V+\tfrac{1}{2})^l[J(J+1)-\Lambda^2]^k. \quad (11)$$

This is for $\Lambda=0$, the familiar expression for the energy of a rotating anharmonic oscillator.[7]

§3. Occurrence of Class A Perturbations

We can take care now of the terms $\mathbf{H}^{(3)}$ and $\mathbf{H}^{(4)}$ neglected so far by considering them as perturbing potentials. $\mathbf{H}^{(4)}$ is independent of the rotational coordinates and therefore any perturbations resulting from it will be of class B. We shall not be any further concerned with perturbations of this type in this paper. The matrix elements $H_{rr'}{}^{(4)}$ are different from zero under almost

[6] The $u(\varphi,\theta)$ are the well-known wave functions of the symmetrical top as (7a) represents the Hamiltonian of the symmetrical top.

[7] Except for terms of higher order (11) is identical with the approximate expression

$$W=W_0+\omega_e(V+\tfrac{1}{2})-x(V+\tfrac{1}{2})^2+\cdots+[B_e-\alpha(V+\tfrac{1}{2})][J(J+1)-\Lambda^2].$$

W_0 is the electronic energy, i.e., the eigenvalue of (1) for the value $r=r_0$ of the parameter and is independent of the masses of the nuclei. As can be easily seen from the derivation sketched above, the higher terms in J are of the form $[J(J+1)-\Lambda^2]^k$ and not simply $J^k(J+1)^k$, as is usually found. For most practical purposes, however, the difference is negligible. The coefficients Y_{lk} have been calculated to a high approximation by Dunham (Phys. Rev. **41**, 721 (1932)).

the same conditions as those of $\mathbf{H}^{(3)}$ (see below). The essential difference is that we must have $\Lambda'=\Lambda$ for $\mathbf{H}^{(4)}$ whereas we have $\Lambda'=\Lambda\pm1$ for $\mathbf{H}^{(3)}$.[8]

In order to calculate the influence of $\mathbf{H}^{(3)}$, we have to know the matrix components

$$S_{\tau\tau'}=H^{(3)}{}_{\tau\tau'}=\int\psi_\tau^*S\psi_{\tau'}dv. \tag{12}$$

We write from now on S instead of $\mathbf{H}^{(3)}$ for the perturbing potential in order to avoid writing too many indices. The integration is extended over all the electronic coordinates, the internuclear distance r, and the rotational coordinates φ and θ. As Kronig showed first, and as can be verified easily, from (12) and (7c) by taking the nature of the wave functions into account, the matrix components $S_{\tau\tau'}$ are different from zero only if the two states τ and τ' fulfill the following conditions.

(a) Both levels must have the same value of J.
(b) Both levels must be positive or both negative.
(c) If the two nuclei are identical, both levels must be even or both odd; furthermore, both must be symmetrical or both antisymmetrical.

These conditions are based entirely on the symmetry properties of the molecule and do not involve any further assumptions.

The integration in (12) over the rotational coordinates can be separated from that over the other coordinates, so that the integral can be split into two factors, one of which is independent of J. If we call it α then Van Vleck showed that

$$S_{\tau\tau'}=\alpha[(J+\tfrac{1}{2}-\bar{\Lambda})(J+\tfrac{1}{2}+\bar{\Lambda})]^{\frac{1}{2}}, \tag{13}$$

$$\alpha(n, L, \Lambda, V; n', L', \Lambda', V')=2(BM_\varphi)_{n, L, \Lambda, V; n', L', \Lambda', V'}, \tag{14}$$

in which $2\bar{\Lambda}=\Lambda+\Lambda'$.

(13) and (14) are still quite general, but in order to go further it is convenient to consider some specialized cases.

1. Assume that the influence of the internuclear axis is comparatively weak. Then the angular momentum M has a constant magnitude L and precesses about the internuclear axis. Let us assume further that the angle which M makes with the internuclear axis has no effect on the equilibrium position, i.e., that r_0 is independent of Λ. Then

$$M_\varphi(n, L, \Lambda, V; n, L, \Lambda\pm1, V)=\tfrac{1}{2}[L(L+1)-\Lambda(\Lambda\pm1)]^{\frac{1}{2}} \tag{15}$$

and all other matrix components are zero. In that case α is zero except when $n=n'$, $L=L'$, $V=V'$, and $\Lambda'=\Lambda\pm1$.

$$\alpha(n, \Lambda, V; n, \Lambda\pm1, V)=B_V[L(L+1)-\Lambda(\Lambda\pm1)]^{\frac{1}{2}}. \tag{16}$$

This gives the regular Λ-doubling, as levels which differ only by the quantum number Λ, can never come accidentally close together. Perturbations, therefore, cannot occur.

2. Assume that the motion is still a regular precession of the constant angular momentum about the figure axis, but that the equilibrium internuclear distance r_0 depends on Λ. In that case (15) still holds true, but

$$B_{VV'}=\int RBR'r^2dr$$

is not even approximately diagonal as R' belongs to a different equilibrium distance than R. We have here a case very similar to that found when the Franck-Condon principle is applied to the matrix components of the electric moment. As long as the equilibrium distance is affected only slightly by the value of Λ the nondiagonal elements of B will be small compared with the elements diagonal in V.

We have now

$$\alpha(n, L, \Lambda, V, n, L, \Lambda\pm1, V')=[B_{VV'}+(r_0'-r_0)\int BR'R(\partial\Phi'/\partial r)_{r=r_0}\Phi dv]\times[L(L+1)-\Lambda(\Lambda\pm1)]^{\frac{1}{2}}. \tag{17}$$

$B_{VV'}$ can be completely calculated if the rotational and vibrational structure of the two perturbing states is known. In general it will be small compared with (16) if $V\neq V'$, and the term in $r_0'-r_0$ will be small compared to $B_{VV'}$ and can be neglected in first approximation.

It may happen now that the levels of n, L, Λ, V and $n, L, \Lambda\pm1, V'$ come very close together. For instance in H_2 we have that the $p\Pi$ levels lie several thousand cm^{-1} above the corresponding

[8] In contrast to $\mathbf{H}^{(3)}$ there are also diagonal elements in $\mathbf{H}^{(4)}$. Their significance has been discussed elsewhere. (G. H. Dieke, Phys. Rev. **47**, 661 (1935).

$p\Sigma$ levels and a high vibrational level of $p\Sigma$ can come very close to a low vibrational level of $p\Pi$. The magnitude and character of the perturbations in such a case can then be completely predicted. It is also apparent that if the rotational states of two such vibrational levels do not actually cross over (see §4) but are close enough that they influence each other notwithstanding the small value of α, irregularities in the Λ-doubling must occur which do not have the character of typical perturbations. From what was said above, we must expect such irregularities to be more pronounced when the equilibrium distance is much affected by the value of Λ.

3. In heavy molecules the motion may be different from a regular precession of a constant angular momentum about the figure axis. In that case (15) does not hold any more and neither the restriction $n'=n$ nor $L=L'$ can be used any longer. However, the restriction $\Lambda'=\Lambda\pm1$ will still hold true as long as the dependence on the azimuth χ about the internuclear axis is given by (2), i.e., as long as everything is symmetrical about the internuclear axis. As soon as this symmetry is disturbed, e.g., by the rotation of the molecule, deviations from the Λ-restriction rule must be expected.[9] Levels can perturb each other now even though their L or n are different. A calculation of the perturbation matrix is then only possible with a more detailed knowledge of the wave function. Very often we can know that the deviations from the motion under 2 cannot be very large, and in that case we can be sure that the interaction elements which are absent in case 2 will be small now.

§4. The Perturbations as Functions of J

We shall investigate now a little more in detail the influence of the perturbation due to $\mathbf{H}^{(2)}$ on the rotational energy levels. We saw that ordinarily the elements of the perturbation matrix are large only when the two levels perturbing each other have all quantum numbers identical except that their value of Λ differs by ±1. Such states are far apart except for the higher levels of light molecules. But even in the latter case there can be no crossing over. (By crossing over is meant that if the levels of the first state are below those of the second state for small values of J, they are above them for large values of J. For intermediate values then they must come very close together and cross over.) We do not have perturbations in the proper sense in this case, but the regular Λ-doubling which is called L-decoupling, when it is very large owing to the proximity of the two states. Although these phenomena are due to exactly the same causes as the real perturbations and there are transition cases between them, they are distinguished from them, because they seem more systematic in character, whereas the real perturbations seem always erratic at a first glance. The reason for this is that the perturbing matrix elements are so much smaller that their influence is not felt, except when the two perturbing states are very close together.

If we are interested in the perturbations of a given state we can restrict ourselves, therefore, on the influence of only those states able to interact with it which are very close. Except for rare cases of coincidence we have, therefore, to consider only one pair of interacting states and shall differentiate them by indices 1 and 2. As the changes in the energy due to the perturbations may be of the order of the distance between the perturbing levels, we must apply the perturbation theory for semidegenerate states. If we call ϵ the energy shift due to the perturbations and δ the energy difference between the unperturbed levels we have

$$\begin{vmatrix} S_{11}-\epsilon & S_{12} \\ S_{21} & S_{22}+\delta-\epsilon \end{vmatrix}=0 \qquad (18)$$

or in the case of class A perturbations for which $S_{11}=S_{22}=0$

$$\epsilon=\delta/2\pm(|S_{12}|^2+\delta^2/4)^{\frac{1}{2}}.$$

If δ is taken positive and ϵ' and ϵ'' are the roots with the negative and positive sign of the square root, respectively, the perturbed energies are

$$W_1+\epsilon' \quad \text{and} \quad W_1+\epsilon''=W_2+\epsilon''-\delta=W_2-\epsilon'.$$

The perturbations of the two levels are of equal

[9] This disturbance of the symmetry about the internuclear axis which results in the L-decoupling will be much more effective in the cases 1 and 2 and therefore the deviations from the Λ-restriction rule will be more pronounced in these cases. A case where this happens is given in §5.

magnitude and opposite sign, so that the levels seem to repel each other. For $\delta \gg |S_{12}|$ we have

$$\epsilon' = -|S_{12}'|^2/\delta. \tag{19}$$

The maximum disturbance occurs when the unperturbed levels coincide. In this case $\epsilon_0 = \pm|S_{12}|$.

The wave functions belonging to the two perturbed levels are linear combinations of the unperturbed ones

$$\begin{aligned} \psi_1' &= a_{11}\psi_1 + a_{12}\psi_2, \\ \psi_2' &= a_{21}\psi_1 + a_{22}\psi_2, \end{aligned} \tag{20}$$

and the coefficients a_{ij} are the solutions of the linear equations

$$\begin{aligned} (S_{11}-\epsilon)a_{11} + S_{12}a_{12} &= 0, \\ S_{21}a_{11} + (S_{22}+\delta-\epsilon)a_{22} &= 0. \end{aligned}$$

As in all similar cases the values of the coefficients are for the limiting cases

$$\begin{aligned} &a_{11} = a_{22} = 1; \quad a_{12} = a_{21} = 0 \quad \text{for} \quad \delta \gg |S_{12}|, \\ &a_{11} = a_{12} = a_{21} = -a_{22} = 1/\sqrt{2} \quad \text{for} \quad \delta = 0. \end{aligned}$$

The first of these relations means that when the two states do not perturb each other appreciably, the perturbed states are identical with the unperturbed ones. When the interaction is not negligible either perturbed state acquires because of (20) the properties of both unperturbed states. For $\delta = 0$ these properties are shared in equal parts. The amplitudes of the electric moment become

$$\begin{aligned} P_1' &= \int \psi_1'^* P \psi \, dv = a_{11}P_1 + a_{12}P_2, \\ P_2' &= \qquad\qquad = a_{21}P_1 + a_{22}P_2, \end{aligned}$$

from which it follows that the intensities are proportional to

$$\begin{aligned} I_1 &= a_{11}^2 I_1 + a_{12}^2 I_2 + 2a_{11}a_{12}I_{12}, \\ I_2 &= a_{21}^2 I_1 + a_{22}^2 I_2 + 2a_{21}a_{22}I_{12}, \end{aligned} \tag{21}$$

in which $I_1 = |P_1|^2$, $I_2 = |P_2|^2$ and I_{12} the real part of $P_1^* P_2$. Always we have, as the matrix of the a_{ij} is a unitary matrix,

$$I_1' + I_2' = I_1 + I_2,$$

but the intensities of the two individual lines may have any value between 0 and $I_1 + I_2$ depending on the particular value of the a_{ij} and of P_1 and P_2.

As is well known everything in this paragraph so far applies equally well to any kind of interaction. We shall apply this now to our special case for which the perturbation matrix is given by (13).

We can write with sufficient approximation

$$W_i = A_i + B_i J(J+1) \tag{22}$$

or $\delta = A_2 - A_1 + (B_2 - B_1)J(J+1) = a + bJ(J+1)$.

If a is positive b must be negative to have a perturbation. For large δ this gives (18)

$$\epsilon' = \alpha^2 \frac{(J+\frac{1}{2}-\bar{\Lambda})(J+\frac{1}{2}+\bar{\Lambda})}{a+bJ(J+1)}. \tag{23}$$

Let us simplify matters still further by restricting ourselves to Σ, Π perturbations for which $\bar{\Lambda} = \frac{1}{2}$. Then

$$\epsilon' = \alpha^2 J(J+1)/(a+bJ(J+1)). \tag{24}$$

If a is sufficiently large the perturbation is negligible for small values of J. For $J=0$ it is exactly zero which can be seen also without any calculation, as there is a level with $J=0$ only for the Σ state which cannot interact with any level of the Π state. For large values of J we have $\epsilon' = -\alpha^2/b$.

We have therefore the following picture: Let us assume that the two states cross over near a certain value J_0 of J. For $J \ll J_0$ the influence of the perturbation is negligible. The rotational levels are represented by the ordinary quadratic formula (21). The vibrational level which is obtained by extrapolation to $J=0$, can therefore never show any perturbation.

For very large values of J the influence of the perturbation does not disappear, however large the distance between the unperturbed levels may become. The reason for this is that the perturbing forces are originated by the rotation of the molecule itself and increase with increasing angular velocity. For large J the interaction results in the constant term α^2/b in the energy so that also in this case the rotational levels are represented by a simple quadratic formula. They are shifted however by the constant amount α^2/b with respect

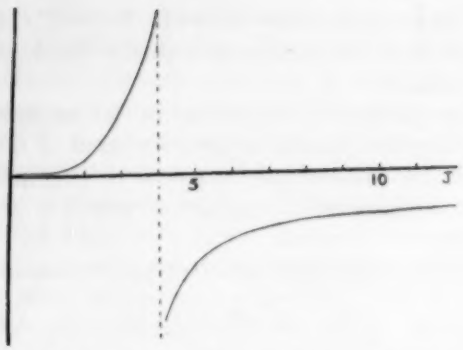

FIG. 1. Class A perturbation. Maximum at $J=4$.

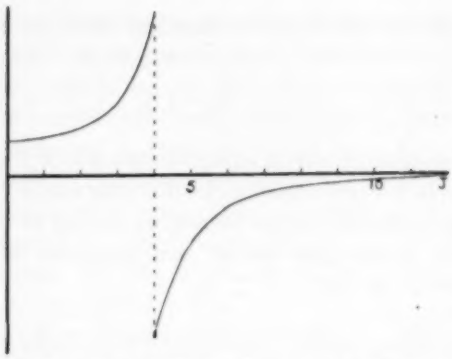

FIG. 2. Class B perturbation. It has a maximum of the same magnitude and at the same place as the perturbation in Fig. 1.

to the levels for low J. In the vicinity of J_0 the levels show strong deviations from the quadratic formula and the lines originating from them may have abnormal intensities.

The occurrence of the constant shift of magnitude a^2/b for large J may be used as a criterion for differentiating between class A and class B perturbations. (See Figs. 1 and 2.) For class B perturbations there is no such constant shift, and the influence of the perturbation disappears completely for large J.

Also for small J the two classes, as we saw above, may show a pronounced difference. Class A perturbations are small for small J and must be completely absent, e.g., in the $J=0$ Σ level. The vibrational levels which are obtained by extrapolating the rotational states to $J=0$ can therefore never be perturbed. For class B perturbations there are no such restrictions and as in Fig. 2, the vibrational level can be perturbed.

§5. Comparison with Experimental Data

Unfortunately the empirical material for testing the results of the preceding paragraph is extremely limited. There are only a few cases known in which both perturbing levels have been investigated. Of these, most represent more complicated cases. The best examples are the perturbations between the $p^3\Pi$ and $p^3\Sigma$ levels of the hydrogen molecule. They will be treated fully elsewhere. The numerous perturbations found in the levels of the CO molecule are complicated by the fact that several perturbations come close together and make accurate calculations impossible.

The perturbations of the He_2 levels[10] offer an interesting example. They are perturbations between $ns\Sigma$ and $nd\Sigma$ levels. As $\Lambda'=\Lambda$ one might think that these perturbations must be of class B. But the fact that there seems to be a constant displacement between the levels with low J values and those with high J values suggests that we may have here nevertheless class A perturbations. This seems to contradict the Λ restriction rule. But as the $d\Sigma$ levels show almost complete L-decoupling, their wave function is a linear combination of the ψ's of a $d\Sigma$, $d\Pi$ and $d\Delta$ state each depending on χ according to (2). The $d\Pi$ part can produce perturbations with the $s\Sigma$ levels. Because of the L-decoupling of $d\Sigma$ the exact dependence on J is somewhat different from the case treated in §4 and the experimental data are too meager to warrant going further into this.

[10] G. H. Dieke, Phys. Rev. **38**, 646 (1931).

Gravitational and Electromagnetic Mass in the Born-Infeld Electrodynamics

(Received March 8, 1935)

BANESH HOFFMANN, *University of Rochester, Rochester, New York*

By postulating that infinite relativistic gravitational potentials are to be rejected in the Born-Infeld theory, it is shown that the gravitational mass of an electron becomes equal to its electromagnetic mass, and that difficulties in the usual relativistic treatment of gravitational mass are avoided. The above postulate is extended and its bearing on the alternative sets of field equations of the Born theory, and on a proposal made by the author is discussed.

§1.

THE classical concept of electromagnetic mass depended on the assumption of a definite size and structure for the electron, but was able to predict that the mass of a body would depend on its state of motion. The special theory of relativity showed, however, that the change of mass with velocity was a property of any inertial mass, whatever its origin, and in consequence the concept of electromagnetic mass has tended to fall into disuse.

Recently Born and Infeld[1] have developed a new system of electrodynamics in which the concept of electromagnetic mass takes on a new significance. Since the Born electron has no infinities in its potential, it is unnecessary to assign a definite radius to it, and its mass is a measure of the total energy of its field over all space. An electron no longer has an "interior" and an "exterior," and no need arises for arbitrarily avoiding the energy of the field "within" the electron since there is no region that can properly be characterized as within it.

In the general theory of relativity, the gravitational mass of a spherically symmetric distribution of matter arises as a constant of integration in Schwarzschild's field, and the gravitational potentials expressing the field contain an infinity at the center of the mass. To avoid this infinity it has been customary to point out that the gravitational potentials of this Schwarzschild field refer only to the region outside the matter producing the field and that, within the matter, other field equations are valid. The interior solution is then fitted to the exterior solution at the surface of the sphere, and this procedure leads to a relationship between the inertial and gravitational masses of the sphere.

In connection with the interior Schwarzschild solution, it is to be noted that an infinity at the origin would arise even here were one not to set equal to zero the integration constant that gives rise to this infinity. That is, one avoids an infinity at the origin, not because such an infinity does not exist in the most general mathematical solution of the interior field equations, but simply because one decides that such an infinity is objectionable on physical grounds.

A difficulty arises in the case of the exterior solution, when this is considered as standing alone, with no reference to a corresponding interior solution; for, since the gravitational mass arises as an arbitrary constant of integration, there is no reason why it should not take on negative values, and a negative mass is not considered desirable, outside the quantum theory. As soon as one relates the exterior solution to a corresponding interior one this difficulty seems to be removed since the gravitational mass is now identified with a quantity which closely approximates the total inertial mass of the sphere, and this will be positive if the density of the sphere is positive. Actually, however, the difficulty has merely been moved rather than removed, for, whereas in the isolated exterior solution we had to choose a positive value for a constant of integration after the general solution had been found, we now have to choose a positive value for the density as soon as the problem is set up.

In this paper we discuss the gravitational mass of an electron according to the Born-Infeld theory and show that the difficulties of the classical relativistic treatment of gravitational

[1] Born and Infeld, Proc. Roy. Soc. **A143**, 410 (1934); **A144**, 425 (1934) and **A147**, 522 (1934). We shall refer to the second of these as II.

mass may be avoided. Since, in the Born-Infeld theory, there are no longer two distinct regions, interior and exterior, to an electron, the one set of field equations must suffice throughout space. It turns out that no recourse is necessary to an interior solution, that the inertial mass of the electron can be related to its gravitational mass, and that this ensures not only that there will be no infinities in the gravitational potentials of the electron, but also that its gravitational mass will necessarily be positive.

§2.

According to Born and Infeld,[2] the field equations of the new theory, when gravitation is taken into account, may be written as

$$R_{ab}-\tfrac{1}{2}g_{ab}R=-8\pi E_{ab},$$

$$\frac{\partial}{\partial x^b}\{(-g)^{\frac{1}{2}}(F^{ab}-GF^{*ab})/(1+F-G^2)^{\frac{1}{2}}\}=0, \quad (1)$$

and $$\partial F_{bc}/\partial x^a+\partial F_{ca}/\partial x^b+\partial F_{ab}/\partial x^c=0,$$

where R_{ab} is the Ricci tensor formed out of the g_{ab}, F and G are defined in II Eqs. (2.16), the energy tensor, E_{ab}, of the electromagnetic field is given by

$$E_{ab}=-g_{ab}\{1-(1+F-G^2)^{\frac{1}{2}}-G^2/(1+F-G^2)^{\frac{1}{2}}\}$$
$$-g^{cd}F_{ac}F_{bd}/(1+F-G^2)^{\frac{1}{2}}, \quad (2)$$

and the units are such that the velocity of light, the gravitational constant, and Born's natural unit of field strength, b, are all taken as unity.

These equations have been solved by the author for the general spherically symmetrical case, and it turns out that the field for this case is necessarily static.[3] The field equations of S.S. were written down with a wrong sign given to the value for the electromagnetic energy tensor E_{ab}, and the interpretation given to the field was different from that to be given in the present paper. If we pay regard to the effects of altering the sign of the electromagnetic energy tensor in S.S., it is seen[4] that the field equations will be satisfied by the line element

$$ds^2=Adt^2-A^{-1}dr^2-r^2(d\theta^2+\sin^2\theta\, d\varphi^2) \quad (3)$$

and the radial electrostatic intensity $F_{14}=\epsilon/(r^4+\epsilon^2)^{\frac{1}{2}}$, ($\epsilon$ a constant of integration), provided that

$$e^{\nu}(rd\nu/dr+1)-1=-8\pi r^2E_4{}^4$$
$$=-8\pi\{(r^4+\epsilon^2)^{\frac{1}{2}}-r^2\}. \quad (4)$$

This equation may be written as

$$(d/dr)(re^{\nu})=1-8\pi\{(r^4+\epsilon^2)^{\frac{1}{2}}-r^2\}$$

and gives the integral

$$A\equiv e^{\nu}=1-2m/r-(8\pi/r)\textstyle\int_0^r\{(r^4+\epsilon^2)^{\frac{1}{2}}-r^2\}dr, \quad (5)$$

where $(-2m)$ is a constant of integration which,[5] in classical relativity, is identified, from a consideration of the trajectories of a test particle in the field, with the gravitational mass of an uncharged sphere. It can be shown to be a first approximation to the inertial mass of the sphere either from consideration of a related interior field or from a general theorem due to Einstein[6] concerning the equality of gravitational and inertial mass in *weak* fields.

The Born theory was propounded in order to remove the infinity in the potential energy of the electron that occurs in the Coulomb field of the Maxwell theory. It is therefore reasonable to make the postulate that not only the electromagnetic potentials and intensities shall contain no infinities, but also that the gravitational potentials shall be free from such singularities.

Now the term involving m in the formula (5) for A becomes infinite as r approaches zero, though the term involving the integral remains finite at the pole despite the factor $1/r$. Thus the above postulate will require that we set m equal to zero.[7] And this requires that we obtain a gravitational mass in (5) from the integral term alone. The integral is not a constant, so that we shall be unable to find an exact duplication of the role played by m.

---

[2] See II, Eqs. (3.2), (3.4), (3.6) and below (4.5).

[3] Hoffmann, *On the Spherically Symmetric Field in Relativity, III*, to appear in Quarterly J. Math. (Oxford). We shall refer to this paper as S.S.

[4] S.S., Eqs. (27α), (27β) and (29); $A=e^{\nu}$.

[5] Cf. the classical relativistic field of a charged sphere, Tolman, *Relativity, Thermodynamics and Cosmology*, Oxford University Press, §107.

[6] Tolman, reference 5, §80.

[7] Cf. Tolman, reference 5, §96, where the constant C is taken as zero on similar grounds.

The integral can be written[8] as

$$\int_0^r r^2 E_4^4 dr = (1/4\pi)\int_0^r\int_0^\pi\int_0^{2\pi} E_4^4 r^2 \sin\theta dr d\theta d\varphi$$
$$= (1/4\pi)\int_0^r\int_0^\pi\int_0^{2\pi}(E_4^4(-g)^{\frac{1}{2}})dr d\theta d\varphi, \quad (6)$$

which measures the amount of $E_4^4(-g)^{\frac{1}{2}}$ in the sphere of coordinate radius r whose center is at the pole of the coordinate system. But $E_4^4(-g)^{\frac{1}{2}}$ is the energy density of the electrostatic field and therefore, in our present units, is equal to the mass density of this energy, i.e., to the electromagnetic mass density of the electrostatic field. Therefore, if we write

$$(1/4\pi)\int_0^r r^2 E_4^4 dr = m_r,$$

the quantity m_r measures the amount of electromagnetic mass contained in a sphere of coordinate radius r about the pole. The relativistic gravitational potential, A, now takes the form

$$A = 1 - 2m_r/r. \quad (7)$$

Though m_r is not a constant, it is very nearly equal to m_∞, the total mass, for values of r appreciably larger than the radius of the classical electron. Furthermore, it is easily seen that m_r is always positive, and it has already been pointed out that m_r/r does not become infinite at the pole. The fact that m_r is not a constant but measures the mass within the sphere of radius r, has a complete analog in the Newtonian theory, since it shows that at a point whose coordinate distance from the center of the electron is r, the gravitational effect is solely due to the matter within the concentric sphere passing through this point, the outer spherically symmetric distribution of mass having no gravitational effect at this point.

Thus by postulating that gravitational potentials that contain infinities are to be rejected, we have found that the electromagnetic and gravitational mass of an electron are equivalent, and this implies that all mass arising from electrons is essentially of an electromagnetic nature. At the same time, the introduction of an extra constant of integration has been avoided.[9]

The gravitational and electromagnetic masses have turned out to be identical in the case of a spherically symmetric electrostatic field, but this is due to the accident that g_{11} and g_{44} are reciprocals for this case. In general the relationship between the masses will be one of only approximate equivalence.

§3.

Born and Infeld have considered two possible sets of field equations for the electromagnetic field,[10] and have not decided which set is to be preferred. Some indication of the respective merits of the two sets of field equations can be obtained by the use of the postulate that all infinities are to be avoided.

In S.S.[11] the general spherically symmetric fields allowed by the two sets of field equations were obtained. If we make allowance for the wrong sign in the field equations of S.S. and ignore the cosmological constant λ and the integration constant m, we may write the two solutions as:

For $G \neq 0$:

$$ds^2 = A dt^2 - A^{-1}dr^2 - r^2(d\theta^2 + \sin^2\theta\, d\varphi^2),$$
$$F_{14} = \epsilon/(r^4+\mu^2+\epsilon^2)^{\frac{1}{2}},$$
$$F_{23} = \mu \sin\theta, \quad (8)$$

with $A = 1 - (8\pi/r)\int_0^r\{(r^4+\mu^2+\epsilon^2)^{\frac{1}{2}} - r^2\}dr$;

For $G = 0$:

$$ds^2 = A dt^2 - A^{-1}dr^2 - r^2(d\theta^2 + \sin^2\theta\, d\varphi^2),$$
$$F_{14} = \epsilon(r^4+\mu^2)^{\frac{1}{2}}/r^2(r^4+\epsilon^2)^{\frac{1}{2}},$$
$$F_{23} = \mu \sin\theta, \quad (9)$$

with $A = 1 - (8\pi/r)\int_0^r[(r^4+\mu^2)(r^4+\epsilon^2)]^{\frac{1}{2}}/r^2 - r^2\}dr$.

Each field represents the effect of a particle having electric pole strength ϵ and magnetic pole strength μ.

In S.S. it was argued that since the $G=0$ field contains infinities at the pole unless μ is taken to

[8] Since $(-g)^{1/2} = r^2 \sin\theta$ here, because g_{11} and g_{44} in (3) are reciprocals.

[9] In classical theories of electromagnetic mass, the possibility of a body having a large mass and zero charge is explained by the fact that charges and masses add algebraically, but the masses associated with positive and negative charges are both positive. In the Born theory, even when gravitation is neglected, the field equations are not linear so that the addition of charges and masses is probably only approximate.

[10] Cf. II, p. 431, Eq. (2.15) and p. 432, Eq. (2.28), the latter being obtained from the former by ignoring the quantity G whenever it appears in the field equations.

[11] S.S. Eq. (30) for the case $G \neq 0$; Eq. (30′) for the case $G = 0$.

be zero, while the $G\neq 0$ field is free from such singularities, the $G\neq 0$ field is preferable if we allow the existence of isolated magnetic poles; but that the relative values of the two fields cannot be determined from these fields if we decide that isolated magnetic poles have no physical existence.

However, in terms of the postulate of the present paper, the situation is reversed. For, since when $\mu\neq 0$, the $G=0$ field involves infinities that are absent from the $G\neq 0$ field, we may argue that the $G=0$ equations require that the constant of integration μ be taken as zero in order that the infinities be avoided. The $G\neq 0$ equations give no reason for rejecting the possibility of a nonvanishing μ. Thus, if isolated magnetic poles are held to be physically nonexistent, the $G=0$ field equations are to be preferred since they require that $\mu=0$. On the other hand, if, in accordance with Dirac's theory,[12] isolated magnetic poles are assumed to exist, the $G\neq 0$ equations have the preference.

When μ is taken to be zero, the two fields become identical and we are back in the situation discussed in the preceding sections.

§4.

So far, we have considered the relationship between gravitational and electromagnetic mass in the Born-Infeld theory for the spherically symmetric case. However, it is to be noted that the particular form given by Born and Infeld for the electromagnetic energy tensor is not necessary to the argument. It will suffice merely that the energy tensor give an electrostatic energy that contains no infinities, is everywhere positive, and approaches zero sufficiently rapidly as r increases. The author has discussed[13] a modified set of field equations that avoids some of the difficulties of the equations proposed by Born and Infeld. However, it encounters other difficulties that are not to be found in the Born theory; the field equations are of the fourth order instead of the second, the spherically symmetric field of a charged particle has not been obtained, and it is shown that this field would differ from the corresponding Born field because of the influence of its own gravitational field, there even being a danger that this influence might introduce an infinity and thus spoil the whole purpose of the theory.

These difficulties lose most of their force when considered in the light of the argument used in the present paper. The fact that the field equations are of the fourth order implies that several unwanted constants of integration will probably arise in the spherically symmetric field; but it is possible that many of these will be removed by the postulate that potentials involving infinities must be avoided. And then, if the gravitational field contains no infinities the formula[14]

$$d\varphi/dr = ke^{\frac{1}{2}(\lambda+\nu)}(1+R)^{\frac{1}{2}}/(2k^2+r^4)^{\frac{1}{2}}$$

that gives the electrostatic intensity, will not be spoiled by infinities in the gravitational potentials e^{λ} and e^{ν}, and there is now considerable likelihood that the electrostatic potential itself will remain finite; which means that the requirement that all infinities, including those in the electrostatic potential, be avoided, will not cause k, essentially the electric charge, to be taken as zero.

I wish to thank Mr. A. G. Hill for the benefit of stimulating discussion.

Note added in proof, May 3, 1935: The criterion used in the present paper for determining infinities in the field is not an invariant one, and some steps in the argument therefore require modification. It is hoped to make this modification the subject of a further paper.

[12] P. A. M. Dirac, Proc. Roy. Soc. **A133**, 60 (1931).
[13] B. Hoffmann, Proc. Roy. Soc. **A148**, 353 (1935).

[14] Reference 13, p. 358, Eq. (30). We are using the notation of that paper here.

LETTERS TO THE EDITOR

Prompt publication of brief reports of important discoveries in physics may be secured by addressing them to this department. Closing dates for this department are, for the first issue of the month, the twentieth of the preceding month; for the second issue, the fifth of the month. The Board of Editors does not hold itself responsible for the opinions expressed by the correspondents.

A Note on the Band Spectrum of Silicon Fluoride

A few years ago Johnson and Jenkins[1] examined the spectrum of a discharge in silicon fluoride gas and found evidence of several band systems. One of these they examined in some detail and attempted a rotational analysis of what is apparently the (0,0) band at λ4368. They found a very large moment of inertia for the emitter which led them to very improbable conclusions as to its structure and nature.

We recently had occasion to examine the data of Johnson and Jenkins and noticed some peculiarities which suggested a possible error in their analysis. Among other things there is an indication of an alternation of intensity in the lines in one region of the λ4368 band and also considerable irregularity in the spacing which suggests that the lines do not all belong to the same band.

We have consequently reexamined under very high dispersion the violet portion of the spectrum obtained in the silicon fluoride discharge and have found some interesting features not previously noted. There are apparently two systems in the region with considerable overlapping of bands from the two. The superposition of two bands at λ4368 is so perfect that it does indeed give the impression at first that all the lines belong to one band. On closer examination one observes two band heads, very close together, which the previous workers apparently did not resolve, and quite strikingly the alternation of intensity and irregularity of spacing which were merely indicated by their data. There is very little doubt that only every other line belongs to one band and the remainder to a second, as there are several bands in the region where overlapping does not occur and which show twice the line spacing of the λ4368 structure. Wherever two bands do practically coincide violent perturbations are observed in some portion of them.

Since Johnson and Jenkins calculated the rotational constants on the assumption that all the lines in the λ4368 structure belonged to one band it is evident that they obtained moments of inertia about twice too large. If one takes half these values and calculates the internuclear distances on the assumption that the emitter is the SiF molecule, one obtains very reasonable results.

A further study of the spectrum is in progress and details will appear shortly.

RICHARD M. BADGER
CHARLES M. BLAIR, JR.

Gates Chemical Laboratory,
California Institute of Technology,
April 29, 1935.

[1] R. C. Johnson and H. G. Jenkins, Proc. Roy. Soc. **A116**, 327 (1927).

Scattering of Neutrons

In view of the recent measurements of Dunning, Pegram, Fink and Mitchell[1] on the absorption of fast and slow neutrons by various metals and of the rather large absorption cross sections shown by some metals for slow neutrons, we have made a preliminary investigation of the scattering of neutrons by several substances.

A bulb S containing radon (240 millicuries to 80 millicuries) and beryllium was placed in a cylinder of paraffin as shown in Fig. 1. After passing through 6 cm of paraffin, the neutrons from the source struck a silver foil, 6×10 cm, and then were scattered from blocks of metal the same size as the silver foil, placed above it. The scattering was measured by observing the increase in the radioactivity of the silver foil caused by the presence of various thicknesses of scatterer.

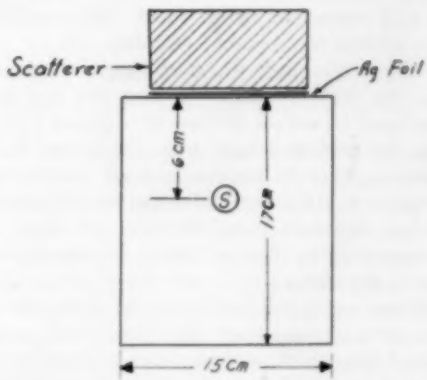

FIG. 1. Arrangement of scattering metal, silver foil and paraffin block containing the neutron source S.

The radioactivity induced in the silver by neutrons was first measured with no scatterer present. This was accomplished by placing the foil in the position as shown and irradiating it for 6 minutes. The sample was then removed and wrapped around a Geiger-Müller tube counter having thin aluminum walls. Counting was begun one minute after removing the sample and was continued until the end of the fifth minute, readings being taken every half minute. The activity of the foil was then given by the total count in this interval minus the natural count of the Geiger-Müller tube. A similar procedure was carried out when the scatterer was placed above the foil as shown in the diagram. The percentage increase in the activity of the silver sample (i.e., activity of the silver with scatterer present minus activity of silver alone, divided by the activity of the silver alone) was plotted as a function of the thickness of the scatterer. On the average about 1000

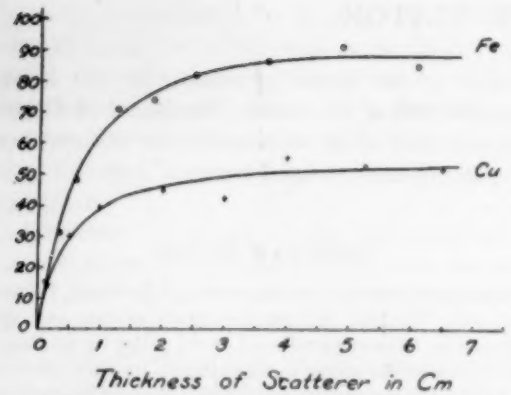

FIG. 2. Activity of Ag + scattering minus activity of Ag divided by activity of Ag alone (in percentage) plotted against thickness of scatterer.

particles were counted in the four minutes when silver alone was present.

The results for iron and copper are shown plotted in Fig. 2. It will be seen that a thickness of about 3.5 cm of either is sufficient to give maximum scattering, which was about 52 percent for copper and 88 percent for iron. It should be noted that the number of atoms per square centimeter is the same in either case, since the atomic densities of iron and copper are about equal. The results are, of course, corrected for the decay of radon.

An attempt was made to get an approximate measurement of the relative number of slow and fast neutrons scattered back by copper. A sheet of cadmium 1 mm thick shielded the neutron source from the silver. With this arrangement about 25 percent as many counts were obtained with Cd as without, indicating that this fraction is due to fast neutrons. A thickness of 4.3 cm of copper placed on top of the silver caused an increase of about 50 per cent in the count.

In another series of experiments the silver foil was not shielded by cadmium from the source, but a sheet of cadmium 1 mm thick, and the same size as the sample, was placed on top of the foil. With this arrangement no change in the activity of the sample was noted. With 4.3 cm of copper placed above the silver and cadmium there was only an 11 percent increase instead of the 52 percent increase obtained without cadmium. This experiment, taken in conjunction with the one just described, indicates that the scattering of fast neutrons by copper is comparable to that of the slow ones.

We should like to thank Dr. Leo Szilard for many suggestions and much helpful discussion. We are indebted to Dr. C. B. Braestrup of the Physical Laboratory of the Department of Hospitals of the City of New York for many favors and also to the American Association for the Advancement of Science for a grant to one of us (A. C. G. M.) with the help of which apparatus has been purchased.

ALLAN C. G. MITCHELL
EDGAR J. MURPHY

Department of Physics,
New York University, University Heights,
May 4, 1935.

[1] J. R. Dunning, G. B. Pegram, G. A. Fink and D. P. Mitchell, Phys. Rev. **47**, 416 (1935).

Precision X-Ray Wavelength Measurements

Precision measurements of the diffraction angles (or wavelengths) of x-ray lines are being made with the double crystal spectrometer with an observational error of 0.0002 to 0.001 percent.[1] The correction due to the divergence of the x-ray beam in the vertical plane which is to be applied to these measured angles is of the order of 0.002 percent.

The most recent and generally used correction formula is[2]

$$\delta\theta = [(a^2+b^2)/24L^2] \tan\theta, \quad (1)$$

where a and b are the effective slit heights, L the distance between the slits and θ the Bragg angle. In view of the demands for increasing precision in wavelength determinations it should be pointed out that the numerator of Eq. (1) is in error and that the correct expression is

$$\delta\theta = [(a+b)^2/24L^2] \tan\theta \quad (2)$$

or, in case $\theta_A \neq \theta_B$, as in different orders or reflection or with dissimilar crystals,

$$\delta\theta = [(a+b)^2/48L^2]\lambda D, \quad (3)$$

where D, the dispersion, is given by

$$D = (1/\lambda)(\tan\theta_A \pm \tan\theta_B). \quad (4)$$

For slits of equal heights Eq. (2) differs from Eq. (1) by a factor of two. This angular shift due to the vertical divergence is toward larger values of θ and consequently $\delta\theta$ must be subtracted from the observed angles. Expressions (2) and (3) are derived from a simplification of Schwarzschild's treatment[3] assuming the instrument is in proper adjustment.

If the diffraction patterns of the crystals are asymmetrical, as predicted by the Darwin-Ewald-Prins theory,[4] a correction for this asymmetry should also be applied to the angle observed in any antiparallel position of the double spectrometer. The center of area of the asymmetrical pattern is shifted to a smaller value of θ and the correction would be added to the observed angle. As mentioned by Compton and Allison,[5] this correction in the (1, +1) position, based on the theoretical diffraction patterns of calcite crystals, at the wavelength 1.54A (Cu $K\alpha_1$) is of the order of magnitude of the correction for the vertical divergence of the beam and the two corrections approximately offset each other. However, the degree of asymmetry of the theoretical patterns varies markedly with wavelength. At the wavelength of, and less than, 0.71A (Mo $K\alpha_1$) (which wavelength has been measured most accurately) the theoretical diffraction pattern of calcite is practically symmetrical. The center of area shift due to asymmetry increases with wavelength to 3.06A, the K absorption limit of calcium. At wavelengths greater than 3.06A the theoretical patterns are again more nearly symmetrical until the region of 5 to 6A is reached where the asymmetry is about the same as, or slightly greater than, at 1.54A.

No positive experimental information has been reported as to the supposed asymmetries of the crystal patterns but indications that such asymmetries do exist are apparent from recent measurements of the shapes of x-ray lines in various antiparallel positions of the spectrometer with various crystals.[6]

Then, unless we assume the validity of the Darwin-Ewald-Prins theory, we are at a loss to correct for the asymmetry of the crystal patterns and this state of affairs reduces the relative importance of an accurate slit-height correction. On the other hand, certain features of the theoretical patterns (but not asymmetries, which as yet cannot be directly checked by experiment) have been shown to give surprisingly good agreement with experimental measurements[4] in the $(1, -1)$ positions and it is likely that the actual pattern asymmetries are given qualitatively by the theory as indicated above. One hesitates to say the experimental crystal effects could be evaluated quantitatively because the theory is based on the assumption of a "perfect" crystal which does not actually exist. Perhaps it is best to apply the slit-height correction and await results of future researches to decide the crystal effects.

The above discussion applies also to wavelength measurements made photographically with a single crystal spectrometer when the appropriate divergence correction is substituted for Eq. (3). The crystal effects in this case are, of course, those due to a single crystal instead of the compound effect of two crystals.

LYMAN G. PARRATT*

Cornell University,
May 1, 1935.

[1] A. H. Compton, Rev. Sci. Inst. **2**, 365 (1931); J. H. Williams, Phys. Rev. **40**, 791 (1932); J. A. Bearden, Phys. Rev. **43**, 92 (1933).
[2] J. H. Williams, Phys. Rev. **40**, 636 (1932).
[3] M. M. Schwarzschild, Phys. Rev. **32**, 162 (1928).
[4] S. K. Allison, Phys. Rev. **41**, 1 (1932); L. G. Parratt, Phys. Rev. **41**, 561 (1932).
[5] Compton and Allison, *X-Rays in Theory and Experiment*, D. Van Nostrand Co., 1935, p. 737.
[6] L. G. Parratt and L. P. Smith, Phys. Rev. **47**, 805A (1935).
* National Research Fellow.

The Scale of X-Ray Wavelengths

In a further effort to settle the question concerning the crystal and ruled grating scale of x-ray wavelengths the writer has carried out two additional experiments. First, the refraction method has been perfected by using a large diamond prism. Second, large ruled gratings have been used with a double crystal spectrometer to measure the wavelength of the copper $K\alpha_1$ line.

It has been shown[1] that the refraction of x-rays may be used as a means of determining the true scale of x-ray wavelengths. In the previous measurements a quartz prism was used and the wavelengths obtained agreed with the ruled grating values. However, there was some uncertainty in the results because of the difficulty of correctly making allowance for the effective number of electrons in the silicon. The present experiment was designed to eliminate this by using a prism of low atomic number. A diamond fulfills all the requirements better than any other substance.

Thus photographic refraction measurements by the method[1] previously described by the writer have been made for the copper $K\beta$ line using the 90° edge of a perfect diamond block 9 mm×9 mm×3 mm. Two surfaces were polished optically flat and intersected in a very perfect edge, though later it was found possible not to allow any part of the x-ray beam to strike the edge. Fig. 1 shows a typical plate. The average of the results from 25 of the best plates is $\delta = 9.224 \pm 0.0005 \times 10^{-6}$. This gives for the wavelength on a $\lambda^{2.75}$ absorption law $\lambda = 1.3924$A. This is 0.26 percent greater than the best crystal value and is in good agreement with the ruled grating wavelengths as is shown in Table I.

FIG. 1. D is the direct beam, β and α the refracted beams of the copper K series.

TABLE I. $(\lambda_g - \lambda_c)/\lambda_c$.

Observer	Grating	Cu $K\beta$	Cu $K\alpha$	Cr $K\beta$	Cr $K\alpha$	Al $K\alpha$
Bearden(1929)	a, b, c	0.24 (10)	0.25 (10)			
Bearden(1931)	1, c	.241(26)	.229(46)	0.229(16)	0.245(28)	
" "	4	.243(4)	.250(11)	.250(15)	.255(27)	
" "	4′	.264(30)	.257(49)	.253(3)	.254(5)	
" "	5	.246(41)	.234(73)	.235(32)	.239(51)	
" "	5′	.259(49)	.250(82)	.256(44)	.255(67)	
" "	6	.239(11)	.244(16)	.240(3)	.240(4)	
Bäcklin(1928)						0.17 (31)
" (1935)						.249(56)
Söderman(1935)			Cu $K\alpha_1$			.255(9)
Bearden(1935)	7		.253(8)			
" "	8		.247(4)			
" "	Refr.	.260(25)				

Weighted average 0.248±0.0016%

One of the objections to the method of using plane gratings for x-rays is that one uses only a small number of lines. Thus in the second experiment a plane grating 75 mm long was used. The entire length was used by placing the grating between the calcite crystals of a double crystal ionization spectrometer. The angles of incidence and diffraction were then measured by the angular displacement of the second crystal. The crystals were set in the $(1, +1)$ position so that the reflected and diffracted lines were essentially in the $(1, -1)$ position. By this method the two most important angular measurements were made with lines which were only 11 seconds to 16 seconds wide. Four carefully calibrated microscopes were used to read the precision circle and since two lines, ten minutes apart, were read in each microscope, eight angular readings were obtained for each individual setting of the circle. Different parts of the circle were used in order to eliminate any errors due to possible erratic rulings on the circle. Two gratings were used, the first (7, Table I) was ruled with 100 lines per mm and the second (8, Table I) was ruled with 300 lines per mm. The average of all 12 results gives for the copper $K\alpha_1$ line, $\lambda = 1.5405$A. This is 0.25 percent greater than the corresponding crystal value and is in excellent agreement with the writer's previous results.[2]

Bäcklin[3] has recently repeated his earlier measurements on the Al $K\alpha$ line and now obtains results almost identical with the writer's 1929, 1931 and the present results. Also Söderman[4] has used a concave grating to compare a high order of the Al $K\alpha$ line with the first order of a known

spark line and obtained good agreement (Table I) with the plane grating results.

The agreement between various ruled grating experiments is actually much better than is obvious from the published reports. This is due to the fact that different crystal constants have been assumed in different reports. In Table I the percent differences between the ruled grating and the crystal values have been recalculated for the best absolute measurements using[5] $d_{\infty}=3.02810$A. The numbers in parentheses are the numbers of independent determinations entering into that particular value. Thus when all the results are referred to the same crystal standard the agreement is very good. The weighted average was obtained by giving each result a weight equal to the number of independent values entering into that particular result. Bäcklin's 1928 result was neglected since his improved technique gave a very much higher value.

Since the many tests made on crystals normally used for x-ray work have indicated no mosaic structure one should be justified in using the absolute x-ray data for calculating some of the fundamental constants. The true x-ray grating constant of calcite crystals which is independent of any theory of crystal imperfection is

$$d_{\infty}=3.03560\pm0.00005\text{A}.$$

Avogadro's number is

$$N=6.0220\pm0.0005 \text{ mole/mole}$$

and using the Faraday $=9648.9$, one obtains the charge on the electron

$$e=4.8036\pm0.0005\times10^{-10} \text{ e.s.u.}$$

The value of Planck's constant as determined from the continuous x-ray spectrum is

$$h=6.607\pm0.001\times10^{-27} \text{ erg. sec.}$$

These values of the fundamental constants differ by 0.75 to 1.0 percent from the present accepted values. Since the three independent methods of determining x-ray wavelengths agree so well it appears that the true scale must be the ruled grating value and not the crystal values. The writer's attempts to use the above values of N, e and h in the interrelationships of the physical constants have not given satisfactory results. Thus, while it appears that one should be able to determine accurately the values of N, e and h from the x-ray data, it does not seem possible at the present time to reconcile such values with existing data on these constants by other methods.

It is a pleasure to acknowledge my indebtedness to the American Academy of Arts and Sciences for funds with which to purchase the diamond prism, and to Professor R. W. Wood for his cooperation in the ruling of the gratings.

J. A. Bearden

Johns Hopkins University,
May 7, 1935.

[1] J. A. Bearden, Phys. Rev. **39**, 1 (1932); J. A. Bearden and C. H. Shaw, Phys. Rev. **46**, 759 (1934).
[2] J. A. Bearden, Phys. Rev. **37**, 1210 (1931).
[3] E. Bäcklin, Zeits. f. Physik **93**, 450 (1935).
[4] M. Söderman, Nature **135**, 67 (1935).
[5] J. A. Bearden, Phys. Rev. **38**, 2089 (1931).

Radiative Auger Effect

The weak forbidden line in the K x-ray spectrum designated as β_5 by Idei[1] and as β_4 by Beuthe[2] has been studied by several workers[3] in the elements from vanadium (23) to antimony (51). It is a close doublet due to the transition $M_{32}M_{32}\rightarrow K$ and has an intensity ratio to α_1 of roughly 0.001. This faint line lies approximately midway between the strong lines β_1 and γ. If, in an effort to gain intensity, polished calcite crystals are used, the feet of the strong lines extend practically to the line β_5, but if etched calcite crystals[4] are used on a double crystal spectrometer with narrow horizontal slits the forbidden line is found in the middle of a broad, flat valley with a distinct plateau on the long wave side. This rise in the "continuous radiation" begins at β_5 and increases in steps until the total increase in ordinates about equals the height of the β_5 line. The phenomenon bears a superficial resemblance to a Compton effect with a very broad modified line.

Fig. 1 shows one set of measurements on molybdenum. The separation of the two components of β_5 indicated in

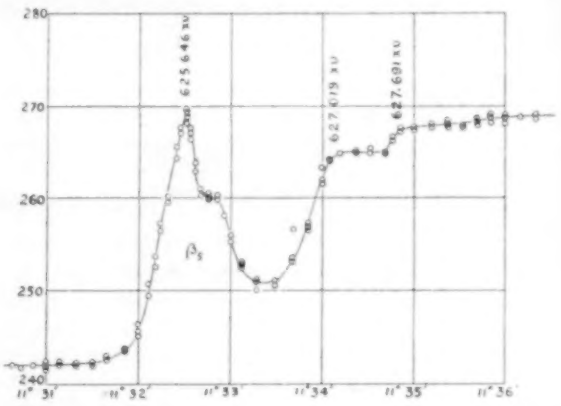

FIG. 1. Molybdenum $K\beta_5$. The strong lines β_1 and γ are at 11° 38′37″ and 11° 25′42″, respectively. The ordinates are electrometer deflections per minute.

this curve would seem to be somewhat too large to agree with accepted values of the $M_{32}M_{32}$ energies. Twelve curves have been run on molybdenum with different crystals, voltages, currents and targets. While slight erratic variations occur because of the faintness of the radiation, the essential characteristics are identical in all. Similar curves but with less precision have been obtained for rhodium, palladium and silver. In each case there is a rise in "background" on the long wave side of β_5, the upward slope extending for about 2 X.U. and then the plateau running with a flat top to β_1. This same peculiar phenomenon is shown in Duane's[5] high dispersion photographs of the Mo K spectrum as distinct increase in background extending from β_5 (called x by Duane) to β_1.

The explanation of this continuum on the long wavelength side of the forbidden line may be seen in the possibility of a radiative Auger effect, i.e., a simultaneous emission of a light-quantum and an electron by the excited atom. As one of us[6] has recently pointed out, such a process can occur by dipole-radiation, while the single electron

transition $M \rightarrow K$ necessitates a quadrupole transition. In an elementary process in which the emitted electron leaves the atom with a kinetic energy E, we would expect a light-quantum to be emitted with a frequency

$$\nu = \nu_{M_1K} - (1/h)(E + I_a),$$

where ν_{M_1K} is the frequency of the β_3-line, I_a the ionization-energy of the ejected electron. Since E, beginning with zero, can assume any positive value, the values of this frequency will likewise lie in a continuous range the high frequency limit of which is given by

$$\nu_{\max} = \nu_{M_1K} - I_a/h.$$

We would interpret each step in the intensity-plateau reported above as the beginning of one such continuum, the short wavelength limit being different from electron groups with different ionization energies I_a. Thus in the case of Mo the continual joining the steps at a wavelength $\lambda = 627.019$ and $\lambda = 627.691$ would correspond to the ejection of an N_2 and N_1 electron, respectively. Expressing the difference in frequency from the step to the forbidden line $\lambda = 625.646$ in units of the Rydberg-frequency, one would thus obtain for the N_1 electron

$$(\nu_{M_1K} - \nu_{\max})_1 = I_{a1}/h = 4.75 \qquad (4.7)$$

and for the N_2-electron

$$(\nu_{M_1K} - \nu_{\max})_2 = I_{a2}/h = 3.19. \qquad (3.8)$$

These values are in satisfactory agreement with those given in the parentheses and determined from limiting frequencies of x-ray series.[7] It is important to notice that the mechanism here proposed yields also the right order of magnitude for the total intensity of the continuum. Taking only the contribution due to the emission of N_2 electrons, we would expect it[8] to stand to the intensity of the K-line in a ratio of about

$$6(e^4/E_a^2)(r_i/r_a^2)^2 \leqq 0.2.$$

E_a is the ionization energy of an M_3-electron, the radii r_i and r_0 of the M_3- and N_2-orbits are estimated from the observed ionization-energies under the assumption of hydrogen-like orbits and the factor 6 is introduced to account for the presence of 6 N_2 electrons. Since the intensity of $K-\gamma$ is about 50 times the intensity of $K-\beta_5$ this means that the total intensity of the continuum would be about $50 \times 0.2 = 10$ times stronger than that of the forbidden line. This agrees with the experimental fact that the height of the plateau is approximately the same as that of the forbidden line; its extension however is about 10–20 times bigger.

F. Bloch
P. A. Ross

Stanford University,
April 22, 1935.

[1] Idei, Sci. Rep. Tohoku Imp. Univ. **19**, 559 (1930).
[2] Beuthe, Zeits. f. Physik **60**, 603 (1930).
[3] Ross, Phys. Rev. **39**, 536 (1932); **43**, 1036 (1933). Carlsson, Zeits. f. Physik **80**, 604 (1933); **84**, 119 (1933); Hulubei and Cauchois, Comptes rendus **196**, 1294 (1933).
[4] Manning, Rev. Sci. Inst. **5**, 316 (1934).
[5] Duane, Proc. Nat. Acad. Sci. **18**, 63 (1932).
[6] Bloch. Soon to be published.
[7] Int. Crit. Tables **6**, 35 (1929).

The Thermodynamic Temperature Scale in the Region Below 1° Absolute[1]

In our first experiments[2] on the production of very low temperatures by adiabatic demagnetization Curie's law, $\chi T = \text{const.}$, was assumed in obtaining the temperature.

Nearly a year ago experiments to determine true thermodynamic temperatures were performed and since we have not yet found time to report these in detail, we wish to publish a brief account of our results here. The full account will be given later, probably in the *Journal of the American Chemical Society*.

The substance investigated was gadolinium phosphomolybdate, $Gd(PMo_{12}O_{40})_3 \cdot 30H_2O$. An 89.28 g sample was used for the measurements.

Hoard[3] has shown that this substance is cubic with the gadolinium atoms occupying positions corresponding to those of the diamond type lattice. Thus all gadolinium atoms are equivalent and since there is but one gadolinium in a total of 250 atoms the magnetic atoms are unusually well diluted. This minimizes the interactions which must at sufficiently low temperatures destroy the validity of Curie's law. This law is, in the limiting case, inconsistent with the third law of thermodynamics.

In a paper, soon to appear,[4] we have shown how the application of the first and second laws of thermodynamics to magnetic and calorimetric data will permit the correlation of magnetic susceptibility, field strength and temperature. Here we will mention only the results for the determination of temperature in the special case of zero magnetic field where $T = de/dS$.

Magnetic susceptibilities were measured by the inductance coil method.[5] The susceptibility could then be used as a reference in correlating entropy and energy measurements. The entropies were fixed by a series of isentropic demagnetizations which started at known temperatures and magnetic field strengths. This procedure has been described in connection with the determination of the heat capacity of $Gd_2(SO_4)_3 \cdot 8H_2O$.[3]

For fixing the energy it was desirable to avoid the use of the usual electrical connections because of heat leak. We considered many possible sources of heat input such as radiation from a filament, from ordinary temperatures or from a radioactive material, the addition of a small amount of solid of known energy content or the condensation of small amounts of helium gas. Although any of these methods might have been employed we finally decided to use an induction heater. The heater consisted of a closed loop of No. 40 (B. and S. gauge) gold wire about 2 cm in diameter. The gold contained 0.1 percent silver. A small current was induced in the heater by means of a relatively large 60-cycle current in the same solenoid magnet used for the demagnetizing process. Although the total amount of energy introduced for a measurement was about 0.001 calorie it could be determined to the order of about 10^{-5} calorie. The measurements showed that for all temperatures down to 0.30°K the Curie scale for gadolinium phosphomolybdate is within 0.01° of the true thermodynamic scale. However, at 0.25° (Curie) the Curie temperature was 5 percent too low; at 0.20°, 11 percent too

low, and at 0.15° it was 22 percent too low. It should be pointed out that the deviations occur at temperatures where thermal equilibrium is more difficult to attain and that they may possibly be due to this effect. Also it is more difficult to obtain accurate derivatives at the end of the curve. It had been expected that the estimates of temperature on the Curie scale would be too high.

During energy input the temperature of the gold induction heater was considerably above that of the calorimeter but since it had to start operating at the low temperature it was possible to conclude that gold is not a superconductor above 0.15°K. Kurti and Simon[5] have recently found that it is still not a superconductor at 0.05° (Curie-$Fe(NH_4)$-$(SO_4)_2 \cdot 12H_2O$).

Since the above deviation from Curie's law is in a ferromagnetic direction, measurements were made to detect any permanent magnetism in gadolinium phosphomolybdate. None was found at any temperature to within an accuracy of 1/5000 of the saturation magnetic moment.

Gadolinium nitrobenzene sulfonate, $Gd(C_6H_4NO_2SO_3)_3 \cdot 7H_2O$ and gadolinium anthraquinone sulfonate, $Gd(C_{14}O_2H_7SO_3)_3 \cdot \chi H_2O$ were investigated in terms of their Curie scales. Their properties lie between those of the sulfate and phosphomolybdate as would be expected from the comparative dilution of the magnetic atoms.

All susceptibilities were independent of frequency to 1000 cycles per sec. Possible hysteresis was investigated calorimetrically with a frequency of 550 cycles per sec. Expressed in terms of the energy transferred to the substance at the maximum of the sine wave, approximately 5 parts in 10,000 were converted to heat at 0.15°. At 0.35°, and above, the effect was less than 5 parts in 100,000 which was the limit of accuracy. These figures apply to all of the above salts except the sulfate which was not investigated for hysteresis with 550 cycles/sec. None of the substances showed a detectable hysteresis at a frequency of 60 cycles/sec.

W. F. Giauque
D. P. MacDougall
Department of Chemistry, University of California,
Department of Chemistry, Harvard University,
April 16, 1935.

[1] The results given here were presented at the meeting of the American Chemical Society in affiliation with the American Association for the Advancement of Science, Berkeley, California, June 18–23 (1934).
[2] Giauque and MacDougall, (a) Phys. Rev. **43**, 768 (1933); (b) **44**, 235 (1933).
[3] Hoard, Zeits. f. Kristallographie, **A84**, 217 (1933).
[4] Giauque and MacDougall, J. Am. Chem. Soc., in press.
[5] Kurti and Simon, Nature **135**, 31 (1935).

The Ultraviolet Absorption Bands of Diacetylene

The absorption spectrum of diacetylene was investigated with a small Hilger quartz spectrograph, by using an absorption length of about 130 cm. A discrete absorption of about seventy bands was found in the region of λλ2900–1900A. At a pressure of 1 mm or lower the most intensive bands set in at λ2430A and extended to the short wavelength limit of the instrument. With increasing pressure, weaker bands in the less refrangible side began to appear until at a pressure of 250 mm the system extended to λ2860A; while in the more refrangible side, the bands broadened to an apparent continuum. Part of the bands are degraded to the red.

The gross structure of the system shows a marked resemblance with the ultraviolet system of dicyanogen.[1] Three distinctive progressions approximately 2100 cm^{-1} apart can be assigned:

(I) ν(cm^{-1})	$\Delta\nu$	(II) ν(cm^{-1})	$\Delta\nu$	(III) ν(cm^{-1})	$\Delta\nu$
41149	2113	41276	2133	41521	2084
43262	2091	43409	2104	43605	2058
45353	2065	45513	2073	45663	
47418		47586			

The bands of these progressions are considered to be due to transitions from the same vibrational level (presumably the vibrationless level) in the ground state to an excited electronic state, (I) with successive excitation of the symmetrical longitudinal vibration ($\nu' \sim 2100$ cm^{-1}) alone, (II) in addition to the successive longitudinal vibration with one quantum excitation of probably the asymmetrical deformation oscillation ($\nu' \sim 130$ cm^{-1}), and (III) in addition to the successive longitudinal vibration with one quantum excitation of probably the symmetrical deformation vibration ($\nu' \sim 370$ cm^{-1}). The resemblance of the structure of diacetylene and dicyanogen has been pointed out by Mecke[2] and his collaborators through an investigation of the infrared and Raman spectra. It is to be pointed out here, that the isosterism between these two compounds is also markedly shown by a comparison of their ultraviolet bands. Because of the complexity of this spectrum, a more detailed investigation with higher dispersion as well as at different temperatures is in progress. A detailed report will appear soon elsewhere.

Sho-Chow Woo
T. C. Chu
National Research Institute of Chemistry,
Academia Sinica, Shanghai, China.
April 19, 1935.

[1] S. C. Woo and R. M. Badger, Phys. Rev. **39**, 932 (1932).
[2] R. Mecke, Eucken-Wolf Hand-und-Jahrbuch der Chem. Physik **9**, II, 392 (1934); B. Timm and R. Mecke, Zeits. f. Physik **94**, 1 (1935).

The Ultraviolet Absorption Spectrum of ND_3

I have recently obtained photographs of the absorption spectrum of very pure ND_3, which was given me by Professor H. S. Taylor of Princeton University. A normal incidence vacuum spectrograph with a 120,000 line 4-inch glass grating, one-meter focus, was used. The spectral region covered was from 2300 to 770A. Six plates showing eighteen spectra at a variety of pressures of ND_3 were obtained. The spectrograph itself filled with the gas acted as the absorbing column, and so the effect of temperature on the absorption could not be observed.

The most interesting result of this work will be a detailed quantitative comparison of the spectra of NH_3 and ND_3, in light of the theory of the vibrational isotope

effect for such molecules. Unfortunately the measurement and reduction of the plates cannot be begun immediately, but a few qualitative facts may be mentioned which are apparent from an inspection of the plates and enlargements.

In the spectrum of NH_3 reported by the writer in this issue of the *Physical Review*, four v' progressions in different electronic states were found. It appears that the analogs of three of these are present in the ND_3 spectrum. The three 0,0 bands of ND_3 almost coincide with the corresponding bands of NH_3, as would be expected. This may be regarded as additional evidence for the correctness of assignment of the 0,0 bands in NH_3. The fact that none of the other strong band heads and subbands of ND_3 coincide with those of NH_3 is additional confirmation of the high purity of the ND_3. The identification of all the weaker absorption requires, of course, a detailed examination, and some of it may prove to be due to NH_2D and ND_2H or even NH_3.

The strong bands in progressions II and III of ND_3 show differences of about 780 and 760. These were very crudely estimated, but appear to be upper state modifications of $\nu_1(745,748)$.[1] The predissociation in progression I appears to start at about the same point in ND_3 as in NH_3.[2] The bands in progressions II and III are very sharp in ND_3 as in NH_3. The rotational fine structure visible in NH_3 is not apparent in ND_3. If the moments of inertia are much larger in ND_3, this may be due to a lack of resolving power. The presence of NH_2D and ND_2H may cause a continuous background also, obscuring the lines of ND_3. This latter effect, if present, does not affect the sharpness of the heads. The subbands are all shaded to the red, as was observed in NH_3.

I am greatly indebted to Professor H. S. Taylor for furnishing the sample of ND_3 which made this work possible.

A. B. F. DUNCAN

Department of Chemistry,
Brown University,
May 15, 1935.

[1] E. F. Barker and Marcel Migeotte, Phys. Rev. **47**, 702 (1935).
[2] The measurements of Dr. W. S. Benedict (Phys. Rev. **47**, 641 (1935)) in this region, which were not available to the writer, will no doubt provide a more accurate value of the predissociation limit.

The Emission of Negative Electrons from Boron Bombarded by Deuterons

In March, 1935, Professor E. O. Lawrence and Dr. R. L. Thornton informed us, in conversation, that they had obtained some evidence indicating the emission of negative electrons of very high energy from boron bombarded with deuterons, and suggested that they might arise from the reaction

$$B^{11}+H^2 \rightarrow B^{12}+H^1 \rightarrow C^{12}+\epsilon^-+H^1. \qquad (1)$$

We have since carried out an investigation of this question, by means of a cloud chamber, and have found such beta-ray emission. Because of the fact that the beta-ray emission does not persist for an appreciable length of time after bombardment, it was necessary to make the observations during bombardment. The experiment was performed in the following way.

A thin walled tube containing the boron (metal) target was constructed so as to project into the cloud chamber through the glass top plate, near one side of the chamber. Of the useful 180° of the target tube, a section extending around 90° was made thin enough to allow the escape of the protons belonging to the 92-cm group, which is known to result from boron bombarded with deuterons.[1] The other 90° section was about three times that thickness, and allowed only electrons to pass. Ample intensity was obtained by running at 550 kv and about ½ microampere deuteron current to the target. The electron tracks were curved by a magnetic field of 1500 gauss, to determine their energy.

Electron Spectrum

In Fig. 1 is shown the energy spectrum obtained from the measurement of 1773 electron tracks. As is evident from the plot, the spectrum is continuous, and similar in form to the usual beta-ray spectrum. The upper energy limit, after adding 0.65 MEV to compensate for the stopping power of the tube surrounding the target, is

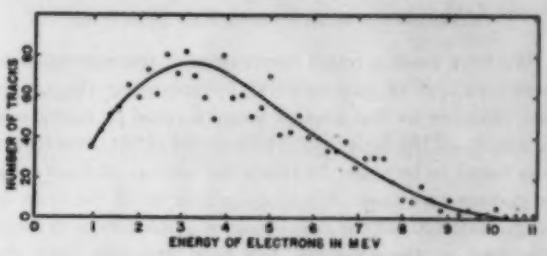

FIG. 1. Energy spectrum of negative electrons from the radioactive isotope B^{12}. To obtain the true energy, 0.65 MEV must be added to compensate for the stopping power of the wall surrounding active substance.

about 11 MEV. The position of the maximum in the curve is not to be taken seriously, since the geometrical conditions of the experimental set-up were such as to favor, to some extent, the lower energy electrons.

Protons

In order to compare the intensity of beta-ray emission with that of some other particle emitted under the same conditions we made a relative count of electrons and 92-cm protons, which were seen to emerge from the thin portion of the target tube. About 20 electrons were observed per proton of the 92-cm group. If we suppose that the beta-rays arise from reaction (1), the proton group associated with the beta-ray emission must necessarily be about 20 times as intense as the 92-cm group. Further, it is known from Cockroft's work that no group of that intensity exists above 10 cm range (2.5 MEV). We may therefore place an upper limit of 2.5 MEV on the energy of the proton in reaction (1).

Energy Balance

The energy release in the reaction

$$B^{11}+H^2 \rightarrow C^{12}+n^1 \qquad (2)$$

obtained from measurements of the maximum neutron energy,[2] is about 13 MEV. Eliminating between this and reaction (1), we see that

$$B^{12} \geq C^{12}+11 \text{ MEV}.$$

The conclusion to be drawn from this is that B^{12}, in disintegrating, loses an amount of mass not less than that corresponding to the *upper limit* of energy of the electron spectrum. The large energy involved in the electron spectrum and the fact that only the mass difference between n^1 and H^1 is made use of, place this conclusion well beyond the limits of experimental error, provided only that the reactions assumed are correct. This result has an important bearing on the neutrino hypothesis and the question of the validity of the principle of the conservation of energy in relation to beta-decay. A similar conclusion has already been reached by Henderson,[3] from a very precise, but less direct, experiment, namely a comparison of the change of energy around the two branches of the Th C to Th D sequence.

Comparison with Gamma-Ray Intensity

We have made a rough comparison of the intensities of beta-rays and of gamma-rays[4] by arranging the target and chamber so that enough paraffin could be interposed to absorb all the beta-rays. The number of beta-ray tracks was found to be about 10 times the number of tracks due to gamma-rays alone. Allowing for a factor of the order of magnitude 100 for the conversion of gamma-rays to recoil electrons in the chamber, we may conclude that the gamma-ray intensity is about 10 times the beta-ray intensity. From other observations[5] it appears that the rate of formation of B^{12} is somewhat greater than that of C^{11} (positron emitter of 20 min. half-life).

By means of an automatic timing device we were able to switch the ion current off a known length of time before each expansion of the chamber. Two runs of 100 pictures each were made, with the ion current stopped 1/25 and 2/25 seconds before the expansion. A total of about 1500 tracks was obtained in the first case, and about one-fourth that number in the second case, indicating a half-life of about 1/50 second for the active constituent.

H. R. Crane
L. A. Delsasso
W. A. Fowler
C. C. Lauritsen

Kellogg Radiation Laboratory,
California Institute of Technology,
May 15, 1935.

[1] Cockroft and Walton, Proc. Roy. Soc. **A144**, 704 (1934).
[2] Bonner and Brubaker, unpublished.
[3] Henderson, Proc. Roy. Soc. **A147**, 572 (1934).
[4] Crane, Delsasso, Fowler and Lauritsen, Phys. Rev. **46**, 1109 (1934).
[5] Lauritsen and Crane, Phys. Rev. **45**, 493 (1934).

Thermal Equilibrium of Slow Neutrons

The question, first attacked by Fermi, of whether the "slow" neutrons, which are so effective in producing nuclear transformations and have such anomalous absorption coefficients, approximate ordinary thermal velocities is of fundamental importance. Following our earlier experiments[1] we have investigated further the effect on the properties of the slow neutrons of the temperature of the hydrogen containing material used to slow them down. Fig. 1 shows the general arrangement used. The Rn-Be

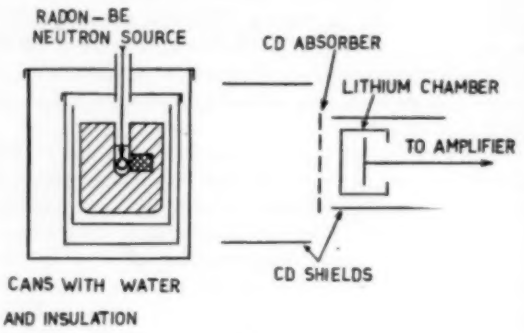

Fig. 1.

neutron source in a Pt container was placed in a cylindrical vessel of water which was inside several thin concentric polished cans to permit cooling to liquid air temperatures and also heating to the boiling point. The neutrons, after being slowed down by impacts with hydrogen nuclei, were detected through the ionizing particles ejected from Li, by means of an ionization chamber-amplifier system and thyratron recorder. In the first series of runs, the chamber had a Li front only; in the second series, runs 4 and 5, the chamber walls and collector were entirely of Li, resulting in much higher efficiency, and reducing the fraction of counts caused by high energy neutrons not highly absorbed by Cd from about 35 to 11 percent. In runs 1, 2 and 3, the Rn-Be bulb was at the same temperature as the water. Since it was found in a test that by cooling the bulb alone, the different modes of condensation of the radon at the low temperatures could produce increases in the number of recorded neutrons of the order of 3 to 8.6 percent, in the runs 4 and 5 the source with a thermocouple and heater was placed inside a soft glass Dewar and the bulb itself held at room temperature. In runs 1 and 2, the inner vessel was one of Cu containing 1100 g of H_2O. In runs 3, 4 and 5, a larger thin Al vessel containing 3400 g of H_2O was used, an amount sufficient to produce nearly the maximum number of slow neutrons. Cd shields were also introduced in the last two runs, as shown in Fig. 1, to reduce room scattering.

Table I shows the results of 5 runs in terms of the percentage change in the number of counts observed (chiefly from Li), and the percentage change in the absorption of Cd as the temperature was lowered from 373° to about 95°K in the first group, and 273° to about 95°K in the second

TABLE I. *Change in the number of observed counts (chiefly Li disintegrations) and in the absorption of Cd as the temperature was lowered to about 95°K.*

Run	Change in Li disintegrations	Change in Cd absorption
	Source at H_2O temperature,	95–373°K
1	+7.8%	+ 2.6%
2	+4.1	+10.7
3	+8.9	+ 2.7
	Source at constant temperature,	H_2O 95–273°K
4	−1.46	+ 3.8
5	−2.8	+ 2.4
	H_2O at constant temperature,	Source 95–273°K
	+3 to 8.6%	

group. Runs 1 and 2 consisted of about 5000 to 7000 counts on each point, run 3 of about 10,000 to 12,000 counts, and runs 4 and 5 of about 12,000 to 20,000 counts on each point. The last two are considered the most reliable, in which cases the accuracy from a purely statistical standpoint should be better than ±1.5 percent.

In regard to the change in the total number of counts observed at the various temperatures as shown in column 2, various factors such as the obvious effect of the condensation of the radon in runs 1, 2 and 3, the possible increased absorption in the walls of the all Li chamber, or the possibility of a slight amount of frost, and other factors which cannot be described in detail here, will have to be taken into account before giving significance to these changes in the total observed count.

The change in the absorption of Cd, as tested by introducing a sheet of about 0.005 cm of Cd (sufficient to absorb about 50 percent of the slow neutrons) is a test of the properties of the neutrons which should be unaffected by factors that may change the number of neutrons. The results, Table I, indicate that the "cold" neutrons are slightly more easily absorbed by Cd. While the effect is small—of the order of 5 percent, it is considerably larger than the probable error, and the possibility of the apparent consistency of the 5 runs being fortuitous is very small. A number of interpretations can be made of these results, such as: (1) No large fraction of these slow neutrons are actually in thermal equilibrium; or (2) a considerable fraction of these neutrons may be in thermal equilibrium, but the absorption of Cd, and the disintegration of Li are not sensitive functions of the neutron energy in this region; or (3) such possible effects as the removal of the slower neutrons from the beam by combination with H or O, or the possibility that the Li detection region does not extend down to near zero energy, etc. may influence the results. The fact that the absorption curve of Cd, when measured with a reasonably parallel beam of slow neutrons, is very nearly exponential, seems to show that the absorption of Cd is not a sensitive function of the energy in this region, and hence that the temperature effect should be small.

J. R. DUNNING
G. B. PEGRAM
D. P. MITCHELL
G. A. FINK

Pupin Physics Laboratories,
Columbia University,
May 22, 1935.

[1] Dunning, Pegram, Fink and Mitchell, Phys. Rev. **47**, 796 (1935).

The Raman Effect in Solutions of Magnesium Sulphate of Varying Concentrations

Previous experiments upon the Raman spectrum of magnesium sulphate have been reported. Embirokos[1] working in Gerlach's laboratory found a frequency shift of 985.7 cm^{-1} in a one-normal solution and 995.7 cm^{-1} in a two-normal solution. The magnitude of the shift was reported verified by Hollaender and Williams,[2] but Woodward and Horner[3] found no change in the frequency shift for solutions of different concentrations. Their values were 982 cm^{-1} for 1.25 and 2.55 normal solutions and 981 cm^{-1} for 5.1 normal. The frequency shift has been remeasured here for solutions of 4.5, 2.3, and 1.1 normal concentrations. The source of light was a glass mercury arc, the spectrograph a Hilger D78, and the plates were measured on a Hilger measuring micrometer. Several plates were taken for each concentration. The strong Raman line excited by Hg 4358A was used for measuring; and for the 4.5 normal solution also the line excited by Hg 4047A. The values found for the shift were 978.9±0.9 cm^{-1}, 980.5 cm^{-1}, 978.1 cm^{-1}. As the individual values for the 1.1 and 2.3 normal solutions lay between the extremes for the 4.5 normal, it is concluded that any change of frequency due to varying concentration must be not more than one or two wave numbers. This is in general agreement with the results of Woodward and Horner.

EDITH M. COON
E. R. LAIRD

Mount Holyoke College,
May 17, 1935.

[1] Embirokos, Zeits. f. Physik **65**, 266 (1930).
[2] Hollaender and Williams, Phys. Rev. **38**, 1739 (1931).
[3] Woodward and Horner, Proc. Roy. Soc. **A144**, 129 (1934).

Temperature Coefficient of the Work Function for Composite Surfaces

At the Washington Meeting, April 27, results were presented of an analysis of the field dependence of the slopes of Richardson plots for electron emission from thoriated tungsten based on a patch distribution of adsorbed atoms. This analysis was sufficient both to account for the experimental results and to establish the patch theory as the most probable explanation. The analysis did not account for the marked decrease of the intercept with increasing applied field, this departure of the intercept from its universal value being a measure of the temperature coefficient of the work function. It was suggested by J. A. Becker that this distribution of patches should also be a function of the temperature. If we let the concentration difference between patches vary with the temperature, we arrive at the following results:

(1) The temperature dependent patch distribution theory accounts for the field dependence of both the slope and intercept of the Richardson plot.

(2) In general, the temperature coefficient of the work function may be resolved into four parts, due, respectively to: (a) the base metal; (b) the uniform layer of adsorbed

atoms; (c) the variation of the distribution of adsorbed atoms; (d) the variation of local fields. Items (c) and (d) are related and are characteristic of the patch distribution.

(3) The sum of (a) and (b) constitute the temperature coefficient at zero applied field.

(4) At applied fields less than the local patch fields at the surface, actual measurement yields the sum of (a), (b), (c) and (d), (d) being a function of the applied field.

(5) At applied fields greater than the local patch fields at the surface, actual measurement yields the sum of (a), (b) and (c).

The temperature coefficient of the work function for composite surfaces has been measured, thermionically, calorimetrically and photoelectrically. To compare any of these reported values it is necessary that not only the applied fields but also the average size and concentration difference of the patches be the same.

A detailed analysis of the observed thermionic constants will appear soon.

ALBERT ROSE

Department of Physics,
Cornell University,
Ithaca, N. Y.,
May 17, 1935.

THE AMERICAN INSTITUTE OF PHYSICS

INCORPORATED

JOURNALS

THE PHYSICAL REVIEW

REVIEWS OF MODERN PHYSICS

PHYSICS

JOHN T. TATE, *Editor*
J. W. BUCHTA, *Assistant Editor*
E. C. BINGHAM, *Rheology Editor*

THE JOURNAL OF THE OPTICAL SOCIETY OF AMERICA

THE REVIEW OF SCIENTIFIC INSTRUMENTS WITH PHYSICS NEWS AND VIEWS

F. K. RICHTMYER, *Editor*

JOURNAL OF THE ACOUSTICAL SOCIETY OF AMERICA

F. R. WATSON, *Editor*

THE JOURNAL OF CHEMICAL PHYSICS

HAROLD C. UREY, *Editor*

THE AMERICAN PHYSICS TEACHER

DUANE ROLLER, *Editor*

The American Institute of Physics is a membership corporation of which five societies are the founding members. These five societies are the principal national societies devoted to pure and applied physics in America. Their names, and those of their representatives who form the Governing Board of the Institute, are given above. The principal work of the Institute is the publication of journals sponsored by the societies or by itself. The names and the editors of the journals are also listed above.

The broad purpose of the Institute is to represent, in all matters of wide or common interest, the five thousand or more members and subscribers associated with the Founder Societies and the journals. It aims to advance the science and profession of physics, and to promote cooperation between pure research, the applied sciences and the industries. To achieve these aims, it is greatly in need of an endowment and is empowered by law to administer grants and funds of any kind.

CONTENTS

PHYS. REV. 47 (1935) JUNE 1

Letters to the Editor:

LANCASTER PRESS, INC., LANCASTER, PA.